

Autonomous Quantum Processing Unit: What does it take to construct a self-contained model for quantum computation?

Florian Meier,^{1,2,*} Marcus Huber,^{1,2,3,†} Paul Erker,^{1,2,3,‡} and Jake Xuereb^{1,2,§}

¹*Atominstitut, TU Wien, 1020 Vienna, Austria*

²*Vienna Center for Quantum Science and Technology, TU Wien, 1020 Vienna, Austria*

³*Institute for Quantum Optics and Quantum Information (IQOQI),
Austrian Academy of Sciences, Boltzmannngasse 3, 1090 Vienna, Austria*

(Dated: February 2, 2024)

Computation is an input-output process, where a program encoding a problem to be solved is inserted into a machine that outputs a solution. Whilst a formalism for quantum Turing machines which lifts this input-output feature into the quantum domain has been developed, this is not how quantum computation is physically conceived. Usually, such a quantum computation is enacted by the manipulation of macroscopic control interactions according to a program executed by a classical system. To understand the fundamental limits of computation, especially in relation to the resources required, it is pivotal to work with a fully self-contained description of a quantum computation where computational and thermodynamic resources are not be obscured by the classical control. To this end, we answer the question; “*Can we build a physical model for quantum computation that is fully autonomous?*”, i.e., where the program to be executed as well as the control are both quantum. We do so by developing a framework that we dub the *autonomous Quantum Processing Unit* (aQPU). This machine, consisting of a timekeeping mechanism, instruction register and computational system allows an agent to input their problem and receive the solution as an output, autonomously. Using the theory of open quantum systems and results from the field of quantum clocks we are able to use the aQPU as a formalism to investigate relationships between the thermodynamics, complexity, speed and fidelity of a desired quantum computation.

I. INTRODUCTION

The earliest conceptions of computation including Babbage’s Analytical Engine [1] and the Turing Machine [2] envisaged computers as objects which receive a mathematical problem as an input and autonomously output its solution, culminating in the modern day realization of these ideas in silicon chips. Quantum physics has ushered in a new paradigm for probabilistic computation also introduced in the form of an input-output device by Benioff [3, 4], Deutsch [5] and Bernstein & Vazirani [6], the quantum Turing Machine. Separately, Feynman [7] and Kitaev [8] also envisaged a method for encoding a quantum computation into a Hamiltonian (also known as the circuit-to-Hamiltonian mapping [9–12]) which maintains the input-output and autonomy features that computation was originally formulated in. Both are successful conceptual frameworks for understanding complexity and computability in the context of quantum mechanics, but have yet to be physically grounded. Instead, current implementations of quantum computation make use of classical systems to continuously control macroscopic fields that change a quantum system to a target state from which an agent probabilistically samples to solve their problem. This is a form of computation which we argue is neither input-output nor autonomous from a

quantum perspective. Beyond this, with the realization that information is indeed physical [13], we understand that any computation will come with energetic costs and dissipated heat. This leaves society with a serious challenge as it becomes more technologically reliant under the constraints of efficiently and sustainably using the energy it produces. Naturally, with the advent of quantum computing the question of its inherent energy consumption has been investigated from different angles [14–16]. One of the challenges in this respect is the fact that there are many factors that are easily conflated, obscuring an understanding of the true fundamental cost of quantum information processing from a thermodynamic perspective. A particular issue being that typically employed time-dependent Hamiltonians involve large classical control costs (such as lasers or large magnetic fields) that contribute far more to the energetics of the quantum computation than that arising from the information processing at the quantum level.

With the challenges of i) recovering an autonomous and input-output quantum computer and ii) completely accounting for its energetics, a natural question arises: *can we build a self-contained physical model of quantum computation?* In this article, we answer this question affirmatively by introducing the autonomous Quantum Processing Unit. A quantum machine that can be fed a quantum state encoding a program to execute and does so by autonomously timing a string of unitaries which result in the desired transformation on a set of target qubits or qudits which can then be measured.

We make use of the framework of quantum thermal machines [17, 18] and recent results from the field of quan-

* florianmeier256@gmail.com

† marcus.huber@tuwien.ac.at

‡ paul.erker@tuwien.ac.at

§ jake.xuereb@tuwien.ac.at

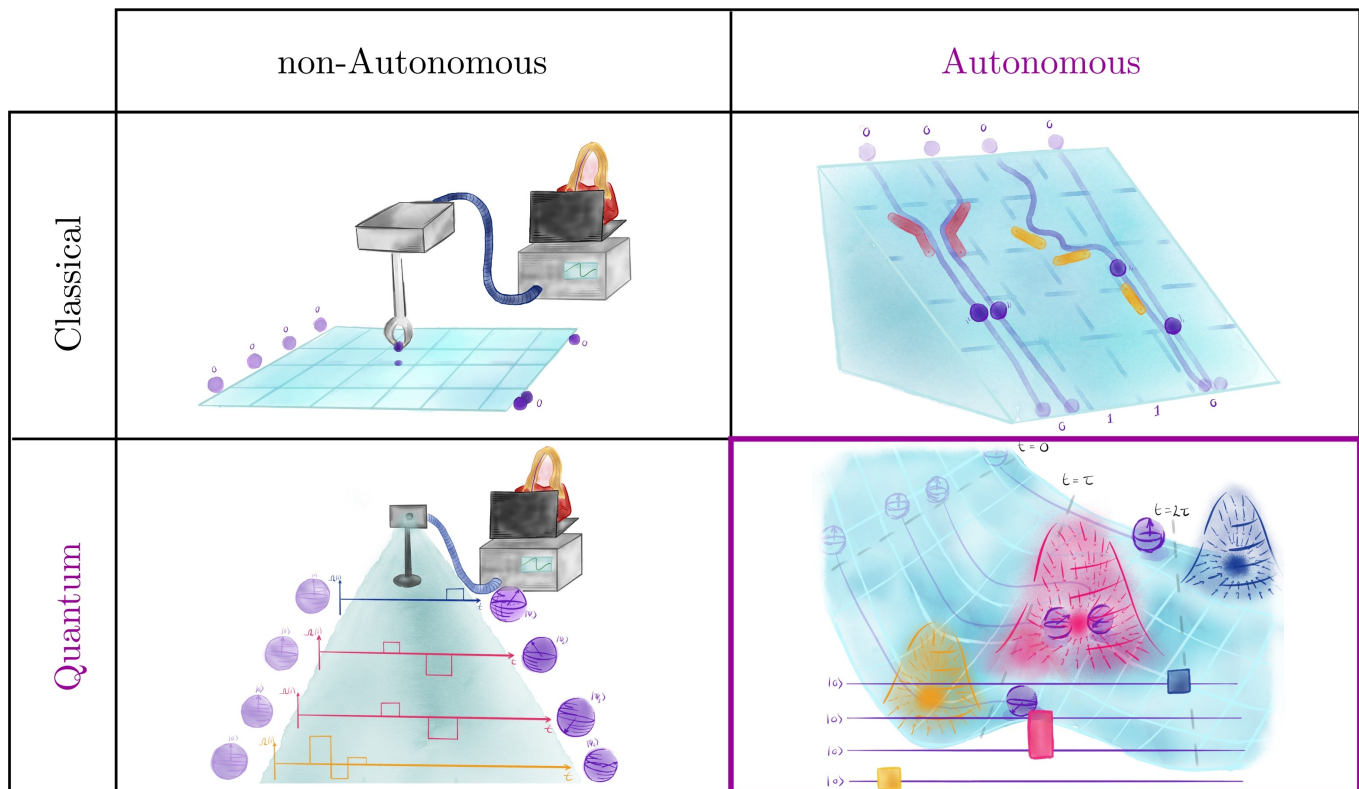


FIG. 1. In these four panels we give artistic impressions illustrating the setting for our proposed model, conveying what we understand by *autonomous*, i.e., the absence of time-dependent classical control mediated by macroscopic fields. In particular in the top right panel we give an illustration of an adaptation of the billiard-ball model of computation and a non-autonomous equivalent of this model in the top left. In the bottom panel we compare quantum computation carried out by a laser pulse according to some control algorithm and the illustrative example described below where spin-1/2 particles progress down a potential landscape with several interaction regions which alter the state of these particles, resulting in an autonomous quantum computation.

tum clocks [19–22] to introduce a model of autonomous quantum computation in the language of open quantum systems [23].

This results in a framework that not only allows us to investigate how finite thermodynamic resources introduce errors within an autonomous computation, but also the thermodynamic cost of a computation of a given complexity and speed. Therefore, ultimately providing a model of autonomous quantum computation that is not only conceptual, but also physically grounded, as suggested in [24].

Autonomy, Computation & Physics In the seminal work titled “Conservative Logic” [25] Fredkin and Toffoli introduced the billiard-ball computer as a model of computation not because it is necessarily efficient, but because it strips computation to its bare bones and allowed them to investigate how physics limits our ability to perform computation. This model is *autonomous*, by which we can understand a *prepare-and-forget* mechanism: after initial preparation, the system evolves without external intervention (see the comparison between left vs. right column in Fig. 1). This means, no control system manipulating the trajectory of the balls over

time is present and so the collisions of the billiards provide a self-contained physical model for the energetics of the computation. In this work we will take on the same perspective lifting it to the setting of quantum computation. Here, *quantum autonomy* means that the Hamiltonian that generates the time-evolution constituting the computation is not time-dependent (and so requires no external clock), nor is the computation encoded in a classical system. This perspective will allow us to develop a framework that connects quantum thermodynamics and quantum computation directly, just as Fredkin and Toffoli were able to connect classical physics and classical computation. It also invites us to reconsider the role of classical control systems within quantum computation.

Before beginning to introduce our model for the autonomous processing of quantum information we consider a motivating example (lower right of Fig. 1) that can help us understand the mechanisms our model for the aQPU requires and why. In this conceptual example a number of spin-1/2 systems sit atop a potential landscape. Once released they progress through the landscape and an arrangement of *interaction regions* acts on them as a *program* for a quantum computation. In analogy to the

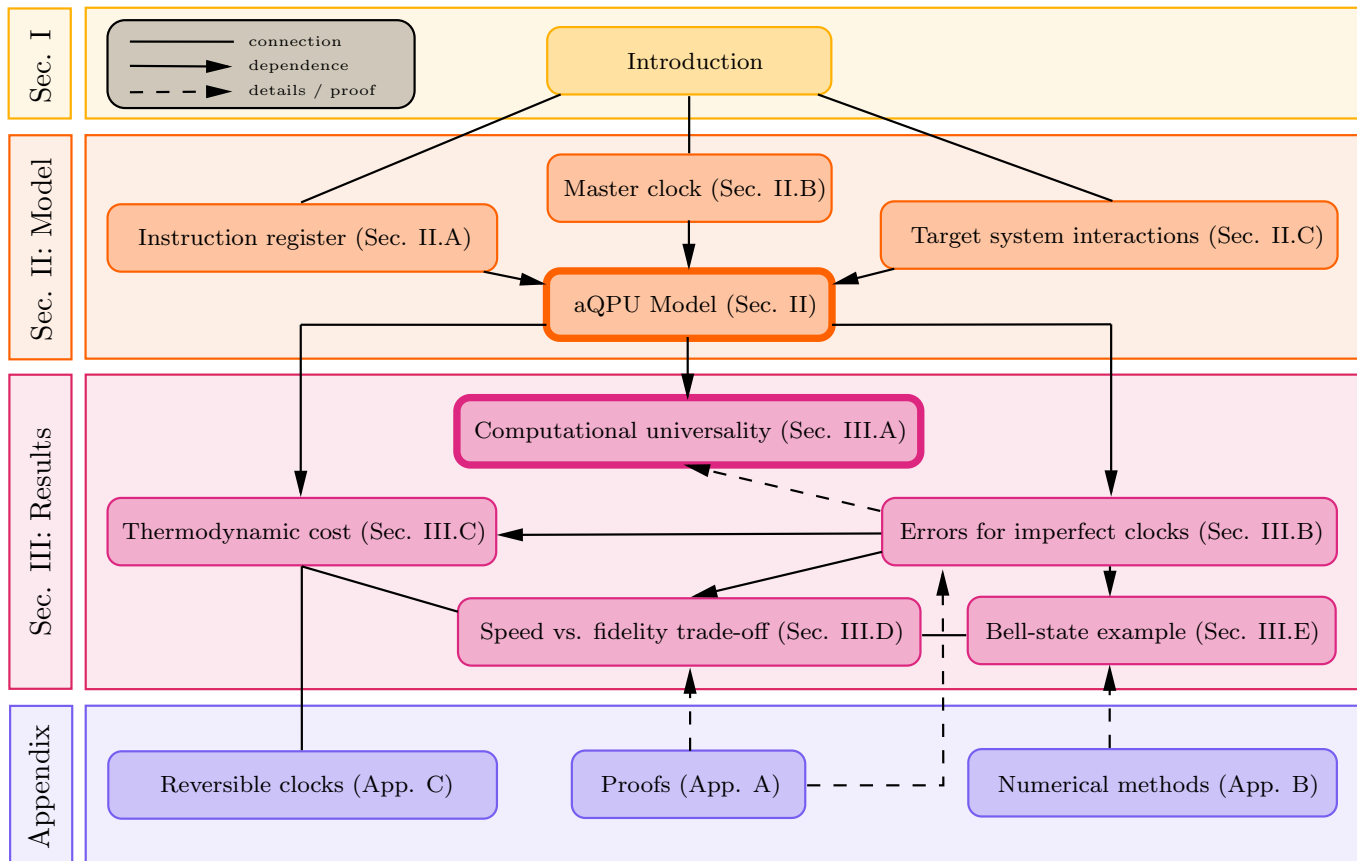


FIG. 2. An overview over the technical parts of the paper including the main sections and concepts. The connections and arrows indicate the hierarchy of the results and how the different topics are linked to each other, and the bold box boundaries indicate integral parts of this work.

billiard-ball example, this model for quantum computation is autonomous for once it is prepared, no further intervention is required. Still, there are some drawbacks, like the agent having to set up new interaction regions and potential landscapes to carry out different computations. What we really want is a quantum mechanical machine which we can feed a quantum input including the program and receive a desired quantum state as an output.

What could such a machine look like? In the illustration so far, the position degree of freedom of the particles encodes the timing of the operations, but this model does not really work with thermal resources making it hard to quantify the energetic cost of the computation. Instead, we want to use a quantum mechanical timing device – a *quantum clock* – to time different gates in a program one by one. For such clocks, open quantum systems are a well-established framework within quantum theory to quantify their non-equilibrium thermodynamic cost [26–29]. Several examples [20, 30, 31] have already shown that quantum clocks can provide accurate timing information only by using the non-equilibrium gradient across different *thermal baths*. Furthermore, whilst an arrangement of interaction regions encodes a computation

the agent would need to rearrange these regions for each computation and is not able to simply input an instruction encoding his desired computation into this setup. Our goal extends beyond this, by having universal interactions that are independent of the program to be carried out. In order to realize this objective, an aQPU would require an *instruction register* to be able to read programs encoded into quantum states which are input into the machine which we call *punch card states*. Together with the quantum clock, the internal aQPU interactions would carry out one instruction after another from the punch card state, completing the computation in an autonomous way.

Implications. We propose the autonomous quantum processing unit firstly as a framework to understand relationships between thermodynamics and the processing of quantum information. By its autonomous nature and structure as a thermal machine, it accounts for all aspects of the thermodynamics of executing a quantum computation and should serve as a conceptual tool for understanding what thermodynamic resources an agent requires to carry out a quantum algorithm of a given complexity at a given fidelity. Secondly, the framework is a novel framing of autonomous computation with an input-output feature

which allows an agent to encode the algorithm they wish to execute into a quantum state. This framework being set in the physics of autonomous thermal machines gives it the potential to be refined into a physical implementation of quantum computation as experimental implementations of thermal machines various platforms such as superconducting qubits [32] continue to improve and others emerge. As a theoretical tool, the aQPU provides a thermodynamically consistent framework for implementing any quantum channel on a subset of its computational register giving insights into the physics of free operations within resource theories of entanglement [33] and quantum thermodynamics [34, 35]. Perhaps most interestingly a subset of the channels one can implement on the aQPU feature indefinite causal order [36, 37] when the instruction register is put in a superposition, suggesting that the aQPU can be used as a tool to investigate the role of superpositions of gate orders (indefinite causal order) in quantum computation [38, 39].

Summary of the results. The remaining article is organized as follows (visualized in Fig. 2):

- In Sec. II, we provide a detailed definition of the aQPU model including the instruction register in Sec. II A, the master clock in Sec. II B and the interactions between clock, instruction state and target system in Sec. II C. This part of the paper is integral to understanding the formal details of the results.
- In Sec. III, we present the results of this work: Sec. III A is about the main result – that the aQPU achieves universal quantum computation if given access to a perfect master clock. Then, in Sec. III B we generalize this result to the case where the clock is not idealized and we quantify how well the aQPU approximates a universal quantum computer. Given these two results, we quantify the thermodynamic cost of running the aQPU in Sec. III C to show that smaller errors in the computation require more thermodynamic resources; furthermore, in Sec. III D we uncover that there is another trade-off, namely between the speed at which a computation can be carried out and by how accurately the aQPU approximates a given target-transformation. We conclude the results section with a numerical example in Sec. III E where we present simulation results of a Bell-state creation.
- In Sec. IV and Sec. V, we provide additional context for our results by showing how the aQPU fits into adjacent fields of quantum information, thermodynamics and causality, but also providing conclusions and an outlook including open problems.
- In the Appendices A, B and C technical results are presented with applicability that goes beyond this work.

II. MODEL

Quantum computation in the traditional circuit-based picture involves carrying out a sequence of unitary gates on a register of qubits which make up the memory of the computer. For generality, we refer to the memory as the target system with Hilbert space \mathcal{H}_T and we do not assume that the memory is made up of qubits, in the sense that it could alternatively be formed of d -dimensional quantum systems, i.e., qudits. Carrying out a computation on the target space requires three additional ingredients, which we will explore in this section (see Table I for the notation).

- (1) First, there is the algorithm which must be encoded in a physical program. We call this the **instruction register** and formalize the concept in Sec. II A.
- (2) Then, secondly, a **master clock** must time the individual instructions and switch from one to the next (see Sec. II B).
- (3) Thirdly, we need appropriate **interactions** between instruction register, clock and the target system for the program to be carried out. In Sec. II C, we propose a fully autonomous model for this.

How these three components combine together to form the aQPU is visualized and explained by Fig. 3 and detailed in the following sections.

System	Subscript
Computational Target Register	T
Instruction Register	R
Clockwork	C
Tick Register (Clock Hand)	H

TABLE I. Throughout this section the following notational shorthand is introduced for denoting different parts of the aQPU.

A. The instruction register

A quantum computation on a target system \mathcal{H}_T comprises some sequence of unitary operations on \mathcal{H}_T . For the aQPU we are interested in the case where we have access to a gate set consisting of a finite number of unitary operations labeled as

$$\mathcal{V} = \{V_T^{(k)} : 1 \leq k \leq K\}, \quad (1)$$

where K is the number of distinct gates in \mathcal{V} . In the special case where the target system is a register of qubits, a particularly relevant choice for \mathcal{V} is one where the gates are drawn from a universal gate set which due to the Solovay-Kitaev Theorem [8, 40–42] allows one to reach

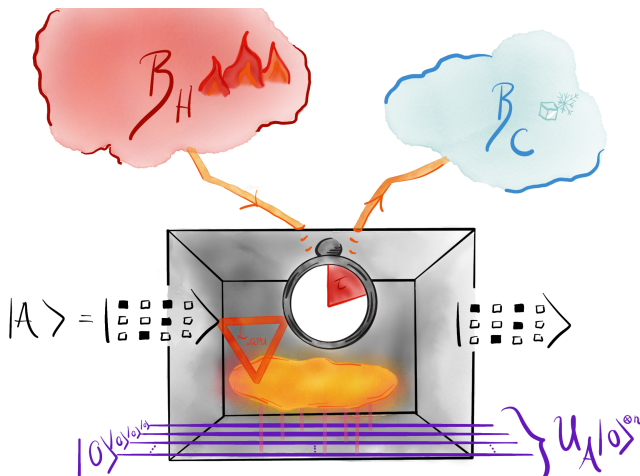


FIG. 3. A qualitative sketch of the autonomous quantum processing unit (aQPU): The aQPU is fed with an instruction register state $|\mathcal{A}\rangle_R$ (see Sec. II A) and an initial state for the target system, here $|0\rangle$, is chosen. The aQPU acts on those two systems jointly by drawing energy from some out-of-equilibrium resources to clock the instructions (more on this part in Sec. II B) and it then carries out the program \mathcal{A} on the initial state of the target system resulting ideally in $V_{\mathcal{A}}|0\rangle$. For finite resources one expects to only reach an approximation of this state. The full model is proposed in Sec. II C.

any quantum state in the Hilbert space with an error which decreases exponentially in the length of a specific sequence (further details can be found in Sec. III D). Generally, we can write each of the gates in \mathcal{V} as the propagator generated by some Hamiltonian for a fixed duration τ . The set of Hamiltonians $\{H_T^{(k)} : 1 \leq k \leq K\}$ is sufficient to generate \mathcal{V} , given that the condition

$$V_T^{(k)} = \exp(-iH_T^{(k)}\tau) \quad (2)$$

is satisfied. The fact that the duration τ has been chosen to be the same for all Hamiltonians is not restrictive, because one can always appropriately rescale the Hamiltonians, such that the product $H_T^{(k)}\tau$ generates $V_T^{(k)}$.

In the circuit model of quantum computation, where we work with a universal gate set for \mathcal{V} , indexing with an integer $1 \leq k \leq K$ as done in Eq. (1) may not be the most natural choice. In the case where each of the elementary gates in \mathcal{V} acts on at most two systems at a time one would rather use a 3-tuple (i, j, ℓ) , where i and j indicate which qubit the gate acts on and ℓ is the index from the list of elementary gates in the universal set. In the end, the set of indices $\{(i, j, \ell)\}$ is still finite and can be mapped to a list of integers $\{k : 1 \leq k \leq K\}$ to encode which elementary gate is performed. For our purposes, we will use the latter labeling for elementary operations throughout the text.

Programs. A program consisting of L computational steps, is given by the ordered set of unitary operations

$V_T^{(a_0)}, V_T^{(a_1)}, \dots, V_T^{(a_{L-1})}$, where each of them is $\in \mathcal{V}$. This means that the index a_n indicating the operation executed at the n th step is given as a number between $1 \leq a_n \leq K$. In this work we examine how the selection of these unitaries and the switching between them can be done autonomously throughout a quantum computation. We will show how the aQPU can be fed an initial state encoding the sequence $(a_0, a_1, \dots, a_{L-1})$, and the initial computational state resulting in the unitaries $V_T^{(a_n)}$ carried out on the target system without any additional time-dependent external control. A main challenge is how such an aQPU can select among the finite number of K Hamiltonians to generate said sequence and moreover how it can time these operations on its own. With respect to the gate set \mathcal{V} , we define a program as follows:

Definition 1 (Program). *With respect to a given set \mathcal{V} of K distinct gates as in Eq. (1) on a target Hilbert space \mathcal{H}_T , we define a program \mathcal{A} of length L to be a finite sequence*

$$\mathcal{A} := (a_0, a_1, \dots, a_{L-1}), \quad (3)$$

where each of the indices $1 \leq a_n \leq K$ encodes the n th operation of the program. This means, \mathcal{A} defines a unitary $V_{\mathcal{A}}$ on \mathcal{H}_T according to the prescription

$$V_{\mathcal{A}} := V_T^{(a_{L-1})} \circ \dots \circ V_T^{(a_1)} \circ V_T^{(a_0)}. \quad (4)$$

One of the goals of an aQPU is to start with some easy-to-prepare initial state featuring a quantum state $\rho_{\mathcal{A}}$ which encodes the program \mathcal{A} . By easy to prepare we understand that the initial state of the aQPU should not be entangled, nor should it feature coherences in the computational basis. Moreover, the initialization would further require an initial state ρ_T on the target system and the clock state ρ_C . Through the evolution of the aQPU, which will be described by some open system dynamics, we desire to achieve a process, where the target system ends up approximately in the state $V_{\mathcal{A}}\rho_T V_{\mathcal{A}}^\dagger$.

Punch card instruction state. Here, we describe an explicit mechanism implementing an aQPU, where the program \mathcal{A} is encoded in a so-called punch card state, and the quantum clock switches from one instruction to the next using a conveyor-belt type mechanism. As the choice of words already suggests, this conveyor-belt-punch card mechanism is designed to switch between the different operations encoded in a given program \mathcal{A} incoherently. We proceed to describe this model which implements an aQPU, starting by describing how the program \mathcal{A} can be encoded in a quantum state.

One physically motivated approach is to use a separate quantum system for each instruction. The Hilbert space for each such instruction being identical. In our setting we can encode the K possible instructions in a $(K+1)$ -dimensional Hilbert space \mathbb{C}^{K+1} to enumerate all elementary gates plus an additional one, the idle gate, which corresponds to doing nothing. Here, \mathbb{C} denotes the complex numbers and \mathbb{C}^{K+1} is the canonical

$(K + 1)$ -dimensional inner product space over the complex numbers. Given the choice of an orthonormal basis $\{|0\rangle, |1\rangle, \dots, |K\rangle\} \subseteq \mathbb{C}^{K+1}$, this would mean that $|0\rangle$ encodes the trivial Hamiltonian $H_T^{(0)} \equiv 0$, and $|k\rangle$ with $1 \leq k \leq K$ encodes the Hamiltonian $H_T^{(k)}$ which generates the elementary gate $V_T^{(k)} \in \mathcal{V}$.

Definition 2 (Punch card state). *Define the punch card state of length M , encoding a program \mathcal{A} of length $L \leq M$ as an element of the form*

$$|\mathcal{A}\rangle_R = |a_0\rangle_{R_0} |a_1\rangle_{R_1} \cdots |a_{L-1}\rangle_{R_{L-1}} |0\rangle_{R_L} \cdots |0\rangle_{R_M}, \quad (5)$$

living in Hilbert space $\mathcal{H}_R = \bigotimes_{m=0}^M \mathcal{H}_{R_m}$, where each factor $\mathcal{H}_{R_m} \cong \mathbb{C}^{K+1}$ encodes instruction $a_m \in \mathcal{A}$, or the idle-instruction $a_{m \geq L} = 0$.

Physically, the quantum systems encoding the individual instruction steps can be thought of as, e.g., $K + 1/2$ -spin systems in an eigenstate of the spin operator. An advantage of this approach where each step is encoded in a separate system is that the question of punch card state preparation can be discussed separately for each instruction and the resources required for the whole program preparation will scale with the number of non-trivial steps L .

B. Autonomous master clock

In this section, we summarize the main notions necessary to understand the workings of autonomous quantum clocks [20, 43], such that in the subsequent arguments, we are able to employ them as the devices controlling the timing of quantum operations on a specific target system.

Model. A ticking clock comprises two systems: first, the clock generating ticks which we denote by the label C and secondly, the ticking register H , that records these ticks in discrete increments. The notation H stands for the hand of the clock. There are theoretical works axiomatically deriving a model for ticking clocks in quantum theory [44, 45] leading to the same model we are using here. We forgo this foundational discussion and we will for the time being simply assume the clock model proposed in the following. Let us start with the ticking register where we can denote the states by labels $|0\rangle_H, |1\rangle_H, |2\rangle_H, \dots$, for 0, 1, 2 or more ticks. One of the main conditions we impose on the ticking register is that it is always in a semi-classical state w.r.t. this basis, i.e., we require that the ticking register is in a diagonal state. The clock's Hilbert space on the other hand is not further specified and we simply denote it by \mathcal{H}_C . At evolution time t , we may therefore write the joint state of the clock and ticking register as

$$\rho_{CH}(t) = \sum_{n \geq 0} \rho_C^{(n)}(t) \otimes |n\rangle\langle n|_H. \quad (6)$$

The state $\rho_C^{(n)}(t)$ can be understood as the non-normalized clock state conditioned on exactly n ticks having occurred, where $n \geq 0$ is an integer.

It is possible to write the equations of motion describing the evolution of $\rho_{CH}(t)$ in the Markovian limit as

$$\dot{\rho}_{CH}(t) = \mathcal{L}_C \otimes \mathbf{1}_H(\rho_{CH}(t)) + \mathcal{D}[J_{\text{tick}}](\rho_{CH}(t)). \quad (7)$$

The operator \mathcal{L}_C describes the internal evolution of the clock, which in this case is assumed to be appropriately described by a dynamical semi-group evolution [44]. This part of the evolution may be understood as the temporal-probability concentration of the clock [21, 30], while the dissipator on the right side of Eq. (7), given by

$$J_{\text{tick}} = \sum_{n \geq 0} J_C^{(n)} \otimes |n+1\rangle\langle n|_H, \quad (8)$$

describes the irreversible tick generation of the clockwork. For each integer $n \geq 0$, the clock can transition between the n th tick state $|n\rangle_H$ to the $(n+1)$ st tick state $|n+1\rangle_H$. At the same time, a quantum jump occurs on the clock defined by the operator $J_C^{(n)}$. In particular, this operator also determines how strongly the clock couples to the transition that generates the $(n+1)$ st tick, leading us to the tick probability as one of the key quantities we need to determine for the clock.

Ticking probabilities. One probability we can immediately look at is the trace $\text{Tr}[(\mathbf{1}_C \otimes |n\rangle\langle n|_H) \rho_{CH}(t)]$, which can be interpreted as the probability $P[N(t) = n]$ of the clock having ticked exactly n times at time t . Normalization of the quantum state $\rho_{CH}(t)$ ensures that the probability $P[N(t) = n]$ is normalized with respect to a sum over all non-negative integers $n \geq 0$, i.e., $1 = \sum_{n \geq 0} P[N(t) = n]$. Using the state decomposition from Eq. (6), we can simplify the trace expression as

$$P[N(t) = n] = \text{Tr}[\rho_C^{(n)}(t)]. \quad (9)$$

This probability ensemble samples over the possible number of times n that the clock has ticked: here, the number n fluctuates. If instead, we are asking about the probability that the n th tick occurs before time t , we are in a different ensemble, where n is fixed, but the time t fluctuates. This probability can be denoted by $P[T_n \leq t]$. We may read the inequality $T_n \leq t$ as the tick time T_n of the n th tick lies before t , i.e., it is smaller than t . We now present a number of useful properties of the tick probability density explored in Appendix A 1, which are necessary to understand the main result of this work. The first of these properties that we prove with a probability theoretic trick in Lemma 2 is the relation

$$\text{Tr}[\rho_C^{(n)}(t)] = P[T_n \leq t] - P[T_{n+1} \leq t]. \quad (10)$$

From this, another useful identity concerning the tick probability density of the n th tick $P[T_n = t] = \partial_t P[T_n \leq t]$ follows. Taking the derivative of Eq. (10) gives

$$\text{Tr}[\dot{\rho}_C^{(n)}(t)] = P[T_n = t] - P[T_{n+1} = t]. \quad (11)$$

Using the equations of motion in Eq. (7) allows us to furthermore express the tick probability density as an appropriate trace over the clock; the details are discussed and proven in Lemma 3, with the main result given by

$$\text{Tr} \left[J^{(n)\dagger} J^{(n)} \rho_C^{(n)}(t) \right] = P[T_{n+1} = t]. \quad (12)$$

With these preliminary results, we are in the position to examine the dynamics of this ticking clock coupled to a target system on which the clock times the desired operations.

C. Clock-instruction-computer interactions

We have finally arrived at a stage where all the main building blocks for the aQPU are together: (1) the target space \mathcal{H}_T where we want to carry out the computation together with the instruction-register \mathcal{H}_R storing the program and (2) the master clock \mathcal{H}_{CH} timing the quantum gates. The missing piece in the puzzle is (3), an interaction term which couples all these three systems together and completes the aQPU. The full Hilbert space we are considering is given by

$$\mathcal{H} \equiv \mathcal{H}_{CH} \otimes \mathcal{H}_R \otimes \mathcal{H}_T, \quad (13)$$

and to begin with the timekeeping we have already established in Sec. II B that the evolution on the clock is governed by an internal clockwork evolution \mathcal{L}_C , which generalizes to the full Hilbert space \mathcal{H} as

$$\mathcal{L}_{cw} = \mathcal{L}_C \otimes \mathbb{1}_{HRT}. \quad (14)$$

Similarly, also the tick generation generalizes to the full space by not acting on the instruction register and the target space, i.e.,

$$\mathcal{L}_{\text{tick}} = \mathcal{D} \left[\sum_{n=0}^{M-1} J_C^{(n)} \otimes |n+1\rangle\langle n|_H \otimes \mathbb{1}_{RT} \right], \quad (15)$$

where contrary to J_{tick} from Eq. (8), we have capped the number of clock ticks to the finite number M . Otherwise, the tick operator behaves the same, and each time the clock ticks, the tick register is shifted by one, until it ends up in the top-state $|M\rangle_H$. The main idea of this finite cap is that once the clock ends up in the last tick register state, the computation is over, and the target-system remains idling.

We now propose a three-body interaction Hamiltonian H_{int} acting on clock, instruction register and target space which ensures the following: *if the the master clock is in the n th tick state $|n\rangle_H$, and the n th punch card state reads $|a_n\rangle_{R_n}$, then, the Hamiltonian $H_T^{(a_n)}$ acts on the target space.* The following Hamiltonian achieves exactly this:

$$H_{\text{int}} = \sum_{\substack{n=0 \\ k=1}}^{M-1, K} \left(|n\rangle\langle n|_H \otimes \mathbb{1}_{R_{m(\neq n)}} \otimes |k\rangle\langle k|_{R_n} \otimes H_T^{(k)} \right). \quad (16)$$

The identity operator $\mathbb{1}_{R_{m(\neq n)}}$ is the identity defined on all punch card instructions but the n th one. The n th instruction is then read out using the term in the second sum on the right-hand side of Eq. (16). Conceptually, one can think of this interaction Hamiltonian as shuffling through filters where the projectors onto the n th tick on the tick register and the k th instruction make sure that the correct computation occurs within the aQPU. Note that there is no contribution from $|M\rangle\langle M|_H$ which ensures that once the the clock has ticked through all instruction steps of the punch card, the interaction on the target system is turned off. This allows us to look at the target system in the late-time limit and thereby ensure that all instruction states have been carried out. The interaction Hamiltonian contributes to the overall evolution on the aQPU with the commutator operator

$$\mathcal{L}_{\text{int}} = -i [\mathbb{1}_C \otimes H_{\text{int}}, \circ]. \quad (17)$$

Finally, the full dynamics are the combination of the terms from Eqs. (14), (15) and (17),

$$\mathcal{L}_{\text{aQPU}} = \mathcal{L}_{cw} + \mathcal{L}_{\text{tick}} + \mathcal{L}_{\text{int}}, \quad (18)$$

such that the time-evolution of the joint state $\rho(t)$ on the full Hilbert space \mathcal{H} from (13) is generated by the equation of motion

$$\dot{\rho}(t) = \mathcal{L}_{\text{aQPU}}[\rho(t)]. \quad (19)$$

Reminding ourselves of the Def. 1 of a program, the goal of the aQPU is that at the end of the evolution the target system is in a state as close as possible to $V_{\mathcal{A}} \rho_T^{\text{init}} V_{\mathcal{A}}^\dagger$, where \mathcal{A} is the program encoded in the punch card state in the beginning. As it turns out, this is indeed achievable in the limit where the master clock is perfect, which means the clock ticks perfectly regularly. In the next section, we formalize this claim and examine in further details the properties of the model we have just defined.

III. RESULTS

In this section, we go into the details of what the aQPU model we have proposed in the previous Sec. II is capable of achieving. We start in Sec. III A by proving that the aQPU is a universal quantum computer if the master clock is perfect. We follow up on this in Sec. III B by exploring how errors propagate in case the clock is non-ideal. Then, in Sec. III C we connect these errors impacting the computational fidelity with the thermodynamic cost of computation. Finally in Sec. III D we discuss how compiling programs on an aQPU with access to a finite set of Hamiltonians and a non-ideal clock presents a trade-off between the speed and fidelity of a computation.

A. The aQPU is universal for ideal clocks

For imperfect clocks, it is of course not expected that that the aQPU computes V_A perfectly on the target system. As we know from previous works [22, 46, 47] non-ideal timing of unitary gates leads to dephasing. What we can show about the aQPU model defined in the previous Sec. II is that under the assumption that the master clock is ideal, the aQPU generates V_A exactly. Ideal in this setting means that the distribution of ticks of the master clock is perfectly regular, i.e., if we set the average time between two ticks as τ , then for an ideal clock,

$$P[T_n = t] = \delta(n\tau - t). \quad (20)$$

We use the terms *perfect* and *ideal* clock interchangeably. Similarly, for the ensemble $N(t)$, we have a window-function-like probability given by the expression

$$P[N(t) = n] = \Theta(t \geq n\tau) - \Theta(t \leq (n+1)\tau), \quad (21)$$

with Θ being the Heaviside step function. Without further ado, the main theorem:

Theorem 1 (Universality for perfect clocks). *Let the aQPU model be defined by the Lindbladian $\mathcal{L}_{\text{aQPU}}$ as in Eq. (18) with access to a finite number of Hamiltonians that generate a universal gate set \mathcal{V} and let \mathcal{A} by any finite program defined on \mathcal{V} . If the master clock is ideal with tick time τ we have that*

$$\begin{aligned} \text{Tr}_{CHR} \left[e^{t\mathcal{L}_{\text{aQPU}}} \left(\rho_C^{\text{init}} \otimes |0\rangle\langle 0|_H \otimes |\mathcal{A}\rangle\langle \mathcal{A}|_R \otimes \rho_T^{\text{init}} \right) \right] \\ = V_{\mathcal{A}} \rho_T^{\text{init}} V_{\mathcal{A}}^\dagger, \end{aligned} \quad (22)$$

for $t \geq M\tau$ large enough.

The statement of this theorem is a consequence of the aQPU's state-structure when subject to the equations of motion in (19). Before we start with the proof of Thm. 1, we focus on the following two preliminaries, at the full level of generality of our model, i.e., we will assume a general master clock that may very well by non-ideal.

- The state-structure of $\rho(t)$: we show that the state can be expanded as an incoherent mixture over the states $|n\rangle\langle n|_H$ of the clock's tick register. We formalize this in Lemma 1.
- Given this specific structure, we can first solve for the clock dynamics and then secondly solve the target system dynamics separately. See Prop. 1.

The aQPU initially starts in a uncorrelated state of clock, tick register, instruction register and target system. Due to the structure of the time-evolution generator $\mathcal{L}_{\text{aQPU}}$, the correlations between different tick numbers that build up over time are only classical, such that we find the following simple structure:

Lemma 1 (State-structure). *Let the initial state defined on the full aQPU Hilbert space \mathcal{H} be given by*

$$\rho^{\text{init}} = \rho_C^{\text{init}} \otimes |0\rangle\langle 0|_H \otimes |\mathcal{A}\rangle\langle \mathcal{A}|_R \otimes \rho_T^{\text{init}}, \quad (23)$$

where ρ_C^{init} is an arbitrary initial state on the clockwork \mathcal{H}_C and ρ_T^{init} an arbitrary initial state on the target system. Then, at any point in time t the state $\rho(t) = e^{\mathcal{L}_{\text{aQPU}}t} \rho^{\text{init}}$ is given by

$$\rho(t) = \sum_{n \geq 0} \rho_C^{(n)}(t) \otimes |n\rangle\langle n|_H \otimes |\mathcal{A}\rangle\langle \mathcal{A}|_R \otimes \rho_T^{(n)}(t). \quad (24)$$

Proof sketch. The three terms that generate the evolution as in (18) are given by a clockwork term \mathcal{L}_{cw} , a tick-generating term $\mathcal{L}_{\text{tick}}$ and a three-body interaction term \mathcal{L}_{int} . In Sec. II B about the master clock we have already established that the terms $\mathcal{L}_{\text{cw}} + \mathcal{L}_{\text{tick}}$ define the clock and tick register evolution. By definition, these terms do not affect the target state, only the term \mathcal{L}_{int} can do so. Since the clock itself is always in a semi-classical mixture over the states $\rho_C^{(n)} \otimes |n\rangle\langle n|_H$ (which we prove in further detail in the Appendix A 2) and H_{int} only couples to $|n\rangle\langle n|_H \otimes |\mathcal{A}\rangle\langle \mathcal{A}|_R$ but does not mix those states, there are no coherences generated between different tick numbers $n \neq m$ and different programs $\mathcal{A} \neq \mathcal{B}$. Consequently, the state $\rho(t)$ will at all times only classically mix the different tick numbers n and always stay in the state $|\mathcal{A}\rangle\langle \mathcal{A}|_R$ of the instruction register, as written in Eq. (24) of the Lemma. For details, we refer the reader to Appendix A 2. \square

Now that we know the state-structure of the aQPU at all times t , we can insert it as an Ansatz into the equations of motion given by (19) and see how the reduced state $\rho_T(t)$ of the target system evolves. To get this done, we resolve the state $\rho(t)$ with respect to the tick numbers n by the looking at the state $\rho_T^{(n)}(t)$. Recalling the general structure from (24), there is some ambiguity regarding the normalization of the clock state $\rho_C^{(n)}(t)$ and the target system state $\rho_T^{(n)}(t)$. We will assume w.l.o.g. that for all n and for all t ,

$$\text{Tr} \left[\rho_T^{(n)}(t) \right] = 1, \quad (25)$$

i.e., the reduced state of the computational target system $\rho_T^{(n)}(t)$ is in a valid quantum state. As a consequence we can keep using the identity from Eq. (9) for the probability $P[N(t) = n]$. All together, this gives us an expression for how to calculate the target system's state,

$$\rho_T^{(n)}(t) = \frac{\text{Tr} \left[(\mathbb{1}_{CRT} \otimes |n\rangle\langle n|_H) \rho(t) \right]}{P[N(t) = n]}. \quad (26)$$

The denominator is to ensure normalization from Eq. (25) by countering the trace over the clock state as in (9). The missing piece towards showing Thm. 1 is the answer to the question: *how does $\rho_T^{(n)}(t)$ evolve?* Whilst

the details can all be found in Appendix A 2 the main idea we use to address this question is to take the time-derivative of Eq. (26) and insert the equations of motion for $\rho(t)$ from (19). As the result, we find

$$\begin{aligned} \dot{\rho}_T^{(n)}(t) &= -i \left[H_T^{(a_n)}, \rho_T^{(n)}(t) \right] \\ &+ p(t) \left(\rho_T^{(n-1)}(t) - \rho_T^{(n)}(t) \right), \end{aligned} \quad (27)$$

where by definition we specifically set $\rho_T^{(-1)} \equiv 0$ for the base case, and furthermore

$$p(t) := \frac{P[T_n = t]}{P[N(t) = n]}. \quad (28)$$

This expression already shows that the state $\rho_T^{(n)}$ evolves according to the Schrödinger equation with Hamiltonian $H_T^{(a_n)}$, given that the program's n th step is a_n . The terms on the right-hand-side with the pre-factor $p(t)$ are perturbations that come from the clock's tick, i.e., there is a constant influx from the state $\rho_T^{(n-1)}(t)$ into $\rho_T^{(n)}(t)$ weighted with $p(t)$ which intuitively corresponds to the tick probability that the n th tick occurs at time t , normalized by the probability $P[N(t) = n]$ that at time t exactly n ticks have occurred. For an ideal clock, this expression becomes singular $p(t) = \delta(t - n\tau)$, where τ is the tick time of the idealized master clock. In that limit, we can already guess from Eq. (27) that $\rho_T^{(n)}(t)$ at time $t = n\tau$ becomes $\rho_T^{(n-1)}(n\tau)$ but for all $t \geq n\tau$, it then evolves exactly according to the Schrödinger equation with Hamiltonian $H_T^{(a_n)}$. Before we discuss this in even more detail we look at how the evolution generally behaves, and for this we have the following result.

Proposition 1 (Target system recursion relation). *The target system's state $\rho_T^{(n)}(t)$ at parameter time t , conditioned on n ticks having occurred takes the following form,*

$$\rho_T^{(n)}(t) = \int_0^t ds \xi(t, s) V_{(a_n)}(t - s) \rho_T^{(n-1)}(s) V_{(a_n)}(t - s)^\dagger. \quad (29)$$

The function $\xi(t, s)$ describes the probability distribution of the n th tick occurring at time s conditioned on n ticks at time $t \geq s$,

$$\xi(t, s) = p(s) \exp \left(- \int_s^t d\tau p(\tau) \right), \quad (30)$$

with $p(\tau)$ as in Eq. (28). Moreover, the unitary $V_{(a_n)}(t)$ is the propagator at time t generated by the Hamiltonian $H_T^{(a_n)}$, i.e., $V_{(a_n)}(t) = \exp \left(-i H_T^{(a_n)} t \right)$.

Proof sketch. Proving the recursion relation boils down to two steps. First, we begin by deriving the equation of motion written in (27) from the global Lindbladian $\mathcal{L}_{\text{aQPU}}$. Following this, we insert (29) into the equation

of motion and prove the recursion relation. The technical details can be found in Appendix A 2 where the key physical insight is the following; the function $\xi(t, s)$ is a probability density with respect to s capturing the probability that the n th tick happens at time $s \leq t$ under the condition that at time t , only n ticks have occurred. The state $\rho_T^{(n)}$ is thus a mixture of $\rho_T^{(n-1)}(s)$ evolved for a time $t - s$ for all possible times s when the n th tick has occurred. The result of this proposition Eq. (29) can be viewed as a generalization of the results in [22] to autonomous quantum computation with arbitrary gates concatenated arbitrarily. \square

A special case of Prop. 1 is the case $n = 0$, which describes the evolution of the target system conditioned on no ticks having occurred yet. This is the base-case of the recursion relation and there, the equations of motion (27) reduce to a standard Schrödinger equation with Hamiltonian $H_T^{(a_0)}$. Thus, we have

$$\rho_T^{(0)}(t) = \exp \left(-i H_T^{(a_0)} t \right) \rho_T^{\text{init}} \exp \left(+i H_T^{(a_0)} t \right), \quad (31)$$

from which we can now derive $\rho_T^{(n)}(t)$ for all $n \geq 1$ by using Prop. 1. An interesting feature recognizable already at this stage is that while $\rho_T^{(0)}(t)$ evolves unitarily, $\rho_T^{(1)}(t)$ evolves according to a mixed unitary channel due to the uncertainty of when the master clock produces its first tick. This trend continues as more operations are concatenated, but the details of this analysis will come in Sec. III B. For the moment, having assembled the requisite tools we will focus on the ideal case where the master clock is perfect and prove Thm. 1 stated at the outset of this section.

Proof of Thm. 1. In the limit where the master clock is ideal, both $P[T_n = t]$ and $P[N(t) = n]$ become distribution-like functions (see Eqs. (20) and (21)) and we have to take special care when applying Prop. 1. A mathematically rigorous treatment of these details can be found in Appendix A 2, where the key insight is that the conditional tick probability density $\xi(t, s)$ in Eq. (29) takes the form of $\delta(s - n\tau)\Theta(t > n\tau)$. The integral (29) then simplifies for $\rho_T^{(n)}(t)$ and $t > n\tau$ to

$$\rho_T^{(n)}(t) = V_{(a_n)}(t - n\tau) \rho_T^{(n-1)}(n\tau) V_{(a_n)}(t - n\tau)^\dagger. \quad (32)$$

We can evaluate this expression for $t = (n + 1)\tau$ to find the equation needed for the next term in the recursion,

$$\rho_T^{(n)}((n + 1)\tau) = V_T^{(a_n)} \rho_T^{(n-1)}(n\tau) V_T^{(a_n)\dagger}, \quad (33)$$

where $V_T^{(a_n)}$ is defined as in (2). Looking at the evolution for $t \geq M\tau$, where M is the maximum number of steps in the program \mathcal{A} , we find that $\rho_T^{(M)}(t)$ is given by the concatenation of all the unitaries $V_T^{(a_0)}, V_T^{(a_1)}, \dots, V_T^{(a_{M-1})}$ applied to the initial state ρ_T^{init} . In mathematical terms, we get

$$\rho_T^{(M)}(t) = V_{\mathcal{A}} \rho_T^{\text{init}} V_{\mathcal{A}}^\dagger, \quad (34)$$

for $t \geq M\tau$. Since for the idealized master clock, the trace $\text{Tr}_{CHR}[\rho(t)]$ will simply yield $\rho_T^{(M)}(t)$ if $t \geq M\tau$ this proves Eq. (22). We conclude that an aQPU with access to a finite set of Hamiltonians that generate a universal gate set and an ideal clock can generate any unitary on the target system \mathcal{H}_T . \square

B. Error propagation for non-ideal clocks

After proving in the previous section that for perfect clocks, the aQPU enables universal quantum computation, we now investigate what happens when the clock's performance deviates from the ideal one. In the idealized case that we have considered, the master clock ticks in intervals of time τ , however, in the non-ideal case, the tick times may be some randomly distributed times t_1, t_2, \dots that are close to $\tau, 2\tau, \dots$ with high probability, but generally not equal (see Fig. 4 for an illustration). In this section, we develop the formal tools necessary for quantifying how a non-ideal distribution of the master clock's ticks affects the fidelity of the computation. To take on this endeavor, we proceed as follows:

- We start by understanding the structure of how the aQPU's master clock times the operations on the target system (see Fig. 4).
- We continue to introduce the necessary notions which allow us to quantify clock performance (Defs. 3 and 4).
- Finally, we connect the notion of clock performance to that of computational fidelity (Prop. 2 and Cor. 1) to show how close imperfect clocks can approximate universal computation.

In our model for autonomous quantum computation, we can use Prop. 1 to separate the clock dynamics and the dynamics of the computational target system. What matters for the controlled operations on the target system is the time between ticks, which we can label as

$$T_{n,n-1} = T_n - T_{n-1}, \quad (35)$$

for the time between the $(n-1)$ st and the n th tick. For a given program \mathcal{A} that is encoded in the instruction register (see Def. 2), the n th Hamiltonian $H_T^{(a_n)}$ is applied for the time $T_{n,n-1}$, which is stochastically distributed. The computation as a whole is given by the tick times $T_{0,1}, T_{1,2}, \dots, T_{N(t)-1, N(t)}$, where $N(t)$ is the number of ticks that the master clock has generated at time t , which is also a probabilistic quantity. As we derive in rigorous detail in Appendix A 3, we can use this argument to write the state $\rho_T(t)$ as an average over all tick times. We summarize a specific sequence of n ticks in a trajectory $\Gamma_n = (\tau_1, \dots, \tau_n)$ where the master clock will have first ticked at $t_1 = \tau_1$ followed by the second tick at $t_2 = \tau_1 + \tau_2$ and so on. Each such trajectory Γ_n

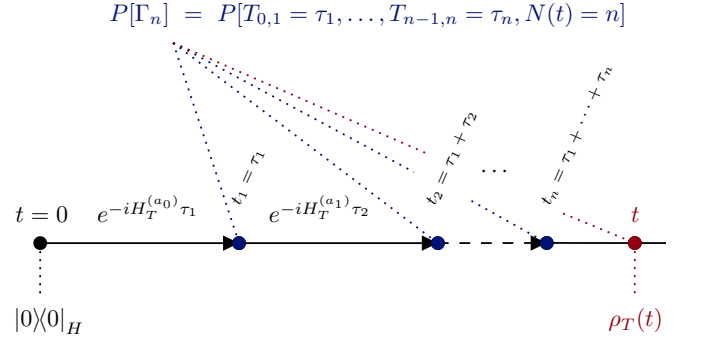


FIG. 4. The evolution of the target system in the aQPU is an average over all possible tick times T_1, \dots, T_n of the master clock. In the above figure we illustrate the evolution of the target system according to the first Hamiltonian $H_T^{(a_1)}$ for some time t_1 given by the first tick of the master clock. The second Hamiltonian $H_T^{(a_2)}$ is applied for some time $t_2 - t_1$, where t_2 is the time at which the master clock ticks the second time. This scheme continues until the time t at which the target system's state $\rho_T(t)$ is considered; said state is given by an average over all the possible times at which the master clock could have ticked, formally given by Eq. (36).

has a probability density $P[\Gamma_n]$ given by the joint probability distribution of all tick times $T_{0,1}, \dots, T_{n-1,n}$ and $N(t) = n$, the probability that number of ticks at time t is given by n . Formally, this results in

$$\rho_T(t) = \sum_{n=0}^M \int d\tau_1 \cdots d\tau_n p[\Gamma_n] \rho(t|\Gamma_n), \quad (36)$$

where one sums over the probabilities that n ticks have occurred in a given trajectory and integrates over the set of possible trajectories with $\rho_T(t|\Gamma_n)$ the unitary evolution of the target system for the tick times in the trajectory Γ_n . As visualized in Fig. 4, this state is given by the target system's initial state $|0\rangle|0\rangle_T$ evolved for duration $\tau_1 = t_1$ according to the first Hamiltonian $H_T^{(a_0)}$ from the program \mathcal{A} . Then, from time t_1 to time t_2 the second Hamiltonian, $H_T^{(a_1)}$, acts on the target system for time $\tau_2 = t_2 - t_1$ and so on until the n th Hamiltonian with index a_n that acts from t_n to time t . A more detailed investigation of properties of this state is given in Appendix A 3. This concludes how we can relate the target system's state $\rho_T(t)$ to the probabilistic distribution of the ticks in a general sense, and in the coming paragraph, we clarify how we can quantify the quality of the clocks that generate these probabilistic tick distributions.

Clock performance. Clock performance can be studied in many ways each of them depending on the particular needs of the application. For our purposes, we are interested in how well the aQPU's master clock can approximate multiples of the duration τ ; to this end, clock resolution and clock accuracy, which have been established well in the field of quantum clocks [20, 31, 44, 48, 49], can be used as a figure of merit for the aQPU. The clock resolution captures how small the time-intervals which a

clock can distinguish are. On a general level, there is no reason why this would have to be the same for each of the clock's ticks, and we can therefore define the clock's resolution for the n th tick as follows:

Definition 3 (Clock resolution). *Given a clock as defined in Eq. (6) with corresponding tick probabilities $P[T_n = t]$. We define the resolution of the n th tick as the following expectation value*

$$\nu_n := \frac{1}{\langle T_{n,n-1} \rangle}, \quad (37)$$

where $T_{n,n-1}$ is the time between $(n-1)$ st and n th tick, as defined in Eq. (35).

Here $\langle \cdot \rangle$ denotes the first moment or expectation value of a random variable and is used in this context as $T_{n,n-1}$ can be different for different runs of a clock. On the other hand, the clock accuracy is a notion of how well clock ticks can be used to estimate the time parameter t of the Hamiltonian evolution.

Definition 4 (Clock accuracy). *The accuracy of the n th tick of a clock as in Eq. (6) is defined as the signal-to-noise ratio given by*

$$N_n := \frac{\langle T_{n,n-1} \rangle^2}{\text{Var}[T_{n,n-1}]}, \quad (38)$$

where $T_{n,n-1}$ is again defined as in Eq. (35).

Going from the ensemble of all ticks that the aQPU generates throughout the evolution to the distribution of the time between two adjacent ticks is convenient for analyzing the interplay between the master clock and the target system. However, in the general case, it is possible that there are correlations between the tick times, e.g., the clock is ticking too fast or too slowly and in such general circumstance only considering the clock accuracy and clock resolution does not capture these correlated errors. These correlated tick errors are coherent errors and can in certain cases be addressed using optimal control and error mitigation strategies [47]. Beyond this, in the limit of ideal clocks as considered in the main Thm. 1, correlated errors would vanish and so it suffices in this work to focus on how varying clock accuracy and resolution for the master clock impacts the performance of the aQPU. A more detailed treatment of correlated ticks can be found in the discussion in Sec. IV A. One particular class of clocks which is therefore of interest to us is that of so-called *reset clocks* [44, 45]. These are examples of clocks whose ticks are independent and identically (i.i.d.) distributed, and hence, there is one random variable that we can label T which describes the time between two adjacent ticks. In this case, the time $T_{n,n-1}$ between the $(n-1)$ st and n th tick, see Eq. (35), is an i.i.d. copy of T and therefore its probability distribution $P[T_{n,n-1} = t]$ is independent of the tick number n and equal to $P[T = t]$. Accuracy and resolution in this special case simplify to

$$\nu = \frac{1}{\langle T \rangle}, \text{ as well as } N = \frac{\langle T \rangle^2}{\text{Var}[T]}, \quad (39)$$

and we can interpret the accuracy N as the average number of times the clock ticks until it goes off by one tick. In this setting of the perfect clock in Thm. 1 can be realized in the limiting case, where $\nu = 1/\tau$ is fixed and the clock accuracy $N \rightarrow \infty$ diverges. In what follows, we will look at finite values for N , but in the limit where N is large. How large precisely and how this impacts the aQPU, we will clarify below.

Clock accuracy vs. computational fidelity. There are two numbers that the clock accuracy N would compete against. Firstly, the (maximum) number of operations of our algorithm M ; we would expect that the clock accuracy must be greater than that number because the clock goes off by one tick on average after N ticks. This leads us to the first requirement that $N \gg M$. Secondly, for each operation, the Hamiltonian $H_T^{(k)}$ is applied for some random time T to the target system. On average this leads to some maximum angle of rotation $\phi^{(k)} = \tau \|H_T^{(k)}\|_\infty$ in the Hilbert space \mathcal{H}_T if the Hamiltonian $H_T^{(k)}$ is applied, where $\|\cdot\|_\infty$ is the Schatten ∞ -norm or operator norm. In this context, the clock accuracy then serves as a notion for how much the rotation in the Hilbert space over- or undershoots the target value on average relative to the total angle of the desired rotation. For a high fidelity computation, we would of course want that this relative over-/undershoot is small. If we demand this not only for a single operation, but for all possible combined operations, we end up with the following condition,

$$\frac{M}{N} \underbrace{\left(\tau \max_k \|H_T^{(k)}\|_\infty \right)^2}_{=:\phi_{\max}^2} \ll 1 \quad (40)$$

where the shorthand ϕ_{\max} has been introduced to denote the maximum angle in the computational state space that the aQPU can generate. If we assume the most general case for how the time T between two ticks can be distributed, under the constraint that the resolution equals $1/\tau$ and the clock accuracy N satisfies Eq. (40) and is much greater than M , some pathological behavior of the clock can still occur. This arises as a result of the fact that under these constraints the higher moments of the probability distribution of T can in principle still take on arbitrary values. In Appendix A 3 we examine the conditions required for the master clock to behave as desired, under the assumption that the tick generation process is exponential decay. In this setting, the higher moments of the tick probability density are bounded due to a probability concentration argument [50, 51]. We can look then at a family of clocks with unbounded accuracy N and fixed resolution $\nu = 1/\tau$. We call the ticks of the master clock *exponentially concentrated*, if there exist constants $\alpha, c > 0$, such that

$$P[|T - \tau| \leq t] \leq \alpha \exp\left(-c\sqrt{N}t\right), \quad (41)$$

for all $t > 0$. This exponential envelope for the tick probability ensures that the dominant contribution to the probability density comes from times closely around τ . Our

goal is to calculate the final state of the computation $\rho_T(t)$ as given in Eq. (36) for a time t large enough such that all operations of the aQPU have been carried out with high probability. As we have assumed i.i.d. ticks for this analysis, the joint distribution of the times $T_{n-1,n}$ between adjacent ticks can be factorized,

$$P[T_{0,1} = \tau_1, \dots, T_{n-1,n} = \tau_n] = \prod_{k=1}^n P[T = \tau_k]. \quad (42)$$

It is therefore tempting to also factorize the expression in Eq. (36), whose integrand is a product with $P[\Gamma_n]$, the probability of a given trajectory with tick durations $\tau_1, \tau_2, \dots, \tau_n$ and $N(t) = n$. The latter condition, i.e., the one that fixes the number of ticks $N(t)$ at time t , breaks the independence of the tick times. At the end of the computation we want that all M ticks have occurred, which is equivalent to the constraint $T_M < t$. Using the concentration inequality (41), we can relax the condition $T_M < t$ up to a small error that vanishes for $t \gg M\tau$ and factorize the integral expression for $\rho_T(t)$ that is given in Eq. (36). We find a recursive expression for $\rho_T(t)$ akin to the one from Prop. 1,

$$\rho_T^{(k)} = \int dt P[T = t] V_{(a_k)}(t) \rho_T^{(k-1)} V_{(a_k)}^\dagger(t), \quad (43)$$

for the special case of i.i.d. ticks and with $\rho_T^{(0)} = \rho_T^{\text{init}}$. The final state $\rho_T(t)$ can be found using the recursion relation up to a small error that vanishes for $t \gg M\tau$,

$$\rho_T(t) = \rho_T^{(M)} + O\left(\exp\left(-cM\sqrt{N}t/2\tau\right)\right). \quad (44)$$

We provide the detailed derivation for this expression in Appendix A 3. To calculate the individual steps of the recursion from (43), we can use the concentration inequality (41) once more. As a result, we find Prop. 2 which captures quantitatively how well a highly accurate clock can control the unitary evolution of the target system in the aQPU.

Proposition 2 (Clock channel). *The i.i.d. recursion relation in Eq. (43) for the case of exponentially concentrated tick time T in the high accuracy limit N can be approximated as*

$$\int dt P[t] V_{(k)}(t) \rho V_{(k)}^\dagger(t) = V_T^{(k)} \rho V_T^{(k)\dagger} + O\left(\frac{\tau^2 \|H_T^{(k)}\|^2}{N}\right). \quad (45)$$

We abbreviate the probability distribution for a single tick with $P[t] = P[T = t]$, and $V_T^{(k)}$ is the Hamiltonian $H_T^{(k)}$ evolved for exactly the desired duration τ as in (2).

Proof sketch. We begin by taking a Taylor expansion of the integrand $V_{(k)}(t) \rho V_{(k)}^\dagger(t)$ around the average τ of $P[t]$. From the zero-th order contribution, we get $V_T^{(k)} \rho V_T^{(k)\dagger}$, but for all higher order contributions it is not

straightforward that the error they give is small. These corrections depend on the higher moments of the distribution $P[t]$ which we can bound using the concentration inequality (41) to leading order in the inverse accuracy $1/N$. The full proof requires a probability theory detour which we provide in detail in Appendix A 3. \square

Considering the recursion relation, we can readily see how the errors of each time step accumulate during the execution of the program by the aQPU. Let us assume that we are still in the limit where the clock accuracy N is high in the sense that $N \gg M, M\phi_{\text{max}}^2$. Here, M is the maximum number of steps that the program \mathcal{A} can have. Furthermore, we make the conventional assumption that the quantum computer starts in a well-defined initial state $|0\rangle_T$ and the desired target state is denoted by $|\Psi(\mathcal{A})\rangle_T = V_{\mathcal{A}}|0\rangle_T$. We can then calculate the fidelity of the desired state $V_{\mathcal{A}}|0\rangle_T$ with the actual state $\rho_T(t)$ of the target system long enough after the expected time it takes for the program \mathcal{A} to finish. This measures how well the aQPU executes the program. For concreteness, we can chose $t = 2M\tau$, and define

$$\mathcal{F}_{\mathcal{A}} := \langle \Psi(\mathcal{A}) | \rho_T(2M\tau) | \Psi(\mathcal{A}) \rangle. \quad (46)$$

Note that the state $\rho_T(t)$ does not vary strongly with t for values $t \geq 2M\tau$ because by construction, the $(M+1)$ st instruction is idle (see eq. (16)). The only corrections to this are of order $O(\phi_{\text{max}}^2/N)$ coming from the imperfection of the clock, because the clock does not tick perfectly at integer multiples of τ . By concatenating the result from Prop. 2 for all the instructions $0 \leq n < M$ as proposed in Eq. (44) we find that

$$\rho_T(t) = |\Psi(\mathcal{A})\rangle\langle\Psi(\mathcal{A})| + O\left(\frac{M}{N}\phi_{\text{max}}^2\right). \quad (47)$$

Thus, the deviations from the desired state for non-ideal clocks depend inverse linearly on the clock accuracy N , with prefactor depending on the number of steps in the program and the maximum angle of rotation that any of the elementary gates of the aQPU can cover. We can rephrase this as a statement about the fidelity $\mathcal{F}_{\mathcal{A}}$ in Cor. 1 below:

Corollary 1 (Program fidelity for non-ideal clocks). *For an aQPU with master clock producing exponentially concentrated i.i.d. ticks at accuracy $N \gg M, M\phi_{\text{max}}^2$, the final program fidelity $\mathcal{F}_{\mathcal{A}}$ for any program \mathcal{A} of length less or equals M is given by*

$$\mathcal{F}_{\mathcal{A}} = 1 - O\left(\frac{M}{N}\phi_{\text{max}}^2\right). \quad (48)$$

Proof. The fidelity $\mathcal{F}_{\mathcal{A}}$ is (by definition) bounded by 1, thus the correction has a negative prefactor. Using the result from (47) together with the definition (46) immediately yields this result. A detailed derivation can be found in Appendix A 3. \square

Notable in this context is our recovery and generalization of the results presented in [22] where we see that the fidelity of the computation executed on the aQPU is impacted by the length of the program and the angle traversed in computational state space. This is intuitive in the sense that the longer the computation the greater the opportunity for the physical error stemming from imperfect timekeeping to grow. Additionally, we confirm our intuition that a better master clock accuracy N results in a higher fidelity of the computation.

C. Thermodynamic cost of computation

Yet, one of the key insights needed to arrive at this model is that circuit-based quantum computation fundamentally relies on clocks for the timing of the computation. The reason behind this being that the process of computation has a well-defined directionality in time, i.e., we want the computer to carry out the instruction step $n + 1$ after step n and so on. Ideally, each of these operations is perfectly timed. The second law of thermodynamics puts an entropic price-tag on dynamics which are biased in one direction of the flow of the parameter time t [52] and hence it is not only natural but also essential to wonder what is the thermodynamic cost of time-keeping. In the field of clocks it is well-established that timekeeping is a deeply thermodynamic process [20, 53] where high clock accuracy comes at a thermodynamic cost and where the unidirectional increase of the clock's tick counter is linked to the entropy production caused by the clock. This source of entropy production dominates during the computation, still there are potential additional contributions during initialization and in the final readout that.

Here, to summarize the possible sources for entropy production for the aQPU, there are three steps that we have to look at: (1) the preparation of the aQPU's initial state, (2) entropy production during the evolution of the aQPU, and (3) measurement or other appropriate readout of the final state. In principle all of these tasks require interactions of the aQPU with some outside environment or control system and therefore, these tasks can produce entropy. We will start with investigating point (2); the entropy production during the aQPU's evolution, and how this is relevant for the computational fidelity. The evolution of the aQPU constitutes three processes: the evolution of the clockwork, the stochastic ticking and the clock-instruction-computer interaction, as one can identify from Eq. (18). Hermitian evolution generators like the clock-instruction-computer interaction do not come at a fundamental thermodynamic cost because they are time-independent and energy-conserving. The open system's component in the clockwork and the tick generation on the other hand are responsible for the unidirectional evolution of the aQPU and therefore, are expected to produce entropy. Examining this entropy production we begin with the clockwork which formally, corresponds to

the contribution from \mathcal{L}_C (see Eq. (7)) in $\mathcal{L}_{\text{aQPU}}$. The entropy-production in the regime that we consider in the main text, i.e., where there is no conjugate tick generation operator $J_{\text{untick}} \propto J_{\text{tick}}^\dagger$, is not well-defined. Including the entropy production of the conjugate ticking process requires that we allow for a non-zero probability of operation $n - 1$ being carried out after operation n . While this does not change anything fundamentally, the mathematics required to deal with this introduce additional challenges which we address in Appendix C.

Applicability of the master equation. The clockwork's evolution is generated by the Lindblad super-operator \mathcal{L}_C , which can be brought into the form

$$\mathcal{L}_C = -i[H_C, \cdot] + \sum_{\ell} \left(L_{\ell} \cdot L_{\ell}^{\dagger} - \frac{1}{2} \{ L_{\ell}^{\dagger} L_{\ell}, \cdot \} \right), \quad (49)$$

with H_C representing the coherent part of the clockwork evolution and the sum with the operators L_{ℓ} the incoherent part of the evolution. This second part is generally necessary to drive the clock, e.g., if the clock's ticks dissipate energy, this energy has to be replenished, and the operators L_{ℓ} can in principle do this, contrarily to H_C which (by definition) acts on the system in an energy-preserving way. The applicability of the master equation description as used here may not be directly apparent but we require such a master equation as it will prove useful in quantifying the thermodynamic cost of the aQPU. To clarify this, we provide a brief discussion on this matter. The master equation description which uses a Lindblad operator to generate the system's evolution is merely an effective description of the system (here: the aQPU) ignoring the degrees of freedom of a bath or environment. Microscopically, the system interacts with some environment and only under specific assumptions is it possible to derive an effective description of the system with a master equation, where the detailed environment behavior can be ignored, and where the description used is a faithful approximation of the true dynamics of the system. A rich variety of literature has been written about this topic, of which some choices are [26–28]. Our approach for the aQPU is to consider the class of systems describable using a master equation, where all the operators of the Lindbladian can in principle be derived microscopically. From a physical point of view, this is in particular true for the clockwork, for which a master equation description has been shown to be derivable from microscopic dynamics in several instances [20, 31].

Entropy production. The entropy production we define here follows from a set of assumptions, which clarify how energy-changes in the system relate to heat dissipation and work. One of these assumptions is that the system-bath interactions are energy-preserving, in that case the entropy production can be identified unambiguously in the separation of Spohn [29, 54]. Furthermore, the jump operators L_{ℓ} must satisfy a property called *local detailed balance* [29, 55, 56]. This means that for every operator L_{ℓ} there exists conjugate operator \bar{L}_{ℓ} , which is

proportional to L_ℓ^\dagger , with the constant of proportionality related to the entropy production $\Delta\sigma_\ell$ per unit population that undergoes the jump L_ℓ . In the regime of local detailed balance jump operators always come in pairs, which we can denote (L_ℓ, \bar{L}_ℓ) and that are related via

$$\bar{L}_\ell = e^{-\Delta\sigma/2} L_\ell^\dagger. \quad (50)$$

On this level of specificity the entropy production can be related to the thermodynamic entropy $\Delta\sigma = \beta\Delta q$ given by the product of the inverse temperature of the bath β generating the transition and heat exchange Δq in the jump process [26–28]. With local detailed balance, we are in a position to quantify how much entropy the clockwork of the aQPU produces. Each unit population undergoing the jump L_ℓ produces $\Delta\sigma_\ell$ entropy, and each reverse jump \bar{L}_ℓ produces $-\Delta\sigma_\ell$ entropy. When working with the master equation evolution we have an ensemble average, which allows us to calculate an average entropy production rate of the clockwork by weighting the probability currents that jump through L_ℓ and \bar{L}_ℓ , such that [29, 54]

$$\langle \dot{\Sigma}_{\text{cw}}(t) \rangle = \sum_\ell \Delta\sigma_\ell \text{Tr} \left[\left(L_\ell^\dagger L_\ell - \bar{L}_\ell^\dagger \bar{L}_\ell \right) \rho_C(t) \right]. \quad (51)$$

Based on this expression the total average entropy production at time T can be calculated using

$$\langle \Sigma_{\text{cw}}(T) \rangle = \int_0^T dt \langle \dot{\Sigma}_{\text{cw}}(t) \rangle. \quad (52)$$

In this case the total entropy production can be resolved into contributions coming from each of the ticks separately. This becomes particularly useful in the case that the entropy per tick, denoted by $\Sigma_{\text{cw},\tau}$, is the same for all ticks and also independent of how long the tick time actually was in each stochastic realization of a clock cycle. We can then derive the integrated entropy production of the clockwork using the identity

$$\langle \Sigma_{\text{cw}}(T) \rangle = \langle N(T) \rangle \Sigma_{\text{cw},\tau}, \quad (53)$$

where $\langle N(T) \rangle$ is the expected number of ticks at time T . If T is chosen to be large enough as in the setting of Cor. 1, for example $T = 2M\tau$, the expected number of ticks at time T would saturate close to M .

Fidelity vs. entropy trade-off – an example. Accurate timekeeping comes at a thermodynamic cost as has been explored in various works [20, 31, 53, 57]. The thermodynamic cost of timekeeping manifests as an inequality of the form

$$N \leq f(\Sigma_{\text{cw},\tau}), \quad (54)$$

for some function f and where N is the clock accuracy as in Eq. (39). An universal form of f for general open quantum systems is not known, but for example in [20] it is found that $f(x) = \frac{x}{2}$ for that specific example or the function $f(x)$ is quadratic as in [31]. Using the fidelity trade-off in Cor. 1 we can obtain a program-fidelity

vs. entropy production trade-off implicitly through the bound Eq. (54) and thus find

$$\mathcal{F}_A \leq 1 - O\left(\frac{M}{f(\Sigma_{\text{cw},\tau})} \phi_{\text{max}}^2\right). \quad (55)$$

The considerations so far have primarily been concerned with the entropy produced in the thermodynamic environments that drive the aQPU. We discuss in the following the implications due to step (1), the initialization, and afterwards step (3), the readout.

Thermodynamic cost of initialization. We continue with the question about what thermodynamic resources one has to invest to generate the aQPU's initial state. The initial state comprises the clockwork, the tick and instruction register and the target system. Modeling the clockwork as an autonomous thermal machine as we have, its state initially does not require any particular preparation since it will tend toward a steady-state. For its tick register, however, it is imperative that it is initially prepared in the $|0\rangle_H$ state. Similarly, the punch card state in the instruction register should encode a program $|\mathcal{A}\rangle_R$ and the target system should be in the initial state of the computation, conventionally labelled as $|0\rangle_T$. Ideally all three systems are initially in a pure state, however if we work in the paradigm where we only have access to thermal resources (e.g., mixed states obtained by thermalizing with macroscopic baths), preparation of a perfectly pure state is impossible with finite resources [58]. We would therefore also expect that if we prepare the aQPU with finite resources, we can only approximate the initial states $|0\rangle_H \otimes |\mathcal{A}\rangle_R \otimes |0\rangle_T$ to finite accuracy and therefore, the program fidelity \mathcal{F}_A would obtain an additional error term. If we work in the paradigm that initially, we only have access to thermal states at inverse temperature $\beta > 0$ then we can investigate the cost of using these resources we have access to freely to improve some subset of them. One way to do this would be to use the pure-state-preparation protocol from [59], which has been used [16, 60] to derive a relationship between entropy production Σ_{init} for state-preparation and the fidelity of the preparation. Let us define the fidelity of the initial state preparation as $\varepsilon > 0$ by

$$\varepsilon := 1 - \langle 0_H, \mathcal{A}_R, 0_T | \tau[\beta]_{HRT} | 0_H, \mathcal{A}_R, 0_T \rangle, \quad (56)$$

where $\tau[\beta]_{HRT}$ is the initial thermal state of tick register (H), instruction register (R) and target system (T). If we assume an preparation protocol in L steps, then we can relate the entropy production Σ_{init} in the thermal baths used for the preparation to ε and L by using results from [16, 60],

$$\varepsilon \geq \frac{1}{\Sigma_{\text{init}}} \exp(-L\Sigma_{\text{init}} + 2W), \quad (57)$$

where W is a measure for the number of qubit equivalents for the registers and target systems HRT that we prepare, and is given by $W = \log(d-1)$, with d being the Hilbert space dimension of HRT . Going back to the

fidelity \mathcal{F}_A , the error ε from the initialization will simply carry over to the final state and provide an upper bound. Thus, we can modify the relationship in Eq. (55) to give

$$\mathcal{F}_A \leq 1 - O\left(\frac{M}{f(\Sigma_{\text{cw},\tau})}\phi_{\text{max}}^2\right) - \frac{e^{-L\Sigma_{\text{init}}+2W}}{\Sigma_{\text{init}}}. \quad (58)$$

This expression gives us a relationship between the fidelity with which we would like the aQPU to execute a program, the complexity of the program captured by $M\phi_{\text{max}}^2$ and the thermodynamic resources in timekeeping $\Sigma_{\text{cw},\tau}$, entropy production Σ_{init} used to purify the initial state of dimension W . Such an expression edifies the fact that accurate quantum computation comes at a cost, which is greater for more *complex* computations. Having detailed the relationship between the thermodynamic cost of preparation (1) and computation (2), we move toward the third and final step, (3) the readout, which we will qualitatively discuss in the coming paragraph.

Thermodynamic cost of readout. Finally, we arrive at step (3), the readout of the final state of the computation. One contribution here comes from the fact that the computation is not performed perfectly, i.e., if we were to start in an initially pure state $|0\rangle_T$, the state $\rho_T(t)$ at the end of the computation would be mixed due to the imperfect timing of the master clock. The main reason comes from the transformation discussed in Prop. 2, which is always entropy increasing. But by the result in Cor. 1 the deviations from the pure state can be bounded by $O\left(\frac{M}{N}\phi_{\text{max}}^2\right)$ which vanishes in the limit for a highly accurate clock. Aside from this, the process of a measurement is known to have divergent resource costs if the measurement is to be perfect [61] and modeled unitarily within the von Neumann measurement scheme. This is due to the *measurement probe* needing to be pure resulting in a situation similar to the case of state-initialization discussed in the previous paragraph. The detailed thermodynamic analysis of this step is not unique to this work and we therefore leave it for future research to investigate.

D. Speed of computation and fidelity

The time-energy uncertainty relation introduced by Mandelstam and Tamm [62] was shown by Margolus and Levitin [63] to bound the rate at which a quantum state can evolve and traverse its state space. This led to the development of the field of *Quantum Speed Limits* [64]. These relations have also been used to bound the speed at which quantum logic gates can be executed and therefore the speed of quantum computation [65, 66]. This however requires imposing a constraint on the energy expectation value of the computational system as well as on the fluctuations thereof. Whilst the same argument can be made to bound the speed of each step in the aQPU's execution of a program, quantum speed limits do not give any operational limitations, for several reasons. First, speed lim-

its do not restrict the speed of quantum operations based on any thermodynamic or physical constraints but only on the geometry of the state space. Second, the speed limits do not take into account the cost of the control required to generate the operation they constrain, e.g., the spectrum of the Hamiltonian generating the operation or the quality of the timekeeping controlling the operation. Third, it has been shown that the speed limits do not impose any fundamental restriction on the speed of computation motivating some to propose arbitrarily fast quantum computation [11]. For these reasons, the question of how the speed of a quantum computation is limited has to be approached from a new and physically grounded angle. We present our attempt at answering this question with our aQPU framework here. With this model, we have a self-contained thermodynamic description for the quantum computer including the master clock, and thus we are in the position to reveal relationships between computational speed, fidelity and resources invested into the computation. The two aspects we consider are the following:

- In the first paragraph, we investigate the speed of executing an arbitrary unitary on the aQPU given access to a finite set of Hamiltonians. Here the notion of speed is captured by the length of the program required to approximate the desired operation. This approximation is known as *compiling* and is known to be possible due to the Solovay-Kitaev theorem [40, 42]. Here we show that one's ability to compile on the aQPU is limited by the thermodynamic resources they have access to, i.e., while longer approximations are more accurate they are more susceptible to physical error on the aQPU. Meaning one might wish to run a shorter, faster and less accurate program on the aQPU to avoid the accumulation of physical error.
- Secondly, we consider a fixed program \mathcal{A} for the aQPU and we investigate the relationship between the clock speed which determines the duration of the entire computation and the computational fidelity. We find a trade-off between clock speed and computational fidelity, showing that slower computation can in principle allow for higher fidelity.

Optimal gate compilation. Since the aQPU is only able to carry out a finite number of Hamiltonians and so generate a finite number of unitaries, these finite number of unitaries must at times be executed as products to approximate a unitary which is outside of the gate set. In other words, a program expressed in an arbitrary gate set must be *compiled* so that it may be executed on the aQPU using the gate set it has access to. The Solovay-Kitaev Theorem [40, 42] states that with access to a universal gate set \mathcal{V} for $SU(2)$, i.e., a set of gates closed under inversion that generate a dense subgroup of $SU(2)$ we can approximate any unitary $U \in SU(2)$ in the following sense: for arbitrarily small $\varepsilon > 0$, the unitary U can be approximated using a product of L gates

$V_i \in \mathcal{V}$. Formally, we can write $V = V_L V_{L-1} \dots V_1$, and the distance of V to the desired unitary U is bounded by

$$\|U - V\|_\infty \leq \varepsilon \quad (59)$$

where $L = O(\log^c(1/\varepsilon))$ for some constant $c > 0$. This means that for a given unitary U , an approximation of a suitable accuracy ε can be found at the cost of increasing the length of the approximation L . This in turn also implies that the time of the compilation scales as $L\tau$ if we reduce the error ε of the approximation, where τ is the average duration required by the aQPU to carry out a single gate. Because the aQPU is a thermodynamic machine that only executes programs perfectly with access to diverging resources to power perfect clocks and run perfectly pure punch card states, we would expect that arbitrarily increasing the length L can not indefinitely increase the quality of the gate compilation. On the contrary, as we have seen in Sec. III B, longer programs are more susceptible to error from finite resources such as imperfect timekeeping which seems to be at odds with the Solovay-Kitaev Theorem which requires longer approximations for higher accuracy. This motivates us to ask *what are the resources required for the aQPU to execute the shortest program with the highest accuracy?* In other words, what is the cost of a program being run on the aQPU at a given speed and accuracy?

Corollary 2 (Compiling with finite resources). *An aQPU featuring a master clock generating exponentially concentrated i.i.d. ticks in the limit of high accuracy $N \gg 1$ and access to a finite set of Hamiltonians which generate a universal gate set \mathcal{V} for $SU(2)$, can approximate any $U \in SU(2)$ using a program $\mathcal{A} = (a_0, \dots, a_{L-1})$ of L unitaries $V_{\mathcal{A}} = V_T^{(a_{L-1})} \dots V_T^{(a_0)}$ with error*

$$\|U |0\rangle\langle 0|_T U^\dagger - \rho_T^{\mathcal{A}}\|_1 \leq O\left(e^{-\alpha L^{1/c}}\right) + O\left(\frac{L}{N} \phi_{\max}^2\right) \quad (60)$$

where α and c are constants. The state $\rho_T^{\mathcal{A}}$ is the target system's state for the aQPU with program \mathcal{A} evaluated at time $t \gg L\tau$.

Proof sketch. Using the triangle inequality, we can relate the distance between $U |0\rangle\langle 0|_T U^\dagger$ and $\rho_T^{\mathcal{A}}$ to the distance coming from the Solovay-Kitaev Theorem,

$$\|U - V_{\mathcal{A}}\|_\infty \leq \varepsilon, \quad (61)$$

between the desired unitary U and the programmed unitary $V_{\mathcal{A}}$, and so a distance

$$\|V_{\mathcal{A}} |0\rangle\langle 0|_T V_{\mathcal{A}}^\dagger - \rho_T^{\mathcal{A}}\|_1 = O\left(\frac{L}{N} \phi_{\max}^2\right), \quad (62)$$

between the target state and the actual output from the computation executed on the aQPU, which will be the result of a channel that is close to the unitary channel of $V_{\mathcal{A}}$ but for a finitely accurate clock, in general not

equal to the unitary channel of $V_{\mathcal{A}}$. Adding up these two error terms together by relating the different norms and distances, we find the desired result (60). More details can be found in Appendix A 4. \square

Whilst the current result captures the impact on any compiled computation on qubits this result can be extended to any unitary in $SU(D)$ with minor alterations using generalizations of the Solovay-Kitaev theorem which can be found in [42] and are out of scope for this work.

Clock speed vs. fidelity trade-off. Let us now consider a fixed program \mathcal{A} to be executed on the aQPU that is encoded by a unitary $V_{\mathcal{A}}$ and examine how it is impacted by being executed at different clock speeds at different clock accuracies. Using the results from Sec. III B, in particular Cor. 1, we know that the aQPU with clock in the high but finite accuracy regime can approximate $V_{\mathcal{A}}$ only up to an error that scales inverse linear in the clock accuracy N .

One naive trick we could play to improve the clock's accuracy whilst ticking at the same rate is the following: we change the clock dynamics, such that only every second tick of the clock, the instruction performed is switched, and each of the generating Hamiltonians from the instruction set is re-scaled by a factor of $1/2$, to compensate for the increase in time between when the instructions are switched. For i.i.d. ticks, this increases the clock accuracy by a factor of 2 at the cost of being twice as slow. More generally, if we switch instructions only every m th tick, we transform

$$\tau \mapsto m\tau, \quad H_T^{(k)} \mapsto \frac{H_T^{(k)}}{m}, \quad N \mapsto mN. \quad (63)$$

The increase in accuracy comes from the fact that summing m i.i.d. random variables increases the average as $\tau \mapsto m\tau$ but the standard deviation only as $\sigma \mapsto \sqrt{m}\sigma$. Since the accuracy N is the ratio $\langle T \rangle^2 / \text{Var}[T]$, we find that $N \mapsto mN$. We find that with the increase in accuracy, the program fidelity $\mathcal{F}_{\mathcal{A}}$ also increases,

$$\mathcal{F}_{\mathcal{A}} = 1 - O\left(\frac{M}{mN} \phi_{\max}^2\right). \quad (64)$$

On the other hand, however, the computational time also increases by a factor of m , due to the increase of the average time between two instructions from τ to $m\tau$. So-far, this has been a specific example for how modifying the clock-instruction interactions leads to a trade-off between fidelity and speed of computation, and next we want to look at a more general case.

If we look at all possible clocks whose tick generating operators $J_C^{(n)}$ have a decay rate bounded by $\Gamma > 0$,

$$\max_{\rho} \text{Tr} \left\{ J_C^{(n)\dagger} J_C^{(n)} \rho \right\} \leq \Gamma, \quad \forall n \geq 0, \quad (65)$$

then, it has been shown in [21] that such a clock's accuracy N and tick frequency (resolution) ν must obey

the trade-off relation $N \leq \Gamma^2/\nu^2$. The clock's frequency $\nu = 1/\tau$ defines the speed of computation and therefore increasing the clock accuracy under the constraint (65) implies a decrease in the computational speed. By inserting the accuracy-frequency trade-off into the expression from Cor. 1, we find

$$\mathcal{F}_A \leq 1 - O\left(\frac{M\nu^2}{\Gamma^2}\phi_{\max}^2\right), \quad (66)$$

a trade-off relation between computational fidelity and the speed of computation ν . Now, one may ask why it was necessary to impose the constraint with Γ on the rate at which ticks are generated. Indeed, if we did not have any assumptions on the timescale, the computational fidelity is timescale invariant and we could simply rescale all energy scales at our will, thus increase the computational speed arbitrarily and at constant fidelity; from that point of view, one may argue that there is no fidelity-speed trade-off. This argument misses important operational constraints, however, namely, if one works with a given physical platform for the aQPU, the decay rate at which ticks are generated is fixed by the physical properties of the system used to build the clock, or at least constrained by its energy scale.

E. Numerical example: Bell-state preparation

The deterministic generation of Bell states has been a fundamental benchmarking task in quantum computation both due to its experimental simplicity (in comparison to tasks of higher complexity) and relationship to quantum advantage in tasks such as quantum cryptography [67, 68], metrology [69] and communication [70]. Below we give a numerical simulation of a minimal aQPU generating a two qubit Bell state to give a sense for how the relationships found in the results section manifest themselves in the dynamics and to investigate what it would take to achieve fidelities on par with those obtained in experiment, on the aQPU. Our minimal aQPU consists of a two qubit computational target register, a qutrit tick register to time the three steps of the computation, a three qutrit punch card state to codify the three different gate positions and lastly a simple quantum clock based on the phenomenon of exponential decay [20] to time the operations. The simulation of this minimal aQPU is publicly available at [71] and we give a brief overview of this simulation below. For a more detailed account of the structure of this simulation we refer the reader to Appendix B.

Bell-state generation program. The way we generate the Bell-pair is by starting with the computational target system in the $|00\rangle_T$ state initially and encoding a sequence of the operations

1. HADAMARD on qubit 1,
2. CNOT on qubit 1 and 2.

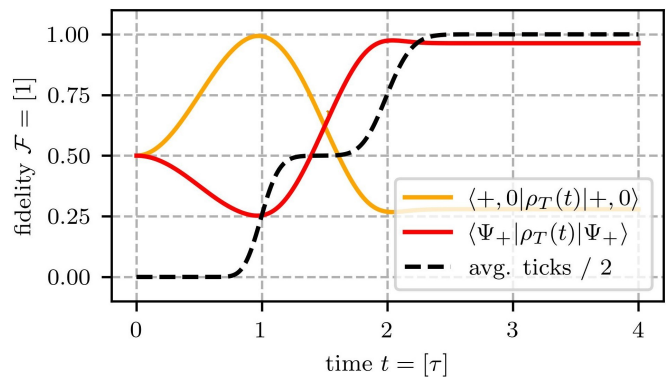


FIG. 5. This figure shows the aQPU evolution for a programmed Hadamard and CNOT gate applied to an initial state $|00\rangle$ on two qubits. The clock used is a coarse-grained exponential decay clock with accuracy $N = 80$. We see how the fidelity of the computational state $\rho_T(t)$ with the $|+, 0\rangle$ state grows to almost unity during the time $[0, \tau]$ of the first tick (orange curve), and then how the fidelity with the Bell-state $|\Psi_+\rangle = \frac{1}{\sqrt{2}}(|00\rangle + |11\rangle)$ grows to almost unity after the second tick at 2τ , albeit with larger error (red curve). The slight decrease in fidelity of the red curve after 2τ comes from the fact that the tick expectation value (black dashed curve) is not yet exactly 2. This corresponds to a small possibility that the clock takes longer to achieve the third tick than expected, leading to the CNOT Hamiltonian running longer than expected, resulting in error.

We achieve this using a gate set

$$\mathcal{V} = \{U_H \otimes \mathbb{1}, U_{\text{CNOT}}\} \quad (67)$$

where $U_H = |+\rangle\langle 0| + |-\rangle\langle 1|$ is the Hadamard and $U_{\text{CNOT}} = |0\rangle\langle 0| \otimes \mathbb{1} + |1\rangle\langle 1| \otimes X$ the CNOT. Both operations are written in the computational basis $\{|0\rangle, |1\rangle\}$, with $|\pm\rangle = \frac{1}{\sqrt{2}}(|0\rangle \pm |1\rangle)$, and X the Pauli- X gate. Further details on the description are given in Appendix B. The main detail is that we have Hamiltonians H_H and H_{CNOT} that generate the two gates in \mathcal{V} if applied for some time interval τ , with $U = \exp(-iH\tau)$ and we must now trigger them in the correct order for the correct duration using a quantum clock and instruction register.

In this minimal aQPU, a numerically efficient way to simulate the clock from [20] is to use the so-called *Erlang-clock*, named after the tick probability distribution (also see the example at the end of Appendix A 3). This clock generates ticks in time intervals τ by counting a fixed number D exponential decays after which it generates a tick. If the decay rate of the underlying exponential process is given by Γ , we have that $\tau = D\Gamma^{-1}$. Possible physical realizations of such a clock are discussed in [20, 72], and one can calculate the clock's accuracy to be $N = D$. To compute the program $\mathcal{A} = (\text{HADAMARD}, \text{CNOT}, \text{IDLE}, \dots)$, the clock ticks at least twice. We plot the aQPU evolution in Fig. 5 for the case where $D = 80$ has been chosen. Between initialization and the first tick the Hadamard Hamiltonian is applied and it is possible to see how the distance of the target system's state $\rho_T(t)$ to

the state $U_{\text{H}}|00\rangle_T$ shrinks. Similarly, for the second tick, when the CNOT is applied, the distance to the Bell-state $|\Psi_+\rangle = \frac{1}{\sqrt{2}}(|00\rangle_T + |11\rangle_T)$ goes down to some steady-state value after which the aQPU is idling.

The program fidelity and its speed trade-off. This final distance between the target system's state and the Bell-state is what tells us how well the aQPU approximates the target unitary for different values of the clock accuracy N . From an operational point of view, we are interested in the state at some finite time t after which the program \mathcal{A} has finished with high probability. As by convention of Cor. 1, we chose $t = 4\tau$ which is twice the expected time for the program to finish and plot the error $1 - \mathcal{F}_{\mathcal{A}}$ between $\rho_T(4\tau)$ and $|\Psi_+\rangle$ in Fig. 6. Since the exponential decay clock satisfies all the assumptions leading to Cor. 1 as we show at the end of Appendix A 3, we would assume the program fidelity to scale as $\mathcal{F}_{\mathcal{A}} = 1 - O(N^{-1})$, which is confirmed by the plot in Fig. 6. The behavior in the given plot can also be interpreted as the *speed-vs-fidelity* trade-off discussed in the second part of Sec. III D, if the decay rate Γ of the exponential decay clock is fixed. Increasing the accuracy N in this case is done by slowing down the clock. According to the prescription in (63), we wait for m exponential decays to happen to define an actual tick and similarly, we re-scale the Hamiltonians by $1/m$, all while keeping Γ fixed. What comes out is a computation time that increases linearly with m and the program fidelity which approaches unity with leading error in $1/m$.

In recent experiment [73] Bell states with an infidelity of 10^{-4} were generated using trapped calcium ions. To achieve such a fidelity for deterministic Bell state generation using the minimal aQPU we have modelled, we can extrapolate the linear relationship it exhibits between clock accuracy and infidelity and conclude that a clock accuracy on the order of 10^4 is required. Physically, this would imply that the aQPU is powered by a clock which ticks 10,000 times before being off by one tick. If as a minimal model for the clock we chose one of the proposals in [20, 72], the entropy production for the entire computation would also be at least of the order $10^4 \times k_B$, using the entropy curve plotted in Fig. 6.

IV. DISCUSSION

The autonomous processing unit framework which we have developed in the prior sections of this work provides a thermodynamically self-contained model of quantum computation. So far, we have used this framework to gain an understanding of the thermodynamic cost of quantum computation as well as physical limitations on the speed of quantum computation. In this section, we address conceptual questions that arise when pondering this new framework and the understandings it allows one to obtain. We start in Sec. IV A by providing insights into whether the *quantum autonomy* we propose is genuine and whether the assumptions we make on the structure

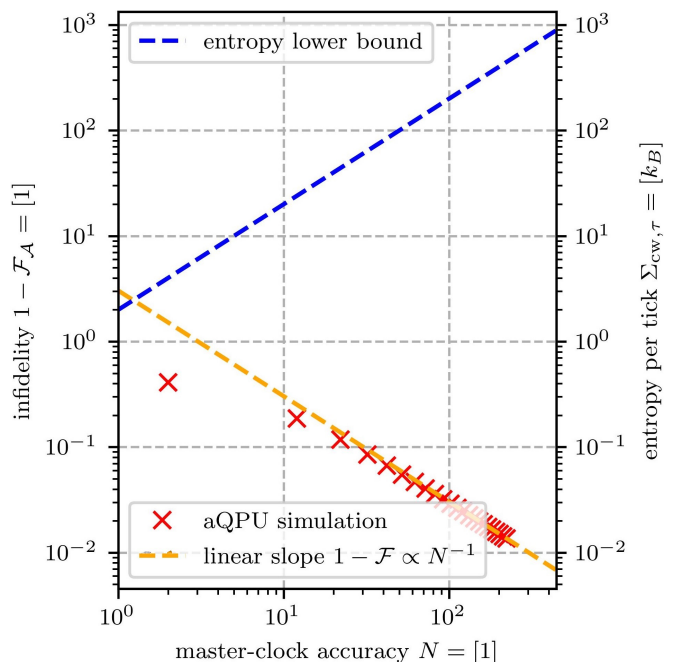


FIG. 6. Here we plot the distance of the target system's state $\rho_T(t)$ at time $t = 4\tau$ to the Bell-state $|\Psi_+\rangle = \frac{1}{\sqrt{2}}(|00\rangle + |11\rangle)$. The distance is measured as an infidelity $1 - \langle \Psi_+ | \rho_T(t) | \Psi_+ \rangle$ plotted in the y -axis and the clock accuracy N on the x -axis both in a loglog-plot. Furthermore, we have inset the lower bound on the clockwork entropy-production $\Sigma_{\text{cw},\tau} \geq 2N$ as derived in [20, 72]. A more in-depth discussion of the clockwork and its entropy production can be found in Appendices B and C. Otherwise, aQPU setup is the same as for the plots in Fig. 5 and we model a aQPU performing a Hadamard and CNOT gate on the initial state $|00\rangle$. What we can recognize in this figure is that as the clock accuracy N asymptotically grows, the distance between $\rho_T(t)$ and $|\Psi_+\rangle$ drops linearly in N , as predicted by Cor. 1. The deviations from the linear curve for small N are consistent with our results which are only proven to hold in the limit of large values of $N \gg M\phi_{\text{max}}^2 = 2\left(\frac{\pi}{2}\right)^2$.

of the master clock used by the aQPU is sensible. Closing off with Sec. IV B we explore how this framework readily provides us with potential insights into fields outside of the physics of quantum computation such as resource theories, indefinite causal order and autonomous thermal machines.

A. Physical desiderata

Why not classical control anyways? We require that the aQPU consists of quantum states and (autonomous) interactions for two main reasons. Firstly, by removing classical control we are able to deal with the obfuscation of the underlying physics of quantum computation and analyze the thermodynamic cost of processing quantum information. Secondly, we feel that it is useful and perhaps thought provoking to provide a model for

quantum computation where instructions and the clock can in principle be quantum. This challenges our preconceptions for how quantum computation *should* be done and forces us to question whether the use of classical physics (e.g., to control the quantum evolution of a register using macroscopic fields) and computation (e.g., to control hardware which implements a quantum algorithm step-by-step) is necessary for quantum computation. In particular the punch card state allows us to circumvent the classical encoding and the quantum clock allows to circumvent the classical control required for timekeeping.

Focusing on the punch card state from both a thermodynamic and a complexity theoretic perspective, we see that the complexity of preparation is essentially trivial, just a classical bit string encoded in a sequence of qubits. But physically, the required perfect purity is prohibited by the third law of thermodynamics. When close to a pure state (even arbitrarily), one can obtain a mixed punch card state autonomously by equilibration with an appropriately chosen thermal bath. Approaching this pure state will come at significant additional thermodynamic cost for its preparation, that may always be bounded by Landauer's bound [58, 59]. Any impurity would result in a classical mixture of different computational sequences carried out, requiring an increasing purity with increasing punch card length. One should note that we are not the first to suggest programming quantum computers using quantum states [74] although our method involves solely incoherent interactions and is markedly different.

Computational errors for non i.i.d. clock. In a number of results we constrained ourselves to the setting where the master clock of the aQPU being considered produces i.i.d. ticks, whose errors are i.i.d. as well. In practice this may not always be the case exactly, and in experimental quantum computation and the field of quantum error mitigation a distinction is made between coherent timekeeping errors and incoherent ones [47]. The latter can usually be mitigated to some extent, for example, if the error were the clock running consistently too fast or too slow, dynamical decoupling [47, 75, 76] or an alternative optimal control strategy could compensate for this. Incoherent errors on the other hand are those that can not be mitigated because the underlying error processes are stochastic and not correlated. Typically, these errors are of much smaller magnitude in practice than coherent ones and therefore affect the computational fidelity much less. On the downside, there is no known error mitigation strategy for incoherent errors which is why it is particularly relevant to understand them in the context of the aQPU.

The errors that occur in the aQPU due to imperfect timekeeping can also be categorized into the two groups of coherent and incoherent. In simple terms, if the master clock's ticks are perfectly i.i.d. and the errors are therefore stochastic and unpredictable, the errors on the computational target system will be incoherent. If, however, the clock ticks are not i.i.d., part of the errors on the

computational target system are coherent and therefore, could in principle be mitigated. When we explored the impact of imperfect timekeeping on the program fidelity for the aQPU in Sec. III B, we provided a general framework that covers master clocks without any assumption on the i.i.d. property of their ticks, hence both coherent and incoherent errors are treated by the result in Prop. 1 and the expression (36). The results in Prop. 2 and Cor. 1 on the other hand only hold under the assumption of i.i.d. ticks.

We now explore two potential generalizations. Firstly, let's consider the scenario where ticks are nearly independent, implying minimal mutual information between different tick times $T_{i,i+1}$ and $T_{j,j+1}$. Under this assumption, it can be demonstrated that $P[T_{i,i+1}, T_{j,j+1}]$ is approximated well by $P[T_{i,i+1}]P[T_{j,j+1}]$. Then, the derivation of the result in Cor. 1 remains valid, albeit with an additional correction introduced to account for tick correlation, dependent on the mutual information between tick times. As a second generalization, let's assume that the master clock is subject to correlated errors of significantly larger magnitude than the incoherent ones. In this instance, the correction to Cor. 1 becomes non-negligible, necessitating the consideration of error mitigation strategies for the aQPU. This avenue becomes particularly intriguing from an autonomy perspective: it prompts the question of which class of errors can be autonomously mitigated and how such strategies compare with their counterparts utilizing classical non-autonomous control. A comprehensive analysis of these two scenarios is deferred to future work.

B. Consequences of our work for other fields

The aQPU beyond unitary quantum circuits. While the main theorem shows that the aQPU can be used for universal quantum computation (Thm. 1), and this generalizes to the case of non-perfect clocks in an approximate sense through Cor. 1, the possible use cases for the aQPU go beyond standard unitary circuits. In particular we can make use of the aQPU to implement any quantum channel $\mathcal{E}(\cdot)$ on a subset of the target register using the Stinespring-dilation Theorem [77] in the following way. Say, the channel $\mathcal{E}(\cdot)$ acts on a k -qubit state ρ . Then, we can find a Kraus representation of this channel which means there exist d bounded operators Λ_i satisfying the completeness-identity $\sum_i \Lambda_i^\dagger \Lambda_i = \mathbb{1}$, and for all states ρ the following equality $\mathcal{E}(\rho) = \sum_i \Lambda_i \rho \Lambda_i^\dagger$. This representation is called *minimal* if d equals the rank of the Choi state corresponding to $\mathcal{E}(\cdot)$ [78]. On the aQPU with access to an n qubit computational register we may execute $\mathcal{E}(\cdot)$ by carrying out a unitary program $V_{\mathcal{E}}$, such that

$$\mathcal{E}(|0\rangle\langle 0|^{\otimes k}) = \text{Tr}_{n-k} \left[V_{\mathcal{E}} |0\rangle\langle 0|^{\otimes k} \otimes |0\rangle\langle 0|^{\otimes n-k} V_{\mathcal{E}}^\dagger \right]. \quad (68)$$

The number of qubits n in the target register of the aQPU must in this case be large enough to accommodate

$d \leq 2^{n-k}$, i.e., the remainder of the register which we use as the auxiliary register has dimension at least equal to the minimum number d of Kraus operators. The input $|0\rangle\langle 0|^{\otimes k}$ can be changed to any other desired pure input state by carrying out a suitable unitary on these k qubits before carrying out this protocol. One should note that the choice of V_ϵ and the state $|0\rangle\langle 0|^{\otimes(n-k)}$ are non-unique and their optimization for an aQPU with access to specific set of Hamiltonians it can execute is an interesting open problem, in particular for studying the implementation of free operations from resource theories [33, 34]. The aQPU can also be used beyond standard quantum information processing, by making use of the fact that the instruction register can in general be in a superposition of different punch card states, leading us to indefinite causal order.

Indefinite causal order. The aQPU can be used to implement arbitrary unitary operations on a designated target system by using the punch card states in Def. 2. The punch card encodes this program in a state of the form $|\mathcal{A}\rangle = |a_1\rangle_{R_1} \otimes \cdots \otimes |a_n\rangle_{R_n}$, represented directly in the canonical product basis $\{|a_i\rangle\}_i$, where a_i are labels for the instructions. One immediate thought experiment possible is to see what would happen if instead of restricting ourselves only to the set of classical instructions \mathcal{A} , we would use quantum instructions, i.e., having the punch card state in a superposition of multiple instructions at the same time. For a program consisting of two steps this could look like

$$|\Psi\rangle_R = \frac{|a_1, a_2\rangle_R + |a_2, a_1\rangle_R}{\sqrt{2}}, \quad (69)$$

where instructions a_1 and a_2 are carried out in a superposition of orderings $(a_1 a_2)$ and $(a_2 a_1)$. Running the aQPU with such an instruction turns out to be a realization of the quantum SWITCH [36] on the unitary channels given by $V_T^{(a_1)}$ and $V_T^{(a_2)}$ applied to some target system. A particular feature of this realization is that it is a thermodynamically autonomous one within standard quantum theory. This model does not contradict the no-go theorem in [36], rather, it circumvents it using the punch card which acts as the quantum program degree of freedom. Similarly, arbitrary permutations of orderings of the program states are possible for the instruction register, and thus, in principle, many varieties of SWITCH-based quantum process matrices/supermaps can be implemented on the aQPU. A classification of the higher order quantum operations [79–81] that the aQPU can generate is left as an open problem. The novel feature of the aQPU is that with this model, it is possible to quantify the thermodynamic resources such non-causal processes require: for one, the contributions already discussed in Sec. III C would enter; for another, the preparation of states of the form (69) may be more costly than preparation of states in the canonical product basis $|a_1, a_2, \dots\rangle_R$ that we have discussed so far. Preparation of a state like $|\Psi\rangle_R$ requires a quantum operation in the first place, for which another aQPU could be used to generate it, where

the instruction is a classical punch card state as in Def. 2. In this sense, a hierarchy of possible operations emerges, where for the SWITCH two layers are required: the first layer aQPU is used for generating (69), and the second layer performs implements the actual SWITCH.

Making thermal machines truly autonomous. One of the longstanding problems in the field of quantum thermodynamics has been the question of whether quantum systems used as thermal machines can exhibit a practical advantage compared to their classical counterparts [17, 24]. The class of quantum thermal machines can be roughly split into two subclasses: ones that are autonomous (like the aQPU) [20, 82] and others that are not autonomous and therefore require external control. An example of the latter is [83]. What such non-autonomous machines have in common that they work in cycles comprising thermalization steps and so-called unitary strokes. That is, one has a sequence of states $\rho_0 \mapsto \rho_1 \mapsto \rho_2 \mapsto \cdots$ of the thermal machine where the individual steps are either unitary maps

$$\rho_{i+1} = U \rho_i U^\dagger, \quad (70)$$

or subsystem thermalization steps

$$\rho_{i+1} = \text{Tr}_A[\rho_i] \otimes \tau_A[\beta], \quad (71)$$

where A is a valid subsystem of the thermal machine and $\tau_A[\beta]$ is the thermal state of said subsystem with respect to some well-define free Hamiltonian H_A of the given subsystem.

The main conceptual issue of these thermal machines is that they require external control to generate these unitaries, using a clock, which is known to come at some non-zero thermodynamic cost [20]. To figure out whether such non-autonomous thermal machines can truly exhibit a thermodynamic advantage compared to their classical counterpart it is therefore imperative to find a self-contained description for these thermal machines including the clock used to control them. Only then is it possible to arrive at a robust conclusion whether such devices are useful or not. This issue has been partly recognized and some attempts have been made towards fixing it using stopwatches, another type of clock that does not tick autonomously, but still degrades over time [48, 84]. While for finite times, the scheme proposed in those works can be used to control thermal machines, eventually the clock state has to be reset due to its degrading. If the reset is done with external control, this defeats the purpose of using the stopwatch in the first place. For the works mentioned before, the reset happens between two highly energy-coherent states of the clock, for which it is unclear whether there exist fundamental processes in nature that generate such transitions. Here the model of the aQPU can provide new insights: as the master clock is a ticking clock, it is resetting repeatedly after every tick, contrary to the coherent stopwatch model that degrade over a longer period of usage and have to be reset manually afterwards. There also exist various models of such clocks [20, 72] which are truly autonomous

in the sense that only thermal resources are required to run the clock. By using the aQPU with this type of master clock, it is possible to promote previously non-autonomous quantum thermal machines to autonomous ones where it is now possible to associate a precise thermodynamic cost of control for the time-steps where a unitary stroke is performed on the machine, by using techniques from Sec. III C. With a slight modification to the aQPU it is also possible to use it for cyclical operations, by introducing a new term in the tick operator that generates a transition $|0\rangle\langle M|_H$ from the maximum tick number state $|M\rangle_H$ to the initial state $|0\rangle_H$.

V. CONCLUSION AND OUTLOOK

In this work we have presented and developed a framework for a thermodynamically self-contained model of quantum computation. This model consists of an autonomous quantum clock which times desired operations, semi-classical quantum states which encode the desired operation and the computational target system whose state at the end of the process is the output. These three parts come together in a three-body open quantum systems interaction driven by thermal baths (see Sec. II C) whose steady state we show is the desired output of the computation making the aQPU universal as shown in Sec. III A. We follow this up by examining how this model changes if it is given access to only finite thermodynamic resources, first by examining the impact of non-ideal master clocks in Sec. III B and later under the impact of thermal imperfect initial states in Sec. III C. This allowed us to examine how the physics of quantum computation constrains the speed and fidelity at which it can be carried out and the corresponding thermodynamic cost of carrying out these computations. We rounded off our presentation of this model by providing a numerical simulation of a minimal aQPU which can be used to generate Bell states in Sec. III E, the code for this example can be found at [71].

We close by listing some open problems the aQPU framework has presented us with which we have not addressed in this work and thank you the reader for engaging with this work till the end.

Physical implementation of the aQPU. Whilst the aQPU is useful as a theoretical framework for analyzing the thermodynamics of quantum computation, it also dares us to think about how necessary classical control is for quantum computation. Just as Feynman challenged the physics community to build the smallest possible heat engine [85], the aQPU challenges the community to build the smallest quantum mechanical computing device. The autonomy and quantum encoding of programs inherent of the aQPU make it a candidate starting point for such a challenge.

Thermodynamics of complexity & computability in quantum computation. Various measures of the complexity of a quantum state have been proposed. Namely

the quantum Kolmogorov complexity [86–88] in its various forms promises to be a measure of the complexity of the operations required to generate a specific quantum state. But none thus far offer a path between the thermodynamic cost of generating a state and its complexity. The aQPU could be a suitable framework within which to examine this framework.

Thermodynamics of Quantum Measurement While the entire computation is indeed autonomous, we have of course left the thermodynamics of the final qubit measurement open. It is clear that a measurement, a transition from quantum to classical, carries with it a thermodynamic cost that is far greater than the energy scale of a single system and comes with its own limitations [61, 89]. As the complexity of the circuit increases, the relative contribution to the total thermodynamic tally might nonetheless improve to the point of negligibility, the full thermodynamics of quantum computation and classical postprocessing is however unresolvable without a thermodynamic understanding of quantum measurements.

Error-correction & mitigation on the aQPU. Without error correction, the only feasible way for autonomous universal computation is a sufficient perfection of the components (well tuned couplings, almost perfect clocks, almost perfect reset). Realistically, one would instead seek to implement error correction within the aQPU. This, however, is challenged by the fact that common error correction techniques often need syndrome measurements, which are, as per our previous point, inherently difficult to give a full thermodynamic account for. There are two possible ways around this for the future: on the one hand one can of course include error correction techniques that require no measurements [90–92], but a far more intriguing possibility is to have an inbuilt mesoscopic measurement mechanism that does not fully transition to the classical, yet features the thermodynamically emergent irreversibility of textbook quantum measurements.

Thermodynamically consistent implementation of indefinite causal order. Usually, the aQPU only needs classical punch card states as input, which are easily prepared classically. For using SWITCH or other circuits building upon the superposition of causal orders, one would need entangled punch card states, which themselves require a quantum computer or a separate aQPU to be prepared. It remains to be seen however whether the thermodynamic cost of the preparation of these quantum punch card states outweighs the potential gain in circuit efficiency from using indefinite causal order [93]. Investigating this trade-off is an interesting line of inquiry opened by the aQPU.

Implementation of free operations for resource theories Resource theories, in particular the resource theory of thermodynamics [34], usually require control and timing for their notion of a free operation. Whilst investigations into the implementation of these operations have been carried out [35] their thermodynamic cost is still uncharacterised. The aQPU framework allows for a full

thermodynamic accounting of the additional control cost contribution, sharpening the core purpose of the resource theory, ie. fleshing out the ultimate thermodynamic limitations of state transformation.

Genuine autonomous advantage in quantum thermal machines. In considering our findings, a pivotal question emerges that is left for future work to be answered: to what extent can (non-autonomous) quantum thermal machines retain a thermodynamic advantage over their classical counterpart once the cost of making the control autonomous are factored in?

Acknowledgements. The authors thank Phila Rembold for suggestions on the clarity of the text. Ralph Silva, Nuriya Nurgaleiva, Elisabeth Bauer, Marek Gluza, Yuri Minoguchi and Gerard Milburn for insightful discussions. F.M., P.E and M.H. acknowledge funding by the European flagship on quantum technologies ('ASPECTS' consortium 101080167). J.X., P.E. and M.H. acknowledge funding from the European Research Council (Consolidator grant 'Cocoquest' 101043705). Lastly, we acknowledge time itself, not only for being such a physically and philosophically interesting notion, but also for allowing us the space to think about and enjoy the ideas presented in this manuscript.

APPENDICES

Appendix A: Proofs

1. Proofs on autonomous clocks

Lemma 2. *Let $N(t)$ be the random variable describing the number of ticks of a clock at time t and let T_n be the random variable describing the time at which the n th tick occurs. Then, the following transformation*

$$P[N(t) = n] = P[T_n \leq t] - P[T_{n+1} \leq t], \quad (\text{A1})$$

converts between the two ensemble formulations.

Proof. Observe that the events $\{N(t) = n\}$ and $\{T_n \leq t \wedge T_{n+1} \geq t\}$ coincide, because n ticks at time t is the case if and only if the n th tick happened before time t and the $(n+1)$ -st tick happens after t . Therefore, we can write

$$P[N(t) = n] = P[T_n \leq t \wedge T_{n+1} \geq t] \quad (\text{A2})$$

$$= P[T_n \leq t] + P[T_{n+1} \geq t] - P[T_n \leq t \vee T_{n+1} \geq t], \quad (\text{A3})$$

where the second line (A3) uses the addition rule. Now we can use that the probability $P[T_n \leq t \vee T_{n+1} \geq t]$, that the n th tick happens before time t or the $(n+1)$ -st tick happens after time t is trivially 1. Thus, we can continue the derivation from before

$$(\text{A3}) = P[T_n \leq t] + P[T_{n+1} \geq t] - 1 \quad (\text{A4})$$

$$= P[T_n \leq t] - P[T_{n+1} \leq t], \quad (\text{A5})$$

which proves the Lemma. \square

If we resolve the clock's state with respect to the tick numbers n we can write down a set of differential equations for the states $\rho_C^{(n)}(t)$. We simply have to calculate

$$\dot{\rho}_C^{(n)}(t) = \text{Tr} \left[(\mathbb{1}_C \otimes |n\rangle\langle n|_H) \dot{\rho}_{CH}(t) \right], \quad (\text{A6})$$

by using Eq. (7). We eventually find

$$\dot{\rho}^{(n)}(t) = \mathcal{L}_C \left[\rho_C^{(n)}(t) \right] - \frac{1}{2} \left\{ J^{(n)\dagger} J^{(n)}, \rho_C^{(n)} \right\} \quad (\text{A7})$$

$$+ J^{(n-1)} \rho_C^{(n-1)}(t) J^{(n-1)\dagger}. \quad (\text{A8})$$

Lemma 3. *Given the clock model with Ansatz as defined in Eq. (6) and equations of motion (7), the tick probability density*

$$P[T_{n+1} = t] = \frac{d}{dt} P[T_{n+1} \leq t], \quad (\text{A9})$$

can be obtained from the state $\rho_{CR}(t)$ as follows,

$$\text{Tr} \left[J^{(n)\dagger} J^{(n)} \rho_C^{(n)}(t) \right] = P[T_{n+1} = t]. \quad (\text{A10})$$

Proof. We show the statement by induction in n . The base case: For $n = 0$ the statement is a consequence of Lemma 2. By definition, $P[T_0 \leq t] = 1$ for all $t \geq 0$ and thus, the previous Lemma gives

$$\text{Tr} \left[\rho_C^{(0)}(t) \right] = 1 - P[T_1 \leq t]. \quad (\text{A11})$$

From this equation, we just have to take the derivative and insert the expression for $\dot{\rho}_C^{(0)}(t)$ (we do not write out the t argument explicitly),

$$-\frac{d}{dt} P[T_1 \leq t] = \text{Tr} \left[\mathcal{L}_C \left[\rho_C^{(0)} \right] - \frac{1}{2} \left\{ J^{(0)\dagger} J^{(0)}, \rho_C^{(0)} \right\} \right] \quad (\text{A12})$$

$$= -\text{Tr} \left[J^{(0)\dagger} \rho_C^{(0)} J^{(0)} \right], \quad (\text{A13})$$

where we have used cyclicity of the trace in the second line and the fact that $\mathcal{L}_C[\rho]$ is always trace-less. This proves the base case.

The induction step: we assume that the theorem holds for some value of n , then, we can show (again using Lemma 2) that it holds for $n+1$. We look again at $P[N(t) = n+1]$ which is the trace of $\rho^{(n+1)}(t)$. Taking the time-derivative of that state (see Eq. (A7)), we find

$$\dot{\rho}^{(n+1)}(t) = \mathcal{L}_C \left[\rho_C^{(n+1)}(t) \right] - \frac{1}{2} \left\{ J^{(n+1)\dagger} J^{(n+1)}, \rho_C^{(n+1)} \right\} \quad (\text{A14})$$

$$+ J^{(n)} \rho_C^{(n)}(t) J^{(n)\dagger}. \quad (\text{A15})$$

Now, we can trace and on the left-hand-side, we get $\partial_t P[N(t) = n+1]$ where we can invoke Lemma 2. On

the right-hand-side, we can use the induction hypothesis and we can replace $\text{Tr} \left[J^{(n)} \rho_C^{(n)} J^{(n)\dagger} \right]$ by $P[T_{n+1} = t]$, which leaves us with

$$\begin{aligned} P[T_{n+1} = t] - P[T_{n+2} = t] \\ = P[T_{n+1} = t] - \text{Tr} \left[J^{(n+1)} \rho_C^{(n+1)} J^{(n+1)\dagger} \right]. \end{aligned} \quad (\text{A16})$$

Simplifying this expression yields the statement for $n+1$, completing the induction step. By induction, the desired statement follows for all values of $n \geq 0$ which is all we wanted to show. \square

2. Proofs on the aQPU universality

In this appendix, we prove the statements from Sec. III A and provide further details. We start by proving our claims related to the semi-classical state-structure of the aQPU.

Lemma 1 (State-structure). *Let the initial state defined on the full aQPU Hilbert space \mathcal{H} be given by*

$$\rho^{\text{init}} = \rho_C^{\text{init}} \otimes |0\rangle\langle 0|_H \otimes |\mathcal{A}\rangle\langle \mathcal{A}|_R \otimes \rho_T^{\text{init}}, \quad (\text{23})$$

$$\mathcal{L}_{\text{tick}}[\rho] = \left(-\frac{1}{2} \left\{ J_C^{(n)\dagger} J_C^{(n)}, \rho_C \right\} \otimes |n\rangle\langle n|_H + J_C^{(n)} \rho_C J_C^{(n)\dagger} \otimes |n+1\rangle\langle n+1|_H \right) \otimes |n\rangle\langle n|_H \otimes |\mathcal{A}\rangle\langle \mathcal{A}|_R \otimes \rho_T, \quad (\text{A19})$$

which also aligns with the required form (A17). Finally, the interaction terms yields

$$\mathcal{L}_{\text{int}}[\rho] = -i\rho_C \otimes |n\rangle\langle n|_H \otimes |\mathcal{A}\rangle\langle \mathcal{A}|_R \otimes \left[H_T^{(a_n)}, \rho_T \right], \quad (\text{A20})$$

where a_n is the n th entry in the program \mathcal{A} . This is also of the desired form and together with the initial remark proves the Lemma. \square

Proposition 1 (Target system recursion relation). *The target system's state $\rho_T^{(n)}(t)$ at parameter time t , conditioned on n ticks having occurred takes the following form,*

$$\rho_T^{(n)}(t) = \int_0^t ds \xi(t, s) V_{(a_n)}(t-s) \rho_T^{(n-1)}(s) V_{(a_n)}(t-s)^\dagger. \quad (\text{29})$$

The function $\xi(t, s)$ describes the probability distribution of the n th tick occurring at time s conditioned on n ticks at time $t \geq s$,

$$\xi(t, s) = p(s) \exp \left(-\int_s^t d\tau p(\tau) \right), \quad (\text{30})$$

where ρ_C^{init} is an arbitrary initial state on the clockwork \mathcal{H}_C and ρ_C^{init} an arbitrary initial state on the target system. Then, at any point in time t the state $\rho(t) = e^{\mathcal{L}_{\text{aQPU}} t} \rho^{\text{init}}$ is given by

$$\rho(t) = \sum_{n \geq 0} \rho_C^{(n)}(t) \otimes |n\rangle\langle n|_H \otimes |\mathcal{A}\rangle\langle \mathcal{A}|_R \otimes \rho_T^{(n)}(t). \quad (\text{24})$$

Proof. It is sufficient to show that for any state ρ of the form

$$\rho = \rho_C \otimes |n\rangle\langle n|_H \otimes |\mathcal{A}\rangle\langle \mathcal{A}|_R \otimes \rho_T, \quad (\text{A17})$$

we have $\mathcal{L}\rho$ is a sum of terms like the one above but possibly different ρ_C, ρ_T and n . The reason this suffices is that the time-evolution is generated by \mathcal{L} , i.e., if we start with a state like that in (A17), at any future point in time t , the state $\rho(t) = e^{\mathcal{L}_{\text{aQPU}} t} \rho$ will be a sum of terms of said form. But this is exactly the statement of the Lemma to prove. Thus, let us look term by term at $\mathcal{L}_{\text{cw}}, \mathcal{L}_{\text{tick}}$ and finally \mathcal{L}_{int} . For this, we simply have to insert:

$$\mathcal{L}_{\text{cw}}[\rho] = \mathcal{L}_{\text{cw}}[\rho_C] \otimes |n\rangle\langle n|_H \otimes |\mathcal{A}\rangle\langle \mathcal{A}|_R \otimes \rho_T, \quad (\text{A18})$$

which is of the desired form. The tick generating term becomes,

with $p(\tau)$ as in Eq. (28). Moreover, the unitary $V_{(a_n)}(t)$ is the propagator at time t generated by the Hamiltonian $H_T^{(a_n)}$, i.e., $V_{(a_n)}(t) = \exp(-iH_T^{(a_n)} t)$.

Proof. The proof of this statement consists of the two steps already pointed out in the main text: first, we show that $\rho_T^{(n)}(t)$ is governed by the equations of motion (27), which, for completeness, we recall here,

$$\dot{\rho}_T^{(n)}(t) = -i \left[H_T^{(a_n)}, \rho_T^{(n)}(t) \right] + p(t) \left(\rho_T^{(n-1)}(t) - \rho_T^{(n)}(t) \right), \quad (\text{A21})$$

with $p(t)$ defined as in Eq. (28), and for convenience we also repeat that definition,

$$p(t) := \frac{P[T_n = t]}{P[N(t) = n]}. \quad (\text{A22})$$

The second step to the proof boils down to inserting the recursion relation (29) from the Prop. 1 into the equation of motion and verify that they are indeed solved. Without further ado, we get started with the first step.

Recall Eq. (26) from the main text which we can

rewrite as

$$P[N(t) = n] \rho_T^{(n)}(t) = \text{Tr}_{CHR} \left[(\mathbb{1}_{CRT} \otimes |n\rangle\langle n|_H) \rho(t) \right]. \quad (\text{A23})$$

Now we take the time-derivative on both sides, and we examine step-by-step the terms that come up. On the right-hand-side, we get $\dot{\rho}(t)$ which can be replaced by $\mathcal{L}_{\text{aQPU}}[\rho(t)]$. So the three terms we have to look at are

- Clockwork term,

$$\text{Tr}_{CHR} \left[(\mathbb{1}_{CRT} \otimes |n\rangle\langle n|_H) \mathcal{L}_{\text{cw}}[\rho(t)] \right]. \quad (\text{A24})$$

- Ticking term,

$$\text{Tr}_{CHR} \left[(\mathbb{1}_{CRT} \otimes |n\rangle\langle n|_H) \mathcal{L}_{\text{tick}}[\rho(t)] \right]. \quad (\text{A25})$$

- Interaction term,

$$\text{Tr}_{CHR} \left[(\mathbb{1}_{CRT} \otimes |n\rangle\langle n|_H) \mathcal{L}_{\text{int}}[\rho(t)] \right]. \quad (\text{A26})$$

The clockwork term (A24) is trivially zero, because we have a factor $\text{Tr}_C \left[\mathcal{L}_C \left[\rho_C^{(n)} \right] \right] = 0$ that vanishes because \mathcal{L}_C acting on anything is zero (traceless property of Lindbladians). The tick-generating term on the other hand yields non-trivial contributions. Let us thus first calculate $\mathcal{L}_{\text{tick}}[\rho(t)]$ in full:

$$\mathcal{L}_{\text{tick}}[\rho(t)] = \sum_{n \geq 0} \mathcal{L}_{\text{tick}} \left[\rho_C^{(n)}(t) \otimes |n\rangle\langle n|_H \otimes |\mathcal{A}\rangle\langle \mathcal{A}|_R \otimes \rho_T^{(n)}(t) \right] \quad (\text{A27})$$

$$\stackrel{(15)}{=} \sum_{n \geq 0} \left(J_C^{(n)} \rho_C^{(n)} J_C^{(n)\dagger} \otimes |n+1\rangle\langle n+1|_H - \frac{1}{2} \left\{ J_C^{(n)\dagger} J_C^{(n)}, \rho_C^{(n)} \right\} \otimes |n\rangle\langle n|_H \right) \otimes |\mathcal{A}\rangle\langle \mathcal{A}|_R \otimes \rho_T^{(n)}(t) \quad (\text{A28})$$

by taking the trace as in Eq. (A25), we find

$$(\text{A25}) = P[T_n = t] \rho_T^{(n-1)}(t) - P[T_{n+1} = t] \rho_T^{(n)}(t). \quad (\text{A29})$$

Next, we look at the contribution from the interaction as written out in Eq. (A26). To understand this term better, recall that \mathcal{L}_{int} is the commutator with the Hamiltonian H_{int} and that H_{int} is a sum over $0 \leq n \leq M$ of terms of

the form

$$\mathbb{1}_C \otimes |n\rangle\langle n|_H \otimes \mathbb{1}_{R_m(\neq n)} \otimes \sum_{k=1}^K |k\rangle\langle k|_{R_n} \otimes H_T^{(k)}. \quad (\text{A30})$$

Lemma 1 ensures that $\rho(t)$ is diagonal with respect to the tick register states $|n\rangle_H$. Thus, the projector $\mathbb{1}_{CRT} \otimes |n\rangle\langle n|_H$ in Eq. (A26) picks out the n th term in the sum of $\rho(t)$ (in the notation of (29)) and similarly, the punch card state $|\mathcal{A}\rangle\langle \mathcal{A}|_R$ of $\rho(t)$ picks out the interaction term where $k = a_n$ and this leads to the following expression:

$$(\text{A26}) = -i \text{Tr}_{CHR} \left[\rho_C^{(n)}(t) \otimes |n\rangle\langle n|_H \otimes \left[\mathbb{1}_{R_m(\neq n)} \otimes \sum_{k=1}^K |k\rangle\langle k|_{R_n} \otimes H_T^{(k)}, |\mathcal{A}\rangle\langle \mathcal{A}|_R \otimes \rho_T^{(n)}(t) \right] \right] \quad (\text{A31})$$

$$= -i \text{Tr}_{CHR} \left[\rho_C^{(n)}(t) \otimes |n\rangle\langle n|_H \otimes |\mathcal{A}\rangle\langle \mathcal{A}|_R \otimes \left[H_T^{(a_n)}, \rho_T^{(n)}(t) \right] \right] \quad (\text{A32})$$

$$= -i P[N(t) = n] \left[H_T^{(a_n)}, \rho_T^{(n)}(t) \right]. \quad (\text{A33})$$

Finally, we can add all the terms (A24), (A25) and (A26) together to find the time derivative of the right-hand side from Eq. (A23). For the left-hand-side, we can take the time-derivative explicitly and we get by using Lemma 2

$$(P[T_n = t] - P[T_{n+1} = t]) \rho_T^{(n)}(t) + P[N(t) = n] \dot{\rho}_T^{(n)}(t) \quad (\text{A34})$$

$$= P[T_n = t] \rho_T^{(n-1)}(t) - P[T_{n+1} = t] \rho_T^{(n)}(t) - i P[N(t) = n] \left[H_T^{(a_n)}, \rho_T^{(n)}(t) \right], \quad (\text{A35})$$

which we can simplify to

$$P[N(t) = n] \dot{\rho}_T^{(n)}(t) = -i P[N(t) = n] \left[H_T^{(a_n)}, \rho_T^{(n)}(t) \right] + P[T_n = t] \left(\rho_T^{(n-1)}(t) - \rho_T^{(n)}(t) \right). \quad (\text{A36})$$

Dividing both sides by $P[N(t) = n]$, we find the desired equation of motion as claimed in Eq. (A21). This completes the first step of the proof.

As for the second step, we want to verify that the expression in (29) solves said equations of motion. We insert (29) into the equations of motion (A21) for this. To simplify the proof, we abbreviate the notation in the following way

$$v(t) \equiv \rho^{(n)}(t), \quad (\text{A37})$$

$$w(t) \equiv \rho^{(n-1)}(t), \quad (\text{A38})$$

$$A \equiv -i \left[H_T^{(a_n)}, \circ \right], \quad (\text{A39})$$

and $p(t)$ as in Eq. (30) from the proposition. In this notation, the equations of motion in Eq. (27) read

$$\dot{v}(t) = Av(t) + p(t)(w(t) - v(t)), \quad (\text{A40})$$

and the ansatz from Eq. (29) can be recast into

$$v(t) = \int_0^t \underbrace{p(s) \exp\left(-\int_s^t d\tau p(\tau)\right)}_{=\xi(t,s)} e^{A(t-s)} w(s). \quad (\text{A41})$$

All we need to do now, is to take the time derivative of $v(t)$ as defined in Eq. (A41). The product rule will give us three contributions,

$$\dot{v}(t) = \xi(t,t)w(t) + \int_0^t ds (\partial_t \xi(t,s)) e^{A(t-s)} w(s) + Av(t). \quad (\text{A42})$$

The partial derivative of $\xi(t,s)$ with respect to t can be calculated by using the definitions from Eq. (30) to give

$$\partial_t \xi(t,s) = -\xi(t,s) \partial_t \int_s^t d\tau p(\tau) \quad (\text{A43})$$

$$= -\xi(t,s)p(t). \quad (\text{A44})$$

Essentially, this result allows us to re-express the middle term on the right-hand side of Eq. (A42),

$$\int_0^t ds (\partial_t \xi(t,s)) e^{A(t-s)} w(s) = -p(t)v(t). \quad (\text{A45})$$

Together with the identity $\xi(t,t) = p(t)$, we can use Eq. (A42), insert Eq. (A45) into the middle term and we finally recover

$$\dot{v}(t) = p(t)w(t) - p(t)v(t) + Av(t), \quad (\text{A46})$$

which is exactly the expression from Eq. (A42). This proves that the ansatz as defined in Eq. (A41) solves this differential equation; moreover, if we revert our notation change from Eqs. (A37), (A38) and (A39), we recover the expression from the proposition, which is all we wanted to show. \square

Let us discuss the different contributions to Eq. (29) in Prop. 1. First of all, we note the resemblance of this expression to the one derived in [22] for the impact of imperfect time-keeping on the evolution of a quantum system under a controlled unitary. Here, it is averaged over the normalized distribution $\xi(t,s)$ (normalized w.r.t. integration over the domain $s \in [0,t]$) the state

$$V_{(a_n)}(t-s)\rho_T^{(n-1)}(s)V_{(a_n)}(t-s)^\dagger, \quad (\text{A47})$$

which is the state at $\rho_T^{(n-1)}(s)$ after $n-1$ ticks at time s , when the n th tick occurs exactly at time s and evolves for another time $t-s$ according to the propagator generated by $H_T^{(a_n)}$. Secondly, we want to understand the expression $\xi(t,s)$ in a probability theoretic sense. For that, we first verify normalization. A longer glance at the definition of $\xi(t,s)$ assures us that $\xi(t,s) = \partial_s \zeta(t,s)$, where

$$\zeta(t,s) = \exp\left(-\int_s^t d\tau p(\tau)\right). \quad (\text{A48})$$

This allows us to analytically calculate the integral of $\xi(t,s)$ and therefore also the normalization condition because

$$\int_0^t ds \xi(t,s) = \int_0^t ds (\partial_s \zeta(t,s)) \quad (\text{A49})$$

$$= \zeta(t,t) = 1, \quad (\text{A50})$$

which was our claim, that $\xi(t,s)$ is a genuine probability distribution over t .

Theorem 1 (Universality for perfect clocks). *Let the aQPU model be defined by the Lindbladian $\mathcal{L}_{\text{aQPU}}$ as in Eq. (18) with access to a finite number of Hamiltonians that generate a universal gate set \mathcal{V} and let \mathcal{A} be any finite program defined on \mathcal{V} . If the master clock is ideal with tick time τ we have that*

$$\begin{aligned} \text{Tr}_{CHR} \left[e^{t\mathcal{L}_{\text{aQPU}}} (\rho_C^{\text{init}} \otimes |0\rangle\langle 0|_H \otimes |\mathcal{A}\rangle\langle \mathcal{A}|_R \otimes \rho_T^{\text{init}}) \right] \\ = V_{\mathcal{A}} \rho_T^{\text{init}} V_{\mathcal{A}}^\dagger, \end{aligned} \quad (\text{22})$$

for $t \geq M\tau$ large enough.

Proof. We provide additional mathematical details to the proof of the theorem. The straightforward way to showing the statement is starting with the non-singular expression in Eq. (A36). That reduces to a well-defined differential equation for $\rho_T^{(n)}(t)$ only for values $t \in [n\tau, (n+1)\tau]$. There, we find

$$\dot{\rho}_T^{(n)}(t) = -i \left[H_T^{(a_n)}, \rho_T^{(n)}(t) \right] \quad (\text{A51})$$

$$+ \delta(t - n\tau) \left(\rho_T^{(n-1)}(t) - \rho_T^{(n)}(t) \right). \quad (\text{A52})$$

Integration yields the initial condition $\rho_T^{(n)}(n\tau) = \rho_T^{(n-1)}(n\tau)$ and once we have the initial condition, we see that the singular expression in line (A52) vanishes, and $\rho_T^{(n)}(t)$ for values $t > n\tau$ follows Schrödinger evolution with Hamiltonian $H_T^{(a_n)}$. This is all we wanted to prove. \square

3. Proofs on errors for non-ideal clocks

We here provide further details for the expansion of the target state evolution under the assumption that the clock is highly accurate but not perfect. In the main text Sec. III B we have provided the corrections as asymptotic expression while here we will provide explicit prefactors. This section is structured to reverse engineer the result from Prop. 2 in the following order:

- As preliminaries, we introduce some abstract probability theoretic notions and results for later use.
- We then at the case of i.i.d. ticks which are *exponentially concentrated*, and derive the asymptotic expansion from Cor. 1.
- In the following step, we argue why the expressions used in the first step follow from the equations of motion in Prop. 1.
- Finally, we argue why our conditions for i.i.d. ticks and exponential probability concentration can generally be satisfied in the high clock accuracy regime.

Preliminaries. In this paragraph we will present adapted results from [50, 51] on concentration inequalities. The idea behind this is that we want to figure out how the aQPU evolves the target system's state in case the clock is highly accurate. To this end, we have to formalize our notion of highly accurate clocks and develop some toolset to rigorously make the necessary statements. We start by considering a generic real random variable X which has without loss of generality mean $\langle X \rangle = 0$. We furthermore assume that X has a *exponentially concentrated* distribution, which we define to be the condition that

$$P[|X| \geq x] = \int_{|x'| > x} dx' P[X = x'] \leq \alpha e^{-cx}, \quad (\text{A53})$$

for two constants $\alpha, c > 0$. Based on this exponential decay condition on the tail of the distribution of X , we can also bound the moments of X and the moment-generating function $M(k) = \langle e^{kX} \rangle$, which will turn out to be useful later.

Lemma 4 (Bounded moments). *Let X be exponentially concentrated as defined in (A53). Then, the absolute moments of X are bounded as follows,*

$$\langle |X|^n \rangle \leq \frac{\alpha n!}{c^n}. \quad (\text{A54})$$

Proof. Here, we use a modified method following Lemma 5.5 from [94]. The trick is to define a positive random variable $Z = |X|^n$ and using partial integration (with special care for the boundaries), we can show

$$\langle |X|^n \rangle = \int_0^\infty dz z P[Z = z] \quad (\text{A55})$$

$$= \int_0^\infty dz P[Z \geq z]. \quad (\text{A56})$$

The inequality $Z \geq z$ is equivalent to $|X| \geq x$, under the change of variables $x^n = z$. Substitution with $dz = nx^{n-1}dx$ allows us to further reexpress the absolute moment according to

$$(\text{A56}) = \int_0^\infty dx nx^n P[|X| \geq x] \quad (\text{A57})$$

$$\leq \int_0^\infty dx \alpha n x^n e^{-cx} \quad (\text{A58})$$

$$= \frac{\alpha n!}{c^n}, \quad (\text{A59})$$

by using the definition of the Γ function and $\Gamma(n) = (n-1)!$ which is all we wanted to prove for this Lemma. \square

Yet another statement we can make by using the assumption that X is exponentially concentrated is about the moment generating function (MGF); by using Lemma 4 we can expand this result to the following.

Lemma 5 (Bounded MGF). *Let X be again exponentially concentrated as in (A53). The resulting MGF is bounded by*

$$M(k) \equiv \langle e^{kX} \rangle \leq \exp\left(\frac{2\alpha k^2}{c^2}\right), \quad (\text{A60})$$

for values $|k| \leq \frac{c}{2}$.

Proof. We can directly expand the MGF in terms of the moments and employ Lemma 4, though note that we also use the fact that the first moment vanishes as we have assumed zero mean for X :

$$M(k) = \sum_{n \geq 0} \frac{\langle (kX)^n \rangle}{n!} \quad (\text{A61})$$

$$= 1 + \sum_{n \geq 2} \frac{\langle (kX)^n \rangle}{n!} \quad (\text{A62})$$

$$\leq 1 + \sum_{n \geq 2} \frac{\langle |kX|^n \rangle}{n!} \quad (\text{A63})$$

$$\leq 1 + \sum_{n \geq 2} \alpha \frac{|k|^n}{c^n} \quad (\text{A64})$$

$$= 1 + \alpha \frac{k^2}{c^2} \sum_{n \geq 0} \frac{|k|^n}{c^n} \quad (\text{A65})$$

$$\leq 1 + 2\alpha \frac{k^2}{c^2} \quad (\text{A66})$$

$$\leq \exp\left(2\alpha \frac{k^2}{c^2}\right) \quad (\text{A67})$$

so long as $|k| \leq \frac{c}{2}$, finalizing our result as desired. \square

What we have done so far is analyzed the behavior of the random variable X . In relation to the clock probability distribution, these would be statements about the

probability distribution of a single tick. When considering many ticks, and under the assumptions those ticks are independent and identically distributed (i.i.d.), we would hope that some of the properties about how well the single tick is concentrated would carry over to the sum over many such ticks. As it turns out, a special case of Bernstein's inequality [95] provides exactly the desired statement.

Lemma 6 (Bernstein's inequality – special case). *Let X_1, \dots, X_n be n i.i.d. copies of the exponentially concentrated random variable X . Define the sum*

$$\bar{X} = \sum_{k=1}^n X_k, \quad (\text{A68})$$

then for any value of t , we always have

$$P[|\bar{X}| \geq x] \leq \exp\left(\frac{\alpha n}{2} - \frac{cx}{2}\right) \quad (\text{A69})$$

Proof. The Chernoff bound [96] can be used directly to upper bound the concentration probability for \bar{X} ,

$$P[|\bar{X}| \geq x] \leq M_n(k)e^{-kx}, \quad (\text{A70})$$

where $M_n(k)$ is the MGF of \bar{X} . By using the i.i.d. property of the random variables X_1, \dots, X_n that sum up to \bar{X} , we can bound $M_n(k)$ from above by using Lemma 5 and the fact that all random variables X_i are exponentially concentrated according to (A53). We find,

$$M_n(k) = M(k)^n \leq \exp\left(\frac{2\alpha nk^2}{c^2}\right), \quad (\text{A71})$$

for all values of k such that $|k| \leq \frac{c}{2}$. Inserting this result into Eq. (A70), we find the bound on the concentration probability,

$$P[|\bar{X}| \geq x] \leq \exp\left(\frac{\alpha n}{2} - \frac{cx}{2}\right) \quad (\text{A72})$$

where we set $k = c/2$ satisfying the conditions from Lemma 5. \square

This Lemma 6 show that if X is exponentially concentrated with constants $\alpha, c > 0$, then also an n -fold i.i.d. sum \bar{X} is exponentially concentrated, however, with slightly heavier tail given by the constants $\exp(\alpha n/2), c/2 > 0$.

Finally, we show an application of these results for the case when we take expectation values of functions with respect to an exponentially concentrated probability distribution. As it turns out (see Lemma 7), it is possible to estimate the expectation value of a function using the Taylor approximation. To this end, we introduce a family of real random variables X_N with zero mean and exponential concentrated probability distribution,

$$P[|X| \geq x] \leq \alpha e^{-x\sqrt{N}x}. \quad (\text{A73})$$

The family parameter $N \in \mathbb{R}_{\geq 0}$ may take any values but must be unbounded. We then find:

Lemma 7 (Taylor trick for expectation values). *Assume $f : \mathbb{R} \rightarrow \mathbb{C}$ is whole and the derivatives in the origin satisfy the following condition,*

$$|f^{(n)}(0)| \leq \gamma^n, \quad (\text{A74})$$

for some constant $\gamma > 0$. Furthermore, take X_N to be a family of exponentially concentrated real random variables as in Eq. (A73), then we have asymptotically

$$\int dx p[X_N = x]f(x) = f(0) + \frac{\sigma^2}{2}f^{(2)}(0) + O\left(\left(\frac{\gamma}{\sqrt{N}}\right)^3\right), \quad (\text{A75})$$

as $N \rightarrow \infty$, where σ^2 is the second moment of X_N .

Proof. For this first step, we can directly use Lemma 4 to derive the following bound on the absolute moments of X_N ,

$$\chi_n := \int dx |x|^n P[X_N = x] \leq \frac{\alpha n!}{(c\sqrt{N})^n}. \quad (\text{A76})$$

Now let us move towards the second step where we expand the integral for the expectation value of f . Since by assumption f is whole, we can expand for any $x \in \mathbb{R}$

$$f(x) = \sum_{n \geq 0} x^n \frac{f^{(n)}(0)}{n!}, \quad (\text{A77})$$

and insert into the integral,

$$\int dx p[X_N = x]f(x) = \sum_{n \geq 0} \int dx p[X_N = x] x^n \frac{f^{(n)}(0)}{n!}, \quad (\text{A78})$$

where switching integral and sum is allowed by the Fubini-Tonelli-theorem [97]. The first three terms of the sum are $f(0) + \frac{\sigma^2}{2}f^{(2)}(0)$ and note that the first moment vanishes because we centered the expansion of $f(x)$ around the mean 0 of X_N 's distribution. The remaining terms can be bounded by using Eq. (A76),

$$\sum_{n \geq 3} \chi_n \frac{f^{(n)}(\mu)}{n!} \leq \alpha \sum_{n \geq 3} \left(\frac{\gamma}{c\sqrt{N}}\right)^n = O\left(\left(\frac{\gamma}{\sqrt{N}}\right)^3\right), \quad (\text{A79})$$

so long as $N > (\gamma/c)^2$ and the series converges. This concludes the proof of the Lemma. \square

We thus conclude this preliminary paragraph, and move towards applying these results for the clock probability distributions.

Step 1. We can always unravel the evolution of the the aQPU into stochastic trajectories. If we look at evolution time t , such a trajectory can have different numbers of total clock ticks n . For given n , a trajectory Γ_n is given by the following labels,

$$\Gamma_n = (\tau_1, \tau_2, \dots, \tau_n), \quad (\text{A80})$$

where τ_k is the time between the $(k-1)$ st and k th tick of the master clock. The relationship to the tick times $t_1 \leq t_2 \leq \dots \leq t_n \leq t$, is given by $t_k = t_{k-1} + \tau_k$, where we set $t_0 = 0$ by definition. Let us furthermore consider the program \mathcal{A} of length $L \geq M$ encoded in a punch card state $|\mathcal{A}\rangle_R$ of length M . For the following analysis we want to look at an explicit trajectory Γ_n of the evolution, where we will find that the computational target system evolves unitarily,

$$\rho_T(t|\Gamma_n) = V_{(a_n)}(t - t_n) \cdots V_{(a_0)}(t_1) \rho_T^{\text{init}} V_{(a_0)}(t_1)^\dagger \cdots V_{(a_n)}(t - t_n)^\dagger. \quad (\text{A81})$$

The probability $p[\Gamma_n]$ that such a trajectory is realized is given by the joint probability that n ticks have occurred at time t , together with the first tick having happened at time t_1 , the second at time t_2 , etc. until the n th tick that must have happened at time t_n . Formally, the probability can be expressed as

$$p[\Gamma_n] = P[T_1 = t_1, \dots, T_n = t_n, N(t) = n] \quad (\text{A82})$$

$$= P[T_1 = t_1, \dots, T_n = t_n \leq t \leq T_{n+1}]. \quad (\text{A83})$$

Summing and integrating over all possible trajectories Γ_n then yields the state of the target computational system at time t on average over all possible times at which the clock could have ticked. This results in the following expression for the target system,

$$\rho_T(t) = \sum_{n=0}^M \int dt_1 \cdots dt_n p[\Gamma_n] \rho(t|\Gamma_n) \quad (\text{A84})$$

$$= \sum_{n=0}^M P[N(t) = n] \underbrace{\int dt_1 \cdots dt_n p[\Gamma_n] N(t) = n \rho(t|\Gamma_n)}_{=\rho_T^{(n)}(t)}, \quad (\text{A85})$$

where we have resolved the density matrix as a sum over the possible numbers of ticks in the second line (A85). Observe first of all, that in the limit of long times t , $P[N(t) = n] \rightarrow 0$ for all values $n < M$. We can quantify

this properly by using the fact that

$$P[N(t) = M] = P[T_M \leq t], \quad (\text{A86})$$

because the clock does not tick more than M times. Now, let us work in the assumption that the clock produces a sequence of i.i.d. ticks, where the time between two adjacent ticks is described by the exponentially concentrated random variable T with mean and variance

$$\tau := \langle T \rangle, \quad \sigma^2 := \text{Var}[T]. \quad (\text{A87})$$

Let $N = \tau^2/\sigma^2$ be the clock accuracy according to Def. 4 or, e.g., Eq. (39). We assume that we have a family of clocks such that the exponential concentration of the tick time T follows the asymptotics

$$P[|T - \tau| \geq t] \leq \alpha \exp\left(-c\sqrt{N}\frac{t}{\tau}\right), \quad (\text{A88})$$

in particular, for growing clock accuracy N , the tail vanishes exponentially quickly. While this may seem like a strong assumption we justify in the third and step of this section that natural choices of clocks satisfy this behavior because the tick generating process is exponential decay. Under this assumption, we can invoke Lemma 6 to bound the probability from Eq. (A86),

$$P[N(t) = M] = 1 - P[T_M \geq t] \quad (\text{A89})$$

$$\geq 1 - \exp\left(\frac{\alpha M}{2} - \frac{c\sqrt{N}(t - M\tau)}{2\tau}\right), \quad (\text{A90})$$

which for $t \geq (M+1)\tau$ and high clock accuracy $N \geq M^2$ guarantees that the clock is in the state with exactly M ticks. Waiting for longer, e.g., $\tau \geq 2M\tau$ would allow for relaxing the condition $N \geq M^2$ on the accuracy to the weaker requirement $N \gg 1$. Let us work in the latter regime and write $P[N(t) = M] = 1 - \varepsilon$, where we remember that $\varepsilon = O\left(\exp\left(-c\sqrt{N}M/2\right)\right)$ as $N \gg 1$. This also implies due to normalization $\sum_n P[N(t) = n] = 1$ that $P[N(t) < M] = \varepsilon$ is small. With this, we can approximate the state $\rho_T(t)$ in Eq. (A85) by the term $n = M$ resulting in the following expression:

$$\rho_T(t) = \int dt_1 \cdots dt_M p[\Gamma_M] \rho(t|\Gamma_M) + O(\varepsilon) \quad (\text{A91})$$

$$= \int d\tau_1 \cdots d\tau_M P[T_{0,1} = \tau_1, \dots, T_{M-1,M} = \tau_M, T_M \leq t] \rho(t|\Gamma_M) + O(\varepsilon) \quad (\text{A92})$$

$$= \int d\tau_1 \cdots d\tau_M P[T_{0,1} = \tau_1, \dots, T_{M-1,M} = \tau_M] \rho(t|\Gamma_M) + O(\varepsilon) \quad (\text{A93})$$

$$= \int d\tau_M P[\tau_M] V_{(\tilde{M})}(\tau_M) \left(\int d\tau_{M-1} \cdots \left(\int d\tau_1 P[\tau_1] V_{(\tilde{1})}(\tau_1) \rho_T^{\text{init}} V_{(\tilde{1})}(\tau_1) \right) \cdots \right) V_{(\tilde{M})}(\tau_M)^\dagger + O(\varepsilon) \quad (\text{A94})$$

where we have used the result from Eq. (A90) in the step to Eq. (A93), which is simply another instance where we use the fact that at time $t \geq 2M\tau$, the contributions from the cases where the aQPU finishes after time t are extremely small and can be bounded by ε . A brief note on the notation in Eqs. (A91) to (A94): the random variables $T_{0,1}, \dots, T_{M-1,M}$ are the M i.i.d. copies of the tick time random variable T . They describe the time between to adjacent ticks as introduced in Eq. (35) of the main text. Between line (A91) and (A92) we switch from the picture of tick times (T_k, t_k) to the picture of the time between ticks, $(T_{k-1,k}, \tau_k)$. Throughout this appendix we will do this step without explicitly mentioning it everytime. In the final line of our derivation here (A94), we denote by $P[\tau_k] = P[T = \tau_k]$ the probability that the time between tick $k-1$ and tick k equals τ_k . It is possible to factorize the equations because the ticks are assumed to be independent. Finally, the unitaries $V_{(\bar{k})}$ are actually generated by the Hamiltonians corresponding to the program \mathcal{A} ,

$$V_{(\bar{k})}(\tau_k) = \exp\left(-iH_T^{(a_{k-1})}\tau_k\right), \quad (\text{A95})$$

evolved for some time τ_k . In this form, we see that approximately, the aQPU acts like a concatenation of mixed unitary channels on the target system, and we can prove the following Prop. 2:

Proposition 2 (Clock channel). *The i.i.d. recursion relation in Eq. (43) for the case of exponentially concentrated tick time T in the high accuracy limit N can be approximated as*

$$\int dt P[t] V_{(k)}(t) \rho V_{(k)}(t)^\dagger = V_T^{(k)} \rho V_T^{(k)\dagger} + O\left(\frac{\tau^2 \|H_T^{(k)}\|^2}{N}\right). \quad (\text{A45})$$

We abbreviate the probability distribution for a single tick with $P[t] = P[T = t]$, and $V_T^{(k)}$ is the Hamiltonian $H_T^{(k)}$ evolved for exactly the desired duration τ as in (2).

Proof. The result follows immediately by using the trick from Lemma 7. We provide the explicit prefactors up to the second order expansion beyond the Eq. (45), and notice the following points: in Lemma 7, the mean of the distribution was assumed to be in the origin; by shifting both the random variable as well as the function f , we can generalize to $\langle T \rangle = \tau > 0$. Our function f is given by

$$f(t) = V_{(k)}(t) \rho V_{(k)}(t)^\dagger, \quad (\text{A96})$$

and is naturally whole and the derivatives are nested commutators with the Hamiltonian such that we can generically bound

$$\left|f^{(n)}(\tau)\right| \leq \|H_T^{(k)}\|^n. \quad (\text{A97})$$

Inserting this into Lemma 7, we find the following result:

$$\int dt P[t] V_{(k)}(t) \rho V_{(k)}(t)^\dagger = V_T^{(k)} \rho V_T^{(k)\dagger} - \frac{\tau^2}{2N} \left[H_T^{(k)} \left[H_T^{(k)}, \rho \right] \right] + O\left(\frac{\tau^3 \|H_T^{(k)}\|^3}{N^{3/2}}\right), \quad (\text{A98})$$

in the limit of high clock accuracy $N \gg \tau^2 \|H_T^{(k)}\|^2$. This was all we intended to prove. \square

We are now in a position to conclude the prove of Cor. 1 from the main text, quantifying the overall fidelity for the computation. For convenience, we repeat:

Corollary 1 (Program fidelity for non-ideal clocks). *For an aQPU with master clock producing exponentially concentrated i.i.d. ticks at accuracy $N \gg M, M\phi_{\max}^2$, the final program fidelity $\mathcal{F}_{\mathcal{A}}$ for any program \mathcal{A} of length less or equals M is given by*

$$\mathcal{F}_{\mathcal{A}} = 1 - O\left(\frac{M}{N} \phi_{\max}^2\right). \quad (\text{A48})$$

Proof. Using Eq. (A94) together with the result from Prop. 2 yields the desired statement. To be more precise, we can introduce a maximum angle of rotation ϕ_{\max} as in Eq. (40) of the main text to upper bound all the contributions from Prop. 2 by one number. All-in-all, the leading order terms will be given by

$$\rho_T(t) = V_{\mathcal{A}} \rho_T^{\text{init}} V_{\mathcal{A}}^\dagger + O\left(\frac{M}{N} \phi_{\max}^2\right) + O(\varepsilon). \quad (\text{A99})$$

The contribution $O(\varepsilon)$ vanishes exponentially in N , hence, we can drop it and conclude the proof of the corollary.. \square

Now we have proven Prop. 2 and Cor. 1 under the assumption that our clock produces exponentially concentrated ticks at high accuracy $N \gg 1$. Furthermore, we have worked with the expression for the target system's state $\rho_T^{(n)}(t)$ from Eq. (A85), which uses a stochastic unravelling of the master-equation [98, 99]. To clear up any doubt, we will justify and prove the assumptions made in the following two steps providing further details on the formalism used.

Step 2. In Eq. (A85), we have given an expression for the target system's state $\rho_T^{(n)}(t)$ at time t , conditioned on n ticks having occurred. For completeness, we verify in this step that the expression as defined in (A85) indeed equals the one found through the equations of motion (27) and Prop. 1. If we manage to show that

$$\rho_T^{(n)}(t) := \int dt_1 \dots dt_n p[\Gamma_n | N(t) = n] \rho(t | \Gamma_n) \quad (\text{A100})$$

satisfies Eq. (27), then we are done. Equivalently, we can look at the equations of motion for $P[N(t) = n] \rho_T^{(n)}(t)$,

which may be simpler to determine,

$$\begin{aligned} \frac{d}{dt} \left(P[N(t) = n] \rho_T^{(n)}(t) \right) &\stackrel{(27)}{=} -P[T_{n+1} = t] \rho_T^{(n)}(t) \\ &\quad - iP[N(t) = n] \left[H_T^{(a_n)}, \rho_T^{(n)} \right] + P[T_n = t] \rho_T^{(n-1)}(t). \end{aligned} \quad (\text{A101})$$

$$\frac{d}{dt} \left(P[N(t) = n] \rho_T^{(n)}(t) \right) = \frac{d}{dt} \int dt_1 \cdots dt_n P[T_1 = t_1, \dots, T_n = t_n \leq t \leq T_{n+1}] \rho_T(t|\Gamma_n) \quad (\text{A102})$$

$$= \frac{d}{dt} \int_0^t dt_n \int dt_1 \cdots dt_{n-1} P[T_1 = t_1, \dots, T_n = t_n, t \leq T_{n+1}] \rho_T(t|\Gamma_n) \quad (\text{A103})$$

$$= \int dt_1 \cdots dt_{n-1} P[T_1 = t_1, \dots, T_{n-1} = t_{n-1}, T_n = t] \rho_T(t|\Gamma_{n-1}) \quad (\text{A104})$$

$$+ \int_0^t dt_n \int dt_1 \cdots dt_{n-1} \left(\frac{d}{dt} P[T_1 = t_1, \dots, T_n = t_n, t \leq T_{n+1}] \right) \rho_T(t|\Gamma_n) \quad (\text{A105})$$

$$+ \int_0^t dt_n \int dt_1 \cdots dt_{n-1} P[T_1 = t_1, \dots, T_n = t_n, t \leq T_{n+1}] \left(\frac{d}{dt} \rho_T(t|\Gamma_n) \right). \quad (\text{A106})$$

We notice that there are exactly three terms appearing in the time-derivative, Eq. (A104) which we will show to equal $P[T_n = t] \rho_T^{(n-1)}(t)$, then Eq. (A105) to be equals the expression $-P[T_{n+1} = t] \rho_T^{(n)}(t)$ and finally Eq. (A106) that will yield the commutator with the Hamiltonian $-iP[N(t) = n] \left[H_T^{(a_n)}, \rho_T^{(n)} \right]$. Let us investigate this term by term, starting with the last one, Eq. (A106):

$$\begin{aligned} \frac{d}{dt} \rho(t|\Gamma_n) &= \frac{d}{dt} V_{(a_n)}(t - t_n) \rho(t_n|\Gamma_{n-1}) V_{(a_n)}^\dagger(t - t_n) \\ &= -i \left[H_T^{(a_n)}, \rho(t|\Gamma_n) \right]. \end{aligned} \quad (\text{A107})$$

In Eq. (A106), we can simply switch the commutator and all the integrals and upon factoring out the conditional probability $P[N(t) = n]$, we find exactly the desired ex-

pression, Let us take the time derivative of the expression in Eq. (A100) times $P[N(t) = n]$, and examine the result term by term:

$$(\text{A106}) = -iP[N(t) = n] \left[H_T^{(a_n)}, \rho_T^{(n)}(t) \right]. \quad (\text{A108})$$

We have thus recovered the part in the equations of motion that generate the unitary evolution. For the two remaining terms, we have to take one step back and examine where the probability $P[T_1 = t_1, \dots, T_n = t_n]$ comes from: the master equation evolution of the clock state together with the tick register $\rho_{CH}(t)$ defines the probability distribution of the tick times. By looking at the trajectories of the clock together with the tick register we can calculate the tick probabilities appearing in Eqs. (A104) and (A105), which will ultimately allow us to show that the derivative reduces to the equation of motion shown in (A101). Let us look at the trajectory of $\rho_{CH}(t|\Gamma_n)$ in a recursive way,

$$\rho_{CH}(t|\Gamma_n) = \exp \left(\mathcal{L}_{CH}^{\text{eff},(n)}(t - t_n) \right) \left[J_C^{(n-1)} \otimes |n\rangle\langle n-1|_H \left(\rho_{CH}(t_n|\Gamma_{n-1}) \right) J_C^{(n-1)\dagger} \otimes |n-1\rangle\langle n|_H \right], \quad (\text{A109})$$

where initially $\rho_{CH}(t|\Gamma_0) = \rho_C^{\text{init}} \otimes |0\rangle\langle 0|_H$. The superoperator $\mathcal{L}_C^{\text{eff},(n)}$ is given by the usual clock Lindbladian \mathcal{L}_{cw} and tick contribution $\mathcal{L}_{\text{tick}}$, but with the tick generation operators unravelled, i.e., we write

$$\mathcal{L}_C^{\text{eff},(n)} = \mathcal{L}_{\text{cw}} - \frac{1}{2} \left\{ J_C^{(n)\dagger} J_C^{(n)} \otimes |n\rangle\langle n|_H, \cdot \right\}. \quad (\text{A110})$$

By taking the trace of the state $\rho_{CH}(t|\Gamma_n)$, we get the probability distribution of the tick times in the trajectory,

$$\begin{aligned} \text{Tr} \{ \rho_{CH}(t|\Gamma_n) \} &= P[\Gamma_n] \\ &= P[T_1 = t_1, \dots, T_n = t_n, T_{n+1} \geq t]. \end{aligned} \quad (\text{A111})$$

Furthermore by taking the derivative of (A111) with respect to t we find the probability distribution $-P[T_1 =$

$t_1, \dots, T_n = t_n, T_{n+1} = t]$ using the expression on the right-hand side, and taking the derivative of the state in (A109), we find the explicit expression

$$\begin{aligned} \frac{d}{dt} \text{Tr} [\rho_{CH}(t|\Gamma)] &= -\text{Tr} \left[J_{CH}^{(n)} \rho_{CH}(t|\Gamma_n) J_{CH}^{(n)\dagger} \right] \\ &= -P[T_1 = t_1, \dots, T_{n+1} = t]. \end{aligned} \quad (\text{A112})$$

where we have defined $J_{CH}^{(n)} = J_C^{(n)} \otimes |n+1\rangle\langle n|_H$. By summing the expression $\rho_{CH}(t|\Gamma_n)$ in Eq. (A109) over all possible trajectories Γ_n for fixed n , we claim to find the same state that we would obtain by integrating the aQPU masterequation with Lindbladian $\mathcal{L}_{\text{aQPU}}$. To be precise, we claim that

$$\rho_{CH}^{(n)}(t) = \int_{0 \leq t_1 \leq \dots \leq t_n \leq t} dt_1 \cdots dt_n \rho_{CH}(t|\Gamma_n). \quad (\text{A113})$$

To prove this equality, we take the derivative with respect to the parameter time t and we find that indeed,

$$\dot{\rho}_{CH}^{(n)}(t) = J_{CH}^{(n-1)\dagger} \rho_{CH}^{(n-1)}(t) J_{CH}^{(n-1)} + \mathcal{L}_{CH}^{\text{eff},(n)} \rho_{CH}^{(n)}(t), \quad (\text{A114})$$

as we also obtain from the equations of motion given by $\mathcal{L}_{\text{aQPU}}$ in (19) projected onto the tick register state $|n\rangle\langle n|_H$. This proves the relation (A111) together with using Lemma 3. More generally such an expression would follow from known results on the relationship between traces of quantum trajectory states and trajectory probabilities which are documented already in the literature, see for example [98, 99]. We use these results at hand and express the two terms in (A104) and (A105) using the trace of $\rho_{CH}(t|\Gamma_n)$ as detailed in Eq. (A111),

$$(\text{A104}) = \int_{t_1 \leq \dots \leq t_{n-1} \leq t} dt_1 \cdots dt_{n-1} \text{Tr} \left[J_{CH}^{(n-1)} \rho_{CH}(t|\Gamma_{n-1}) J_{CH}^{(n-1)\dagger} \right] \rho_T(t|\Gamma_{n-1}) \quad (\text{A115})$$

$$= \text{Tr}_{CH} \left[J_{CH}^{(n-1)} \left(\int_{t_1 \leq \dots \leq t_{n-1} \leq t} dt_1 \cdots dt_{n-1} \rho_{CH}(t|\Gamma_{n-1}) \otimes \rho_T(t|\Gamma_{n-1}) \right) J_{CH}^{(n-1)\dagger} \right] \quad (\text{A116})$$

$$= \text{Tr}_{CH} \left[J_{CH}^{(n-1)} \left(\rho_{CH}^{(n-1)}(t) \otimes \rho_T^{(n-1)}(t) \right) J_{CH}^{(n-1)\dagger} \right] \quad (\text{A117})$$

$$= P[T_n = t] \rho_T^{(n-1)}(t). \quad (\text{A118})$$

Note that the step from (A116) to (A117) is not is not trivial. To work, it requires Lemma 1 and the generalization of the equality (A113) to the case where the system T is included. To show this, we can use the Eq. (A114) but modified to include the interaction terms with T . All-in-all, the expression in Eq. (A118) correctly cancels the last term appearing in Eq. (A101) as we desired. Similaly, we can show

$$(\text{A105}) = - \int_{t_1 \leq \dots \leq t_n \leq t} dt_1 \cdots dt_n \text{Tr} \left[J_{CH}^{(n)} \rho_{CH}(t|\Gamma_n) J_{CH}^{(n)\dagger} \right] \rho_T(t|\Gamma_n) \quad (\text{A119})$$

$$= -\text{Tr}_{CH} \left[J_{CH}^{(n)} \left(\int_{t_1 \leq \dots \leq t_n \leq t} dt_1 \cdots dt_n \rho_{CH}(t|\Gamma_n) \otimes \rho_T(t|\Gamma_n) \right) J_{CH}^{(n)\dagger} \right] \quad (\text{A120})$$

$$= -P[T_{n+1} = t] \rho_T^{(n)}(t), \quad (\text{A121})$$

using the same arguments as for Eq. (A104). This cancels the last remaining term in (A101), and proves that (A102) indeed reduces to the usual equations of motion for $\rho_T^{(n)}(t)$. What we have proven with this statement is that the target system's state as defined in Eq. (A100) is the same as obtained from the recursion relation in Prop. 1 by uniqueness of the solution to the equation of motion given the same initial conditions.

Step 3. After having successfully argued in the previous two steps how Prop. 2 and Cor. 1 come about, we check the validity of the assumptions that have lead to these results. In particular, we want to check

- Under which conditions is a family of clocks with unbounded accuracy N exponentially concentrated as assumed in Eq. (A88)?
- Which examples of quantum clocks exhibit this behavior?

Let us start with the first item, and we remind ourselves of the assumption that we consider clocks producing i.i.d. ticks. Following the results in [21], we can express the cumulative probability distribution $P[T \geq t]$ as follows,

$$P[T \geq t] = \exp \left(-\Gamma \int_0^t dt' f(t') \right), \quad (\text{A122})$$

where $\Gamma = \max_{\rho} \text{Tr} \left[J_C^{\dagger} J_C \rho \right]$ is the maximum rate of the clock's tick generating channel, and $f(t)$ some func-

tion with values in $[0, 1]$ describing the conditional tick probability of the clock. This form already reveals the main reason why we would expect exponential concentration of the clock's ticks: the tail for $t \rightarrow \infty$ of the distribution is naturally exponentially suppressed because the tick generating process is exponential decay, and for $t \rightarrow -\infty$, the distribution is bounded because by definition the tick must happen after $t \geq 0$. For the purpose here, we are interested in a family of such clocks, where the clock's average tick time is fixed to τ but the decay rate Γ is growing, giving a growing clock accuracy N which is proportional to Γ^2/τ^2 . Looking at the left tails to bound $P[T \leq \tau - t]$ for $t \geq 0$, we notice that $P[T \leq 0] = 0$ by definition, which reduces the problem of finding an exponential envelope to an optimization problem on the compact interval $[0, \tau]$. For the right tails of the tick probability distribution $P[T \geq \tau + t]$, where again $t \geq 0$, we notice that if there exists some constant $c > 0$ such that $f(t + \tau) \geq c$ for all $t \geq 0$, then we can bound $P[T \geq \tau + t]$ from above using the exponential envelope $e^{-c\Gamma t}$. The exponent can be rewritten in terms of the clock accuracy to yield $e^{-c'\sqrt{N}t/\tau}$, where the constant c' is chosen to satisfy $c'\sqrt{N} = c\Gamma\tau$. The parameter α in the definition for exponential probability concentration in Eq. (A88) can now be chosen such that the sum of the left and right tail are bounded by $\alpha e^{-c'\sqrt{N}t/\tau}$, which may be understood as a general recipe to examine whether a family of tick probability distributions satisfies exponential concentration.

Going towards the second item, we want to consider clocks which do indeed exhibit an exponential concentration of their tick probability according to Eq. (A88). Given the framework introduced in Sec. II B of the main text, the most basic clock is the one whose tick distribution is exponential decay, $P[T \geq t] = e^{-\Gamma t}$. A modification which improves this clock's accuracy is concatenating several ticks and say have only every k th decay count as an actual tick, but to ensure that the average time between two ticks that we count stays the same, we replace $\Gamma \rightarrow k\Gamma$. The resulting probability distribution is given by the sum of k i.i.d. exponential random variables with same rate $k\Gamma$, which is also known as the Erlang distribution [100],

$$P[T_{(k)} \geq t] = \sum_{n=0}^{k-1} \frac{(k\Gamma t)^n}{n!} \exp(-k\Gamma t). \quad (\text{A123})$$

A clock with this cumulative tick distribution has accuracy $N = k$ at average tick time $\langle T_{(k)} \rangle = \tau = 1/\Gamma$. Since T is exponentially concentrated almost by definition with parameters $\alpha = 2$, and $c = \Gamma$, we can use Lemma 6 with a small change (see, e.g., Thm. 1.13 in [51]) to account for the rescaling $\Gamma \rightarrow k\Gamma$ to yield

$$P[|T_{(k)} - \tau| \geq t] \leq 2 \exp\left(-\frac{N}{2} \min\left\{\frac{t}{\tau}, \frac{t^2}{\tau^2}\right\}\right), \quad (\text{A124})$$

with $N = k$ the accuracy. While this is slightly different from the assumptions in Lemma 7 for $t \leq \tau$, the first order correction in Prop. 2 hold for this tick distribution, because in the asymptotic limit, for $t \geq \tau$, the tails of the distribution are again bounded by the exponential. For an illustration how this clock can be used for the aQPU, we refer the reader to Sec. III E and Figs. 5 and 6 where an example is simulated numerically.

4. Proofs for speed of computation and fidelity

In this section we provide the proof to Cor. 2 about the trade-off between two error sources in gate-compilation with an imperfect clock.

Corollary 2 (Compiling with finite resources). *An aQPU featuring a master clock generating exponentially concentrated i.i.d. ticks in the limit of high accuracy $N \gg 1$ and access to a finite set of Hamiltonians which generate a universal gate set \mathcal{V} for $\text{SU}(2)$, can approximate any $U \in \text{SU}(2)$ using a program $\mathcal{A} = (a_0, \dots, a_{L-1})$ of L unitaries $V_{\mathcal{A}} = V_T^{(a_{L-1})} \dots V_T^{(a_0)}$ with error*

$$\|U|0\rangle\langle 0|_T U^\dagger - \rho_T^{\mathcal{A}}\|_1 \leq O\left(e^{-\alpha L^{1/c}}\right) + O\left(\frac{L}{N} \phi_{\max}^2\right) \quad (60)$$

where α and c are constants. The state $\rho_T^{\mathcal{A}}$ is the target system's state for the aQPU with program \mathcal{A} evaluated at time $t \gg L\tau$.

Proof. Let the aQPU have access to a finite set \mathcal{V} of K Hamiltonians which generate a dense subset of unitaries (\mathcal{V}) in $\text{SU}(2)$. Furthermore, we look at an aQPU with clock accuracy N satisfying the fidelity relationship from Cor. 1 given a program length $L \equiv M$. If we want to execute a unitary $U \in \text{SU}(2)$ on a qubit having access only to the elementary gates in \mathcal{V} , the Solovay-Kitaev Theorem implies that this is possible approximately with an error $\varepsilon > 0$ using a product $V_{\mathcal{A}} = V_T^{(a_{L-1})} \dots V_T^{(a_0)}$, where $V_T^{(a_\ell)} \in \mathcal{V}$ and $\mathcal{A} = (a_0, \dots, a_{L-1})$ is the program of the aQPU. The error is quantified such that the distance between target unitary U and the compiled program $V_{\mathcal{A}}$ is bounded by $\|V_{\mathcal{A}} - U\|_\infty \leq \varepsilon$ where the error ε and the length L of the program are related via $L = O(\log^c(1/\varepsilon))$ for some constant $c > 0$ that is independent of the desired gate.

The quantity we actually want to calculate is the distance between $U|0\rangle\langle 0|_T$ and the state $\rho_T^{\mathcal{A}}$ that the aQPU with imperfect clock can generate. To this end, we consider the trace distance between the target unitary U applied to an initial state $|0\rangle\langle 0|_T$ and the approximation executed on the aQPU

$$\begin{aligned} \|U|0\rangle\langle 0|_T U^\dagger - \rho_T^{\mathcal{A}}\|_1 &\leq \|U|0\rangle\langle 0|_T U^\dagger - V_{\mathcal{A}}|0\rangle\langle 0|_T V_{\mathcal{A}}^\dagger\|_1 \\ &\quad + \|V_{\mathcal{A}}|0\rangle\langle 0|_T V_{\mathcal{A}}^\dagger - \rho_T^{\mathcal{A}}\|_1, \end{aligned} \quad (\text{A125})$$

where we have used a midpoint trick and a triangle inequality to split this distance into the first term which captures the quality of the approximation and a second term which captures how well the aQPU executes the approximation program. The trace-distance used here is defined as

$$\|\rho - \sigma\|_1 := \frac{1}{2} \text{Tr} \left[\sqrt{(\rho - \sigma)^\dagger (\rho - \sigma)} \right]. \quad (\text{A126})$$

Focusing on the second term, we may readily apply Prop. 2 to obtain

$$\left\| V_{\mathcal{A}} |0\rangle\langle 0|_T V_{\mathcal{A}}^\dagger - \rho_T^{\mathcal{A}} \right\|_1 = O \left(\frac{L}{N} \phi_{\max}^2 \right) \quad (\text{A127})$$

since $\rho_T^{\mathcal{A}} = V_{\mathcal{A}} |0\rangle\langle 0|_T V_{\mathcal{A}}^\dagger + O \left(\frac{L}{N} \phi_{\max}^2 \right)$ by Eq. (47). This leaves the first term which we bound by considering that the approximation is guaranteed to satisfy $\|U - V_{\mathcal{A}}\|_\infty \leq \varepsilon$ by the Solovay-Kitaev Theorem [42]. By definition of the Schatten ∞ -norm we have

$$\begin{aligned} \varepsilon &\geq \|U - V_{\mathcal{A}}\|_\infty = \sup_{|\psi\rangle \in \mathcal{H}} \|(U - V_{\mathcal{A}})|\psi\rangle_T\|_2 \quad (\text{A128}) \\ &= \sup_{|\psi\rangle \in \mathcal{H}} \sqrt{\langle \psi | (U^\dagger - V_{\mathcal{A}}^\dagger)(U - V_{\mathcal{A}}) | \psi \rangle_T}. \end{aligned}$$

Squaring both sides and making use of the definition of the supremum we obtain

$$\begin{aligned} \varepsilon^2 &\geq \sup_{|\psi\rangle \in \mathcal{H}} \langle \psi | (U^\dagger - V_{\mathcal{A}}^\dagger)(U - V_{\mathcal{A}}) | \psi \rangle_T \\ &= \langle 0 | (U^\dagger U + V_{\mathcal{A}}^\dagger V_{\mathcal{A}} - U^\dagger U_{\mathcal{A}} - V_{\mathcal{A}}^\dagger U) | 0 \rangle_T \\ &= 2 \left(1 - \Re \{ \langle 0 | U^\dagger V_{\mathcal{A}} | 0 \rangle_T \} \right) \\ &\geq 2 \left(1 - |\langle 0 | U^\dagger V_{\mathcal{A}} | 0 \rangle_T| \right), \quad (\text{A129}) \end{aligned}$$

where we have used $\Re\{z\} \leq |z|, \forall z \in \mathbb{C}$ in the last inequality. By multiplying and dividing Eq. (A129) by the same factor $1 + |\langle 0 | U^\dagger V_{\mathcal{A}} | 0 \rangle_T|$, we get

$$\varepsilon^2 \geq 2 \left(\frac{1 - |\langle 0 | U^\dagger V_{\mathcal{A}} | 0 \rangle_T|^2}{1 + |\langle 0 | U^\dagger V_{\mathcal{A}} | 0 \rangle_T|} \right). \quad (\text{A130})$$

Since states are normalized, Cauchy-Schwarz implies that $1 \geq |\langle 0 | U^\dagger V_{\mathcal{A}} | 0 \rangle_T|$ and we can further bound

$$\varepsilon^2 \geq 1 - |\langle 0 | U^\dagger V_{\mathcal{A}} | 0 \rangle_T|^2, \quad (\text{A131})$$

which will allow us to complete our proof. The trace distance of two pure states $|\psi\rangle, |\phi\rangle$ simplifies to $\| |\psi\rangle\langle\psi| - |\phi\rangle\langle\phi| \|_1 = \sqrt{1 - |\langle\psi|\phi\rangle|^2}$ and so the first contribution to Eq. (A125) reduces to

$$\left\| U |0\rangle\langle 0|_T U^\dagger - V_{\mathcal{A}} |0\rangle\langle 0|_T V_{\mathcal{A}}^\dagger \right\|_1 = \sqrt{1 - |\langle 0 | U^\dagger V_{\mathcal{A}} | 0 \rangle_T|^2} \quad (\text{A132})$$

and so by Eq. (A131) we can bound the contribution by

$$\left\| U |0\rangle\langle 0|_T U^\dagger - V_{\mathcal{A}} |0\rangle\langle 0|_T V_{\mathcal{A}}^\dagger \right\|_1 \leq \varepsilon, \quad (\text{A133})$$

giving the desired result as a combination of Eqs. (A127) and (A133),

$$\|U |0\rangle\langle 0| U^\dagger - \rho_T^{\mathcal{A}}\|_1 \leq \varepsilon + O \left(\frac{L}{N} \phi_{\max}^2 \right), \quad (\text{A134})$$

a modified Solovay-Kitaev theorem. This shows that whilst any unitary can be approximated with an error ε that scales inversely in the length L of the approximation, finite thermodynamic resources introduce errors which scale with the length of the approximation. The Solovay-Kitaev construction gives $L = O(\log^c(1/\varepsilon))$ as the inverse scaling relationship and can be derived from the inequality given in [41, 101]

$$L < \frac{5}{4} \left(\frac{\log(1/C^2\varepsilon)}{\log(1/C\varepsilon_0)} \right)^c L_0, \quad (\text{A135})$$

where L_0 is the length of an initial guess approximation with error ε_0 from which Solovay-Kitaev algorithm starts, c is a bounded constant depending on the choice of compiling algorithm but independent of the desired gate and C is an error scaling constant. Inverting this inequality one obtains

$$\varepsilon < \frac{1}{C^2} \exp \left(\log \left(\frac{1}{C\varepsilon_0} \right) \left(\frac{4L}{5L_0} \right)^{1/c} \right), \quad (\text{A136})$$

meaning that the error ε in the gate approximation scales with the length of the approximation L as $\varepsilon = \mathcal{O}(\exp(-\alpha L^{1/c}))$, where $\alpha > 0$ is a constant. The modified Solovay-Kitaev theorem can now be stated as

$$\|U |0\rangle\langle 0| U^\dagger - \rho_T^{\mathcal{A}}\|_1 \leq O \left(\exp(-\alpha L^{1/c}) \right) + O \left(\frac{L}{N} \phi_{\max}^2 \right),$$

where the first contribution corresponding to the error ε in the approximation decays exponentially fast with the length $L^{1/c}$ of the approximation. The second contribution grows in L because the errors from the aQPU approximation of the program \mathcal{A} add up the longer the program and thus this error scales linearly with L , which is all we wanted to show. \square

Appendix B: Additional details on the numerics of the Bell-state example

In this appendix we provide additional details about Sec. III E, particularly how the Figs. 5 and 6 have been generated. All the numerical methods we here refer to are available freely on the GitHub repository [71] in the version used to generate this paper's figures.

Setup. When modeling the aQPU explicitly for an example, we have to make a choice about which family of clocks we want to use for timing the gates and which gate-set we encode. Since the goal is to generate a Bell-state of two qubits initially starting in their $|0\rangle$ state, the set of gates we want to have access to is given by

$\mathcal{V} = \{U_{\text{H}} \otimes \mathbb{1}_2, U_{\text{CNOT}}\}$, the Hadamard gate U_{H} and the CNOT gate U_{CNOT} ,

$$U_{\text{H}} = \frac{1}{\sqrt{2}} \begin{bmatrix} 1 & 1 \\ 1 & -1 \end{bmatrix}, \quad U_{\text{CNOT}} = \begin{bmatrix} 1 & 0 & 0 & 0 \\ 0 & 1 & 0 & 0 \\ 0 & 0 & 0 & 1 \\ 0 & 0 & 1 & 0 \end{bmatrix}. \quad (\text{B1})$$

These two gates are generated by the Hamiltonians

$$H_{\text{H}} = -\frac{\pi}{2} (\mathbb{1}_2 - U_{\text{H}}), \quad (\text{B2})$$

for the Hadamard gate U_{H} , and

$$H_{\text{CNOT}} = \frac{\pi}{2} \begin{bmatrix} 0 & 0 \\ 0 & 1 \end{bmatrix} \otimes \begin{bmatrix} 1 & -1 \\ -1 & 1 \end{bmatrix}. \quad (\text{B3})$$

To be explicit, the Hamiltonians are related to the gates via $U_{\text{H}} = \exp(-iH_{\text{H}})$ and $U_{\text{CNOT}} = \exp(-iH_{\text{CNOT}})$. The punch card state as from Def. 2 which encodes our desired program can be made up of the three states $|0\rangle_{\text{R}}$ for the idle state, $|\text{C}\rangle_{\text{R}}$ for the CNOT gate and $|\text{H}\rangle_{\text{R}}$ for the Hadamard gate. Note that the dimension of this punch card state is not exhaustive for the set of mentioned Hamiltonians for which in principle one could also apply the Hadamard gate to the second qubit and apply the CNOT with qubit number two instead of one as the control. To keep the description minimal, we stick with the instruction set that only encodes the two required operations and idling.

As for the master clock, we work with the example given in [20]. Physically, this quantum clock is made-up of a D -dimensional ladder and a two-qubit heat engine. The engine is coupled to two out-of-equilibrium heat baths that drive up the ladder's state until it decays and generates a tick. The dynamics of this clock are well approximated by what is called the *Erlang-clock*, also discussed as an example at the end of Appendix A 3, see Eq. (A123). This clock is run by a sequence of exponential decays of the same rate Γ such that only every D th decay is counted as an actual tick of the clock. Modeling this clock requires a clockwork of dimension D , with

internal state-space given by $|0\rangle_{\text{C}}, \dots, |D-1\rangle_{\text{C}}$. As for the evolution, we have jump processes $|k\rangle_{\text{C}} \rightarrow |k+1\rangle_{\text{C}}$ that can be described with a Lindblad jump operator

$$L_{\text{C}} = D \sum_{k=0}^{D-2} |k+1\rangle\langle k|_{\text{C}}. \quad (\text{B4})$$

Here, we have chosen unitless time, and a jump rate that increases with the dimension D of the clockwork. The operator L_{C} describes the incoherent jumps from $|0\rangle_{\text{C}}$ all the way up to $|D-1\rangle_{\text{C}}$. Given that the clock initially starts in $|0\rangle\langle 0|_{\text{C}}$, this evolution is entirely classical, which simplifies the computational resources required for the numerical analysis. The jump operator (B4) scales with D to ensure that the average time until one clock-cycle is completed is always 1, regardless of how large D is. For larger dimension D , the clock has to jump through more levels, but the larger the prefactor, the faster the clock cycles through these levels. One part that is still missing to close the clock cycle, that is, once the clock reaches $|D-1\rangle_{\text{C}}$ bringing the state back down to $|0\rangle_{\text{C}}$, is the clock's tick. To solve this problem, we introduce the clock's tick register H . For our example the tick register can work with three states, $|0\rangle_{\text{H}}, |1\rangle_{\text{H}}$ and $|2\rangle_{\text{H}}$, such that we can implement the Hadamard and CNOT step needed for the Bell-state creation and one final state in which the aQPU can idle after the two previous steps. These clock's tick here is defined by

$$J_{\text{CH}} = D |0\rangle\langle D-1|_{\text{C}} \otimes \sum_{j=0}^1 |j+1\rangle\langle j|_{\text{H}}. \quad (\text{B5})$$

One can verify using (A123) that for the clock whose evolution is defined by the operators in Eqs. (B4) and (B5), the average time between two ticks is given by $\langle T \rangle \equiv \tau = 1$ and the variance by $\text{Var}[T] = \frac{1}{D}$. Hence, the clock accuracy here equals $N = D$, and we would expect for larger clockwork dimensions D , the computational fidelity to increase.

Finally, going to the interaction Hamiltonian, we are following entirely the scheme in Eq. (16), which for pedagogical completeness we write out here in detail,

$$H_{\text{int}} = |0\rangle\langle 0|_{\text{H}} \otimes (|\text{H}\rangle\langle \text{H}|_{\text{R}_1} \otimes \mathbb{1}_{\text{R}_2\text{R}_3} \otimes H_{\text{H}} + |\text{C}\rangle\langle \text{C}|_{\text{R}_1} \otimes \mathbb{1}_{\text{R}_2\text{R}_3} \otimes H_{\text{CNOT}}) \\ + |1\rangle\langle 1|_{\text{H}} \otimes (\mathbb{1}_{\text{R}_1} \otimes |\text{H}\rangle\langle \text{H}|_{\text{R}_2} \otimes \mathbb{1}_{\text{R}_3} \otimes H_{\text{H}} + \mathbb{1}_{\text{R}_1} \otimes |\text{C}\rangle\langle \text{C}|_{\text{R}_2} \otimes \mathbb{1}_{\text{R}_3} \otimes H_{\text{H}}). \quad (\text{B6})$$

After the second tick, the tick register ends in the subspace spanned by $|2\rangle_{\text{H}}$, where H_{int} does not have any support, hence the clock is idling after that final jump. To encode the program for the Bell-state generation, we will now use the following punch card state following

Def. 2,

$$|\mathcal{A}\rangle_{\text{R}} = |\text{H}, \text{C}, 0\rangle_{\text{R}}, \quad (\text{B7})$$

corresponding to the desired gate-sequence Hadamard, $U_{\text{H}} \otimes \mathbb{1}_2$ and then CNOT, U_{CNOT} . Applied to the initial

state $|0\rangle$, we would get out the state

$$|00\rangle_T \mapsto V_{\mathcal{A}} |00\rangle_T = \frac{1}{\sqrt{2}} (|00\rangle_T + |11\rangle_T) = |\Psi_+\rangle. \quad (\text{B8})$$

The goal of the aQPU evolution given by the Lindbladian $\mathcal{L}_{\text{aQPU}}$ is to approximate this state. By starting with the initial state

$$|\Psi_{\text{init}}\rangle = |0\rangle_C \otimes |0\rangle_H \otimes |\mathcal{A}\rangle_R \otimes |00\rangle_T, \quad (\text{B9})$$

and evolving the aQPU Lindbladian for some time $t = 4$, that is twice the time we would expect to be required for completing the Hadamard and CNOT gate, we get

$$\rho_T^A(t) = \text{Tr}_{CHR} [e^{t\mathcal{L}_{\text{aQPU}}} |\Psi_{\text{init}}\rangle\langle\Psi_{\text{init}}|]. \quad (\text{B10})$$

Ideally, we would find that $\rho_T^A(4)$ is approximately $|\Psi_+\rangle_T$, and quantitatively, this corresponds to minimizing the error

$$1 - \mathcal{F}_{\mathcal{A}} = 1 - \langle\Psi_+|\rho_T^A(4)|\Psi_+\rangle. \quad (\text{B11})$$

One may convince themselves using the final example in Appendix A3 that the family of clocks at hand, parametrized by $D \in \mathbb{N}$, satisfies all the assumptions by Cor. 1, which shows that as $D \rightarrow \infty$, the program fidelity $\mathcal{F}_{\mathcal{A}}$ approaches 1 asymptotically with leading error $1/D$. This scaling is also verified by the numerics presented in Fig. 6.

Numerical methods. Numerically simulating the aQPU using directly the standard Lindblad master-equation approach would be unfeasible because the dimensionality of the matrix superoperator $\mathcal{L}_{\text{aQPU}}$ is $(D \times 3 \times 3^3 \times 4)^4$. However, one can take advantage of the sparsity of the problem directly, owing the fact that the clockwork evolution is purely classical; hence, instead of working in the space of density matrices for the clock, tick register and punch card, we can use classical probability distributions, effectively improving the performance quadratically. We implement this using a matrix of dimension $D^2 \times 3^2$ for joining the clock, tick-register and punch card together, detailed on the repository [71]. For integration of $e^{t\mathcal{L}_{\text{aQPU}}}$, the library `scipy.integrate.solve_ivp` is used.

Appendix C: Generalization for backwards-ticking clocks

In Sec. III C we provided a preliminary discussion of the thermodynamic cost of running the aQPU taking into account the master clock, and state-preparation but not including the cost of tick generation. The bound we provided in that setting can be understood as a lower estimate for the entropic cost of the clock. For a tighter and more universal relationship between entropic cost and clock quality, the cost of tick generation has to be accounted for as well. Since the tick is a stochastic jump process described by the operator J_{tick} , detailed balance

implies the need for a reverse jump process J_{untick} proportional to J_{tick}^\dagger . The constant of proportionality between J_{untick} and J_{tick}^\dagger is related to the entropy production $\Delta\sigma_{\text{tick}}$ in the thermal baths mediating the jump process and given by [55, 56],

$$J_{\text{untick}} = e^{-\Delta\sigma_{\text{tick}}/2} J_{\text{tick}}^\dagger, \quad (\text{C1})$$

as already pointed out in Eq. (50) in the main text for the internal clockwork dynamics. Formally, only for divergent $\Delta\sigma_{\text{tick}} \rightarrow \infty$, this reverse process vanishes completely. In this appendix, we discuss what implications a finite value for $\Delta\sigma_{\text{tick}}$ has on the aQPU, following up on the work [45] treating this topic from a perspective on quantum clocks. The main result we discuss here are the equations of motion that describe the aQPU in the fully reversible case with finite entropy production $\Delta\sigma_{\text{tick}}$ for the tick generation, which – unsurprisingly – reduce to the established equations (27) from the main text in the limit of an irreversible clock.

Reversible clock ticks. We start this appendix with a note on the physics of clocks which *can* tick reversibly. In an everyday picture of clocks, a wall-clock for example, it is most unlikely that the second hand jumps backwards, but it is not impossible. Thermal fluctuations in the clockwork in general allow for such a process, unless the clock is run at absolute zero temperature. Nonetheless, if said clock jumps back by one second, for an observer reading the clock, time does not jump backwards by one second. The observer will simply see the clock undergoing a stochastic fluctuation in the direction opposed to its more likely path of evolution. In a similar way, we can think of the J_{untick} process in the clock description used for this work: if the master clock including the tick register are run at finite temperatures (implying finite $\Delta\sigma_{\text{tick}}$), the tick register can jump backwards. This does not mean time runs backwards, and in principle an observer measuring the tick register can detect these jumps by creating a temporal record of the register’s state. Analogous to how it would be possible to see the hand of a wall-clock jump back by one second. Nonetheless, if the interactions between the master clock, instruction register and target system are given by the state in which the tick register finds itself in, these reverse jumps affect the computation. As a result, if the clock jumps backwards it may be that the sequence of instructions from the punch card state $|\mathcal{A}\rangle_R$ that are carried out is $\dots a_n \rightarrow a_{n-1} \rightarrow a_n \rightarrow a_{n+1} \dots$ instead of $\dots a_n \rightarrow a_{n+1} \dots$ as one would usually desire. To quantitatively capture how these different processes affect the computation, we need to discuss the two points:

- How does the aQPU target system evolve in the case both forwards and backwards ticks are possible?
- What is the relationship between entropy production of the clock and the reverse tick processes?

Equations of motion. The only change to $\mathcal{L}_{\text{aQPU}}$ as defined in (18) in the main text is that we add a term corresponding to J_{untick} . We remind ourselves of how J_{tick} is defined in (8),

$$J_{\text{tick}} = \sum_{n \geq 0} J_C^{(n)} \otimes |n+1\rangle\langle n|_H, \quad (\text{C2})$$

which allows us to determine the reverse process through (C1) and the operator

$$J_{\text{untick}} = \sum_{n \geq 0} \bar{J}_C^{(n)} \otimes |n\rangle\langle n+1|_H. \quad (\text{C3})$$

Here, we have chosen that the prefactor $e^{-\Delta\sigma_{\text{tick}}/2}$ to be the same for all tick numbers $n \geq 0$, for simplicity, but in principle nothing prevents a different factor for each pair of jump operators $J_C^{(n)}, \bar{J}_C^{(n)}$. The conceptual discussion, however, does not change in that case. For the case where there is only the forward ticking process, and the ticks happen with unit probability in the infinite time limit, one can define the tick probability density $P[T_n = t]$ as done in Eq. (12). For the case where the clock's register can jump both forward and backward, the notion of a tick probability density function stops being well-defined, and one has to switch to a different picture. One immediate generalization also considered in [45] are tick currents which in our case would be given as

$$p_n(t) = \text{Tr} \left[J_C^{(n-1)\dagger} J_C^{(n-1)} \rho_C^{(n-1)}(t) \right], \quad (\text{C4})$$

for the forward tick current of the n th tick, the generalization of Eq. (12). One can think of tick currents as a tick rate, i.e., the number density of ticks per unit time, which does not necessarily have to be normalized quantity. For the reverse process, we would have

$$\bar{p}_n(t) = \text{Tr} \left[\bar{J}_C^{(n)\dagger} \bar{J}_C^{(n)} \rho_C^{(n+1)}(t) \right], \quad (\text{C5})$$

the reverse current of the n th tick. We can then follow the steps outlined already in Appendix A 2 to derive the equations of motion for the target system's state $\rho_T^{(n)}(t)$. The only change is that now, there is a new term in $\mathcal{L}_{\text{aQPU}}$ given by the dissipator $\mathcal{D}[J_{\text{untick}}] \otimes \mathbb{1}_{RT}$, and furthermore we have

$$\frac{d}{dt} P[N(t) = n] = p_n(t) - p_{n+1}(t) + \bar{p}_n(t) + \bar{p}_{n-1}(t), \quad (\text{C6})$$

instead of $d/dt P[N(t) = n] = p_n(t) - p_{n+1}(t)$ as in Eq. (11). Combining all terms together, we arrive at the equations of motion for $\rho_T^{(n)}(t)$, where a new term with prefactor $\bar{p}_n(t)$ appears as the contribution from the reverse-ticks. One consequence is that it is not possible anymore to find a recursion relation as in Prop. 1 because now $\dot{\rho}_T^{(n)}(t)$ depends not only on $\rho_T^{(n)}(t)$ and $\rho_T^{(n-1)}(t)$, but also on $\rho_T^{(n+1)}(t)$ due to the backwards ticks,

$$\dot{\rho}_T^{(n)}(t) = -i \left[H_T^{(an)}, \rho_T^{(n)}(t) \right] + \frac{1}{P[N(t) = n]} \left(p_n(t) \left(\rho_T^{(n-1)}(t) - \rho_T^{(n)}(t) \right) + \bar{p}_n(t) \left(\rho_T^{(n+1)}(t) - \rho_T^{(n)}(t) \right) \right). \quad (\text{C7})$$

As we take the limit $\Delta\sigma_{\text{tick}} \rightarrow \infty$ of divergent entropy production per unit population undergoing a tick of the clock, the term $\bar{p}_n(t) \rightarrow 0$ vanishes. For example, in the case where the tick register models a macroscopic memory where for all practical purposes one can assume $\bar{p}_n(t) = 0$, we recover the previous equations of motion from the main text.

Tick entropy production. For all the cases, where $\Delta\sigma_{\text{tick}} < \infty$ takes a finite value, the entropy production for the ticking process can be calculated from detailed balance and for a more detailed estimate of the true thermodynamic cost of the aQPU, this contribution has to be taken into account as well. Similar to the internal clockwork contribution $\Sigma_{\text{cw}}(t)$ discussed already in Sec. III C, the additional entropic contribution from the ticks can be derived as

$$\langle \dot{\Sigma}_{\text{tick}}(t) \rangle = \Delta\sigma_{\text{tick}} \text{Tr} \left[\left(J_{\text{tick}}^\dagger J_{\text{tick}} - J_{\text{untick}}^\dagger J_{\text{untick}} \right) \rho(t) \right], \quad (\text{C8})$$

and added to the other contributions coming from Eq. (52). While in the asymptotic limit of $t \rightarrow \infty$, the entropy rate (C8) approaches a constant, for timescales we are interested in, this may not be the case. In Sec. III B, we found that a high fidelity computation is possible if we satisfy $N \gg M$, i.e., the clock accuracy must be much greater than the maximum number of instructions carried out by the aQPU. For an i.i.d. clock, the accuracy N can be understood as the average number of ticks the clock produces until it goes wrong by one tick [20]; the assumption that $N \gg M$ thus implies that in the timescale $t \leq M\tau$ relevant for the aQPU, where τ is the average time between two ticks, the clock has not yet reached its steady-state. This is because for tick numbers $n \leq M$, the n th tick and the $(n+1)$ st tick probability densities still have negligible overlap. If we were to look at Eq. (C8) ignoring the contribution from J_{untick} , we could resolve the trace $\text{Tr} \left[J_{\text{tick}}^\dagger J_{\text{tick}} \rho(t) \right]$ with respect to a sum

over the tick numbers, resulting in a sum over $p_n(t)$ times $\Delta\sigma_{\text{tick}}$. Integrating over time up to $t = 2M\tau$ would give the accumulated entropy production due to the ticks of the master clock at the time we chose to evaluate the target system's state $\rho_T(2M\tau)$ (see Sec. III B). Formally, we find $\Sigma_{\text{tick}}(2M\tau) = \Delta\sigma_{\text{tick}} \int_0^{2M\tau} dt \sum_{n=0}^M p_n(t)$, which due to normalization of the $p_n(t)$ in the irreversible clock case gives $\Sigma_{\text{tick}}(2M\tau) = M\Delta\sigma_{\text{tick}} + \text{err.}$ where the error term comes from the small but non-zero probability that the clock has not yet ticked M times at time $2M\tau$. The prefactor in front of $\Delta\sigma_{\text{tick}}$ is given by M and not by $2M$ because in our model, see Sec. II B, the maximum tick number of our clock is assumed to be M .

The discussion so far has been about irreversible clocks, but working with the expression (C8) for the tick entropy production. In the truly reversible case, J_{untick} can't be set to zero, else the pre-factor $\Delta\sigma_{\text{tick}}$ would diverge as already pointed out earlier in this appendix. The analysis for the irreversible clock case can not be carried

over directly, because for example the notion of clock accuracy N has to be generalized as well as the tick probability densities. Here, we do not provide an exhaustive answer to how Σ_{tick} factors into the thermodynamic cost, though coming from a heuristic perspective, we would still expect that in the limit where the reverse tick process is strongly suppressed, the contribution of J_{untick} would still be negligible. This is also what we would expect, as for a high fidelity computation, we would intend to suppress the backwards ticks, thus $\int dt \text{Tr} \left[J_{\text{untick}}^\dagger J_{\text{untick}} \rho(t) \right]$ which is the integrated number of reverse ticks should be much smaller than 1. Hence the contribution from J_{untick} in Eq. (C8) would be negligible compared to the one from J_{tick} , leading us towards the conclusion that even in the reversible case, the tick entropy production in the limit we are interested in is given by $M\Sigma_{\text{tick}}$. Corrections to this expression are of the order of the probability that the clock has not yet ticked M times or that it has ticked backwards once, both of which we assume to be much smaller than 1.

-
- [1] A. G. Bromley, Charles babbage's analytical engine, 1838, *Annals of the History of Computing* **4**, 196 (1982).
- [2] A. M. Turing, On computable numbers, with an application to the entscheidungsproblem, *Proceedings of the London Mathematical Society* **s2-42**, 230 (1937).
- [3] P. Benioff, The computer as a physical system: A microscopic quantum mechanical hamiltonian model of computers as represented by turing machines, *Journal of Statistical Physics* **22**, 563–591 (1980).
- [4] P. Benioff, Quantum mechanical models of turing machines that dissipate no energy, *Phys. Rev. Lett.* **48**, 1581 (1982).
- [5] D. Deutsch, Quantum theory, the Church-Turing principle and the universal quantum computer, *Proceedings of the Royal Society of London Series A* **400**, 97 (1985).
- [6] E. Bernstein and U. Vazirani, Quantum complexity theory, *SIAM J. Comput.* **26**, 1411–1473 (1997).
- [7] R. P. Feynman and T. Hey, Quantum mechanical computers, in *Feynman Lectures on Computation* (CRC Press, 2023) p. 169–192.
- [8] A. Y. Kitaev, A. Shen, and M. N. Vyalyi, *Classical and Quantum Computation*, Graduate Studies in Mathematics, Vol. 47 (American Mathematical Society, 2002).
- [9] K. G. H. Vollbrecht and J. I. Cirac, Quantum simulators, continuous-time automata, and translationally invariant systems, *Phys. Rev. Lett.* **100**, 010501 (2008).
- [10] J. Bausch, T. S. Cubitt, and M. A. Ozols, The complexity of translationally invariant spin chains with low local dimension, *Annales Henri Poincaré* **18**, 3449 (2016).
- [11] S. P. Jordan, Fast quantum computation at arbitrarily low energy, *Phys. Rev. A* **95**, 032305 (2017).
- [12] J. Bausch and E. Crosson, Analysis and limitations of modified circuit-to-hamiltonian constructions, *Quantum* **2**, 94 (2018).
- [13] R. Landauer, Information is a physical entity, *Physica A: Statistical Mechanics and its Applications* **263**, 63 (1999), proceedings of the 20th IUPAP International Conference on Statistical Physics.
- [14] A. Auffèves, Quantum technologies need a quantum energy initiative, *PRX Quantum* **3**, 020101 (2022).
- [15] D. Jaschke and S. Montangero, Is quantum computing green? an estimate for an energy-efficiency quantum advantage, *Quantum Science and Technology* **8**, 025001 (2023).
- [16] F. Meier and H. Yamasaki, Energy-consumption advantage of quantum computation, *arXiv:2305.11212 [quant-ph]* (2023).
- [17] J. Goold, M. Huber, A. Riera, L. d. Rio, and P. Skrzypczyk, The role of quantum information in thermodynamics—a topical review, *Journal of Physics A: Mathematical and Theoretical* **49**, 143001 (2016).
- [18] M. T. Mitchison, Quantum thermal absorption machines: refrigerators, engines and clocks, *Contemporary Physics* **60**, 164–187 (2019).
- [19] P. Erker, *The quantum hourglass: Approaching time measurement with quantum information theory* (2014).
- [20] P. Erker, M. T. Mitchison, R. Silva, M. P. Woods, N. Brunner, and H. Marcus, Autonomous Quantum Clocks: Does Thermodynamics Limit Our Ability to Measure Time?, *Phys. Rev. X* **7**, 031022 (2017).
- [21] F. Meier, E. Schwarzthans, P. Erker, and M. Huber, Fundamental accuracy-resolution trade-off for timekeeping devices, *Phys. Rev. Lett.* **131**, 220201 (2023).
- [22] J. Xuereb, P. Erker, F. Meier, M. T. Mitchison, and M. Huber, Impact of imperfect timekeeping on quantum control, *Phys. Rev. Lett.* **131**, 160204 (2023).
- [23] H.-P. Breuer and F. Petruccione, *The Theory of Open Quantum Systems* (Oxford University Press, 2007).
- [24] J. A. M. Guzmán, P. Erker, S. Gasparinetti, M. Huber, and N. Y. Halpern, Divincenzo-like criteria for autonomous quantum machines, *arXiv:2307.08739 [quant-ph]* (2023).
- [25] E. Fredkin and T. Toffoli, Conservative logic, in *Collision-Based Computing* (Springer London, 2002) p.

- 47–81.
- [26] P. P. Hofer, M. Perarnau-Llobet, L. D. M. Miranda, G. Haack, R. Silva, J. B. Brask, and N. Brunner, Markovian master equations for quantum thermal machines: local versus global approach, *New Journal of Physics* **19**, 123037 (2017).
- [27] H. Carmichael, *Statistical methods in quantum optics : 1. Master equations and Fokker-Planck equations*, 1st ed., Texts and monographs in physics No. ISBN 9783642081330 (Berlin [u.a.] : Springer, Berlin [u.a.], 2002) pp. XXIII, 365 S., graph. Darst.
- [28] D. Walls and G. J. Milburn, eds., *Quantum Optics* (Springer Berlin Heidelberg, 2008).
- [29] G. T. Landi and M. Paternostro, Irreversible entropy production: From classical to quantum, *Rev. Mod. Phys.* **93**, 035008 (2021).
- [30] E. Schwarzthans, M. P. E. Lock, P. Erker, N. Friis, and M. Huber, Autonomous Temporal Probability Concentration: Clockworks and the Second Law of Thermodynamics, *Phys. Rev. X* **11**, 011046 (2021).
- [31] A. P. T. Dost and M. P. Woods, Quantum advantages in timekeeping: dimensional advantage, entropic advantage and how to realise them via berry phases and ultraregular spontaneous emission, [arXiv:2303.10029 \[quant-ph\]](https://arxiv.org/abs/2303.10029) (2023).
- [32] M. A. Aamir, P. J. Suria, J. A. M. Guzmán, C. Castillo-Moreno, J. M. Epstein, N. Y. Halpern, and S. Gasparinetti, Thermally driven quantum refrigerator autonomously resets superconducting qubit (2023), [arXiv:2305.16710 \[quant-ph\]](https://arxiv.org/abs/2305.16710).
- [33] E. Chitambar and G. Gour, Quantum resource theories, *Rev. Mod. Phys.* **91**, 025001 (2019).
- [34] M. Lostaglio, An introductory review of the resource theory approach to thermodynamics, *Reports on Progress in Physics* **82**, 114001 (2019).
- [35] P. Faist, M. Berta, and F. G. S. L. Brandao, Thermodynamic implementations of quantum processes, *Communications in Mathematical Physics* **384**, 1709–1750 (2021).
- [36] G. Chiribella, G. M. D’Ariano, P. Perinotti, and B. Valiron, Quantum computations without definite causal structure, *Phys. Rev. A* **88**, 022318 (2013).
- [37] V. Vilasini and R. Colbeck, General framework for cyclic and fine-tuned causal models and their compatibility with space-time, *Phys. Rev. A* **106**, 032204 (2022).
- [38] G. Rubino, L. A. Rozema, A. Feix, M. Araújo, J. M. Zeuner, L. M. Procopio, Č. Brukner, and P. Walther, Experimental verification of an indefinite causal order, *Science Advances* **3**, e1602589 (2017).
- [39] V. Vilasini and R. Renner, Embedding cyclic causal structures in acyclic space-times: no-go results for indefinite causality (2023), [arXiv:2203.11245 \[quant-ph\]](https://arxiv.org/abs/2203.11245).
- [40] A. Y. Kitaev, Quantum computations: algorithms and error correction, *Russian Mathematical Surveys* **52**, 1191 (1997).
- [41] M. A. Nielsen and I. L. Chuang, *Quantum Computation and Quantum Information*, 10th ed. (Cambridge University Press, 2010).
- [42] C. M. Dawson and M. A. Nielsen, The Solovay-Kitaev algorithm, *Quantum Info. Comput.* **6**, 81–95 (2006).
- [43] F. Meier, Performance limits of decay clocks: Fundamental accuracy and resolution limits of quantum clocks with exponential ticking mechanism (2022).
- [44] M. P. Woods, Autonomous Ticking Clocks from Axiomatic Principles, *Quantum* **5**, 381 (2021).
- [45] R. Silva, N. Nurgalieva, and H. Wilming, Ticking clocks in quantum theory, [arXiv:2306.01829 \[quant-ph\]](https://arxiv.org/abs/2306.01829) (2023).
- [46] J. Åberg, Catalytic coherence, *Phys. Rev. Lett.* **113**, 150402 (2014).
- [47] H. Ball, W. D. Oliver, and M. J. Biercuk, The role of master clock stability in quantum information processing, *npj Quantum Information* **2**, 16033 (2016).
- [48] M. P. Woods, R. Silva, and J. Oppenheim, Autonomous Quantum Machines and Finite-Sized Clocks, *Annales Henri Poincaré* **20**, 125 (2019).
- [49] M. P. Woods, R. Silva, G. Pütz, S. Stupar, and R. Renner, Quantum clocks are more accurate than classical ones, *PRX Quantum* **3**, 010319 (2022).
- [50] S. Boucheron, G. Lugosi, and P. Massart, *Concentration Inequalities: A Nonasymptotic Theory of Independence* (Oxford University Press, 2013).
- [51] P. Rigollet, Sub-gaussian random variables, in *18.S997: High Dimensional Statistics* (Massachusetts Institute of Technology, 2015) MIT OpenCourseWare.
- [52] G. E. Crooks, Entropy production fluctuation theorem and the nonequilibrium work relation for free energy differences, *Phys. Rev. E* **60**, 2721 (1999).
- [53] G. J. Milburn, The thermodynamics of clocks, *Contemporary Physics* **61**, 69 (2020).
- [54] H. Spohn, Entropy production for quantum dynamical semigroups, *Journal of Mathematical Physics* **19**, 1227–1230 (1978).
- [55] U. Seifert, Stochastic thermodynamics, fluctuation theorems and molecular machines, *Reports on Progress in Physics* **75**, 126001 (2012).
- [56] C. Maes, Local detailed balance, *SciPost Phys. Lect. Notes* , 32 (2021).
- [57] A. N. Pearson, Y. Guryanova, P. Erker, E. A. Laird, G. A. D. Briggs, M. Huber, and N. Ares, Measuring the Thermodynamic Cost of Timekeeping, *Phys. Rev. X* **11**, 021029 (2021).
- [58] P. Taranto, F. Bakhshinezhad, A. Bluhm, R. Silva, N. Friis, M. P. Lock, G. Vitagliano, F. C. Binder, T. Debarba, E. Schwarzthans, F. Clivaz, and M. Huber, Landauer Versus Nernst: What is the True Cost of Cooling a Quantum System?, *PRX Quantum* **4**, 010332 (2023).
- [59] D. Reeb and M. M. Wolf, An improved Landauer principle with finite-size corrections, *New Journal of Physics* **16**, 103011 (2014).
- [60] J. Xuereb, T. Debarba, M. Huber, and P. Erker, Quantum coding with finite thermodynamic resources, [arXiv:2311.14561 \[quant-ph\]](https://arxiv.org/abs/2311.14561) (2023).
- [61] Y. Guryanova, N. Friis, and M. Huber, Ideal Projective Measurements Have Infinite Resource Costs, *Quantum* **4**, 222 (2020).
- [62] L. Mandelstam and I. Tamm, The uncertainty relation between energy and time in non-relativistic quantum mechanics, in *Selected Papers* (Springer Berlin Heidelberg, 1991) p. 115–123.
- [63] N. Margolus and L. B. Levitin, The maximum speed of dynamical evolution, *Physica D: Nonlinear Phenomena* **120**, 188–195 (1998).
- [64] S. Deffner and S. Campbell, Quantum speed limits: from heisenberg’s uncertainty principle to optimal quantum control, *Journal of Physics A: Mathematical and Theoretical* **50**, 453001 (2017).
- [65] S. Lloyd, Ultimate physical limits to computation, *Nature* **406**, 1047–1054 (2000).

- [66] L. B. Levitin and T. Toffoli, Fundamental limit on the rate of quantum dynamics: The unified bound is tight, *Phys. Rev. Lett.* **103**, 160502 (2009).
- [67] A. K. Ekert, Quantum cryptography based on bell's theorem, *Phys. Rev. Lett.* **67**, 661 (1991).
- [68] J. Yin, Y.-H. Li, S.-K. Liao, M. Yang, Y. Cao, L. Zhang, J.-G. Ren, W.-Q. Cai, W.-Y. Liu, S.-L. Li, R. Shu, Y.-M. Huang, L. Deng, L. Li, Q. Zhang, N.-L. Liu, Y.-A. Chen, C.-Y. Lu, X.-B. Wang, F. Xu, J.-Y. Wang, C.-Z. Peng, A. K. Ekert, and J.-W. Pan, Entanglement-based secure quantum cryptography over 1,120 kilometres, *Nature* **582**, 501 (2020).
- [69] R. Demkowicz-Dobrzański, J. Kołodyński, and M. Guţă, The elusive heisenberg limit in quantum-enhanced metrology, *Nature Communications* **3**, 1063 (2012).
- [70] H. Buhman, Lukasz Czekaj, A. Grudka, M. Horodecki, P. Horodecki, M. Markiewicz, F. Speelman, and S. Strelchuk, Quantum communication complexity advantage implies violation of a bell inequality, *Proceedings of the National Academy of Sciences* **113**, 3191 (2016).
- [71] F. Meier, aQPU Numerics Code, <https://github.com/aspects-quantum/aqpu> (2024).
- [72] A. C. Barato and U. Seifert, Cost and precision of brownian clocks, *Phys. Rev. X* **6**, 041053 (2016).
- [73] C. R. Clark, H. N. Tinkey, B. C. Sawyer, A. M. Meier, K. A. Burkhardt, C. M. Seck, C. M. Shappert, N. D. Guise, C. E. Volin, S. D. Fallek, H. T. Hayden, W. G. Rellergert, and K. R. Brown, High-fidelity bell-state preparation with $^{40}\text{Ca}^+$ optical qubits, *Phys. Rev. Lett.* **127**, 130505 (2021).
- [74] M. Kjaergaard, M. E. Schwartz, A. Greene, G. O. Samach, A. Bengtsson, M. O'Keeffe, C. M. McNally, J. Braumüller, D. K. Kim, P. Krantz, M. Marvian, A. Melville, B. M. Niedzielski, Y. Sung, R. Winik, J. Yoder, D. Rosenberg, K. Obenland, S. Lloyd, T. P. Orlando, I. Marvian, S. Gustavsson, and W. D. Oliver, Programming a quantum computer with quantum instructions, *arXiv:2001.08838 [quant-ph]* (2020).
- [75] M. J. Biercuk, H. Uys, A. P. VanDevender, N. Shiga, W. M. Itano, and J. J. Bollinger, Optimized dynamical decoupling in a model quantum memory, *Nature* **458**, 996 (2009).
- [76] A. Soare, H. Ball, D. Hayes, J. Sastrawan, M. C. Jarratt, J. J. McLoughlin, X. Zhen, T. J. Green, and M. J. Biercuk, Experimental noise filtering by quantum control, *Nature Physics* **10**, 825 (2014).
- [77] W. F. Stinespring, Positive functions on c^* -algebras, *Proceedings of the American Mathematical Society* **6**, 211 (1955).
- [78] J. Watrous, *The Theory of Quantum Information* (Cambridge University Press, 2018).
- [79] G. Chiribella, G. M. D'Ariano, and P. Perinotti, Theoretical framework for quantum networks, *Phys. Rev. A* **80**, 022339 (2009).
- [80] E. Castro-Ruiz, F. Giacomini, and i. c. v. Brukner, Dynamics of quantum causal structures, *Phys. Rev. X* **8**, 011047 (2018).
- [81] P. Taranto, M. T. Quintino, M. Murao, and S. Milz, Characterising the hierarchy of multi-time quantum processes with classical memory (2023), *arXiv:2307.11905 [quant-ph]*.
- [82] N. Linden, S. Popescu, and P. Skrzypczyk, How small can thermal machines be? the smallest possible refrigerator, *Phys. Rev. Lett.* **105**, 130401 (2010).
- [83] V. Scarani, M. Ziman, P. Štelmachovič, N. Gisin, and V. Bužek, Thermalizing quantum machines: Dissipation and entanglement, *Phys. Rev. Lett.* **88**, 097905 (2002).
- [84] M. P. Woods and M. Horodecki, Autonomous quantum devices: When are they realizable without additional thermodynamic costs?, *Phys. Rev. X* **13**, 011016 (2023).
- [85] R. P. Feynman, There's plenty of room at the bottom, *Engineering and Science* **23**, 22 (1960).
- [86] M. Müller, Strongly universal quantum turing machines and invariance of kolmogorov complexity, *IEEE Transactions on Information Theory* **54**, 763–780 (2008).
- [87] C. E. Mora, H. J. Briegel, and B. Kraus, Quantum kolmogorov complexity and its applications, *International Journal of Quantum Information* **05**, 729–750 (2007).
- [88] M. Lemus, R. Faleiro, P. Mateus, N. Paunković, and A. Souto, Quantum Kolmogorov complexity and quantum correlations in deterministic-control quantum Turing machines, *Quantum* **8**, 1230 (2024).
- [89] E. Schwarzahans, F. C. Binder, M. Huber, and M. P. E. Lock, Quantum measurements and equilibration: the emergence of objective reality via entropy maximisation, *arXiv:2302.11253 [quant-ph]* (2023).
- [90] V. V. Albert, S. O. Mundhada, A. Grimm, S. Touzard, M. H. Devoret, and L. Jiang, Pair-cat codes: autonomous error-correction with low-order nonlinearity, *Quantum Science and Technology* **4**, 035007 (2019).
- [91] H. Kwon, R. Mukherjee, and M. Kim, Reversing lindblad dynamics via continuous petz recovery map, *Physical Review Letters* **128**, 10.1103/physrevlett.128.020403 (2022).
- [92] O. Shtanko, Y.-J. Liu, S. Lieu, A. V. Gorshkov, and V. V. Albert, Bounds on autonomous quantum error correction (2023), *arXiv:2308.16233 [quant-ph]*.
- [93] M. Araújo, F. Costa, and Č. Brukner, Computational advantage from quantum-controlled ordering of gates, *Physical Review Letters* **113**, 10.1103/physrevlett.113.250402 (2014).
- [94] R. Vershynin, Introduction to the non-asymptotic analysis of random matrices, in *Compressed Sensing: Theory and Applications*, edited by Y. C. Eldar and G. Kutyniok (Cambridge University Press, 2012) p. 210–219.
- [95] S. N. Bernstein, On a modification of Chebyshev's inequality and of the error formula of Laplace, *Uchenye Zapiski Nauch.-Issled. Kaf. Ukraine, Sect. Math* **1**, 38–48 (1924), (Russian).
- [96] H. Chernoff, A Measure of Asymptotic Efficiency for Tests of a Hypothesis Based on the sum of Observations, *The Annals of Mathematical Statistics* **23**, 493 (1952).
- [97] H. Bauer, *Measure and Integration Theory* (De Gruyter, Berlin, New York, 2001).
- [98] A. J. Daley, Quantum trajectories and open many-body quantum systems, *Advances in Physics* **63**, 77 (2014).
- [99] D. A. Lidar, *Lecture notes on the theory of open quantum systems* (2019).
- [100] D. R. Cox, *Renewal Theory* (Methuen & Co Ltd, 1962).
- [101] M. Ozols, *The Solovay-Kitaev theorem*, Essay at University of Waterloo (2009).